ABSTRACT

WEBB, ELIZABETH LYNN. Process control parameters for Skipjack tuna (*Katsuwonas pelamis*) precooking. (Under the direction of S. Andrew Hale).

The purpose of this research was to define the critical process control parameters that influence texture and yield for the precook unit operation in the commercial canning of Skipjack tuna. To accomplish this goal, the impact of precook temperature and time combinations on the Instrumental Texture Profile Analysis (ITPA) texture parameters, protein state, weight loss, and moisture content of hydrothermally treated tuna loin meat was investigated. It was found that temperature was the primary influence for all ITPA parameters, however time influenced texture when samples were held at 55°C. Auto proteolysis was suspected at this temperature, as some ITPA parameters declined with increased time.

Data from small steamed and small hydrothermally treated samples were compared with data from whole steamed fish to ascertain whether small sample results could be extrapolated to data from whole precooked fish. Weight loss, moisture content, and ITPA values reacted similarly, regardless of experiment method. For all treatments, weight loss and moisture content decreased with increased temperature, and hardness, instantaneous springiness, and retarded springiness increased with increased temperature. Cohesiveness did not vary with temperature. Linear conversion equations were written to predict texture, weight loss, and moisture content results of whole precooked fish from small steamed and small hydrothermal samples.

Process inputs which are available from a commercial precooking unit operation were used to model effects of precooking Skipjack tuna. Fuzzy logic, neural network, and multiple linear regression models were written to predict precook time, weight loss,

friability, and edible weight of precooked fish from final backbone temperature, frozen weight, and storage time inputs. Both fuzzy logic and neural net models perform better than traditional multiple linear regression models in predicting cook time and weight loss. Friability and edible weight were difficult to quantify with all models, and more data was needed to better quantify these variables.

PROCESS CONTROL PARAMETERS FOR SKIPJACK TUNA (*Katsuwonas pelamis*) PRECOOKING

by

Elizabeth Lynn Webb

A dissertation submitted to the Graduate Faculty of
North Carolina State University
in partial fulfillment of the
requirements for the Degree of
Doctor of Philosophy

BIOLOGICAL AND AGRICULTURAL ENGINEERING

Raleigh

2003

APPROVED BY

_____	_____	_____
Dr. Brian Farkas	**Dr. James Young**	**Dr. Kevin Keener**

_____
Dr. Andrew Hale
Chair of Advisory Committee

DEDICATION

This work is dedicated to Mema, my greatest teacher.

BIOGRAPHY

Elizabeth Webb was born in Ocala, Florida and grew up nearby in the small towns of Ocklawaha and East Lake Weir. She is a ninth generation native Floridian, and the oldest of four daughters of Ricki and Jack Webb. Her roots are in oranges, grapefruit, and tangerines, not tuna, as she is the fifth generation of her family to work in citrus. She spent her free time during her youth enjoying sports, horseback riding, hunting, fishing, occasional waterskiing, and other tomboyish activities.

Elizabeth received her Bachelors in Agricultural Engineering from the University of Florida, Gainesville, Florida in September 1994. After graduating, she was employed for two years as a process engineer with Brown Citrus Systems in Winter Haven Florida where she provided technical advice and engineering solutions to domestic and international citrus processing plants. She earned her Masters of Science degree in engineering by studying the graduate Chemical Engineering curriculum from the University of South Florida, Tampa, Florida in May 1997. Her thesis was titled "Describing a Citrus Pulp Wash System Using a Modified McCabe-Thiele Method". After graduating with her Masters, she joined the Biological and Agricultural Engineering department as a doctoral student, where she worked until December 2000 when she rejoined Brown Citrus Systems Inc. as their Technical Services Director.

ACKNOWLEDGEMENTS

I thank my family, Will, Jack, and Willie, for their patience and sacrifices during all the time I spent on this work. Thanks also to Dr. Andy Hale for the latitude to pursue my research, the guidance when things went bad, and his kindness for understanding life. I am indebted to Dr. Brian Farkas, who has given me much encouragement and needed direction throughout my doctoral endeavours. My gratitude goes to Dr. Tyre C. Lanier for sharing his wealth of seafood knowledge with me. I also appreciate Dr. Kevin Keener and Dr. Jim Young for their input during my studies.

My work is only one part of a research project on tuna and tuna processing. I owe the rest of The Tuna Group, as we were collectively called, a big thank you for their group spirit and willingness to help – kudos to Jon Bell, Janet Zhang, Nicola Stagg, Heather Stewart, and Penny Amato. I especially thank Tim Seaboch for his help and camaraderie throughout my stay in North Carolina, some of which was imparted during the many, many experiments I ran in 117.

I would like to recognize StarKist Seafoods and the USDA for providing funds and support for my research project. I want to thank two StarKist employees in particular - Jaime Citron and Joe Emmer - for coordinating the shipment of the all the frozen, cannery grade tuna used in my research.

Thanks to Dr. Bob Braddock and Dr. William Miller of the UF/IFAS Citrus Research and Education Center. They provided good advice, abundant moral support, and great impetus for finishing this dissertation. Words fall flat when describing the credit deserved by Pam Russ, the librarian at the Citrus Research and Education Center, who gave me a cubby, a T1 connection, all the journal article reprints I could generate, and a friendly ear during the last two months of writing this dissertation.

TABLE OF CONTENTS

LIST OF TABLES

3.0 MANUSCRIPT 1

4.0 MANUSCRIPT 2

5.0 MANUSCRIPT 3

LIST OF FIGURES

2.0 LITERATURE REVIEW

3.0 MANUSCRIPT 1

4.0 MANUSCRIPT 2

5.0 MANUSCRIPT 3

1.0 INTRODUCTION

Today, as is the trend with most mass produced, consumable agricultural products, canned tuna has changed from a high profit margin product to a commodity product. In the commodity product business model, several ways exist for a company to remain profitable, including bulk processing, overhead reduction, and decreased raw product waste. To bulk process, a plant must increase production volume while maintaining the same, or slightly elevated, fixed costs. To use this strategy, food plants can increase throughput while maintaining the same amount of processing machinery, or produce more product in the same amount of production time. Reduced overhead, for most processors, means a reduced workforce and more plant automation. For inordinately high labor markets, some companies relocate their entire processing facility to a region with less expensive labor costs. A processor can also decrease the amount of wasted raw material used to make a finished product to increase profit.

The tuna industry has already learned the lesson of "running volume", as processing plants currently exist which turn out millions of cans of tuna per day (Bell, 2000). They have also learned the lesson of overhead reduction through workforce relocation – one example is StarKist tuna's closing of the Mayaguez, Puerto Rico plant due to high labor costs. The tuna industry's profit margin has been adversely affected by the high cost of fish; therefore decreased raw product waste translates into increased profit.

The tuna canning industry is not very automated, as cannery unit operations have largely stayed the same for 50 years (Finch, 1963; Horner, 1992). Automation, sensing, and control are not widely implemented in tuna canning, possibly due the diversity of incoming raw materials (Choudhury and Bublitz, 1996), high initial investment

in machinery and worker training (DeSilva, 1992), and undefined process variables which relate to controllable parameters.

Canned tuna is heated twice during processing – once to change the meat texture for hand cleaning of the whole fish, and again during canning to achieve a commercially sterile product. The first heating, or precook, directly impacts a cannery's profit, as it is the single biggest impact on final product quality and yield (Wheaton and Lawson, 1985; Lassen, 1965). Mistakes made during precook cause yield loss by either unnecessary water loss or undesirable texture changes that cause edible meat loss. A complicating factor during precook is the natural variation of the raw product. Cooked tuna can also suffer from mushy texture after precooking, called mushy tuna syndrome (MTS). MTS is thought to be caused by auto proteolytic enzymes which can be active in the precook temperature range (Stagg, 1999). MTS decreases yield, as light to moderately MTS affected fish are difficult to clean, and fish severely affected by MTS are not suited for canning. The ability to control the precook unit operation would help processors reduce raw product waste and increase profits.

The ultimate goal of this research was to control the canned tuna process for a more predictable yield. To achieve this goal, critical process control parameters needed to be defined for the precook unit operation, as the precook step is the single biggest influence on plant yield. The purpose of this work was to –

- Define the influence of temperature and time, using ranges seen in commercial processing, on texture changes of precooked tuna
- Investigate whether texture degradation and yield reduction occurs at a certain temperature during precooking
- Investigate the effect of temperature and time on tuna mass and moisture changes
- Compare the effect of cooking whole and small samples

- Model the outcome of final temperature and fish size on cook time, weight loss, edible weight, and friability in whole fish.

- Learn how to manipulate process control parameters to achieve maximum yield while minimizing texture degradation and friability

1.1 REFERENCES

Bell, J.W., 2000. Liquid mass transport in Skipjack tuna muscle (Katsuwonas pelamis) during canned tuna processes [PhD dissertation]. North Carolina State University, Raleigh, NC.

Choudhury, G. S., and Bublitz, C. G., 1997. Computer based controls in the fish processing industry. Ch 19 in *Computerized Control Systems in the Food Industry*, G. S. Mittal, Ed. Marcel Dekker, Inc., New York, NY.

DeSilva, C. W., 1992. Research laboratory for fish processing automation. Robotics and Computer Integrated Manufacturing 9 (1) p 49-60.

Finch, R., 1963. The tuna industry. Ch 7 in *Industrial Fishery Technology*, M. E. Stansby and J. A. Dassow, Eds. Reinhold Publishing Corp., New York.

Horner, W. F. A., 1992. Canning fish and fish products. Ch 5 in *Fish Processing Technology*, G. M. Hall, Ed. Blackie Academic and Professional, published in North American by VCH Publishers, New York, NY.

Lassen, Sven 1965. Tuna Canning and the Preservation of the Raw Material through Brine Refrigeration. Ch. 4 in *Fish as Food*, v 4, part 2, G. Borgstrom (Ed.) p. 207-245, Academic Press, New York and London.

Stagg N. 1999. Response of Skipjack tuna muscle protein to thermal processing [MSc thesis]. Raleigh NC: North Carolina State University. 128 p.

Wheaton, F.W. and Lawson, T.B., 1985. Heat processing and canning: canning of tuna. In Processing Aquatic Food Products, John Wiley and Sons, New York, NY.

2.0 LITERATURE REVIEW

2.1 Skipjack tuna

Tuna was first canned in 1903, when a disastrous sardine catch forced Mr. A. P. Halfhill of San Pedro, California to search for alternate fish to preserve in an effort to keep his cannery afloat (Finch, 1963). Fourteen species of tuna can be legally canned in accordance with the 1998 Code of Federal Regulations, but canned tuna sold in the United States primarily consists of light meat harvested from Bluefin, Albacore, Yellowfin, or Skipjack. Skipjack tuna (*Katsuwonus pelamis*) has become the most popular commercially fished tuna, and currently comprise fifty percent of the worlds catch (Wheaton and Lawson, 1985; Gardieff, 2003; Joseph, 2003). Skipjack also represent the majority of meat canned for chunk light tuna (Bell, 1998).

Skipjack (Figure 1) is epipelagic, inhabiting waters with temperature ranges of 14.7°C to 30°C, and are distributed circumtropically, however also occur along the European coast and the North Sea (Figure 2). Skipjacks tend to school, sometimes with other tuna species. Schooling frequently occurs under a drifting object, or larger marine animals such as whales or sharks. Skipjack often school by size, as smaller fish might not be able to maintain top speeds achieved by larger fish. The maximum recorded length for this species is 108 cm from head to tail fork, and the maximum recorded weight is 34.5 kg. Tuna caught for commercial purposes more commonly attain a length of 50 to 80 cm and weight between 2.7 to 10 kg. Cannery Skipjack are commercially fished at the surface, primarily with purse seine nets. Artificial flotsam and other manmade floating structures are regularly used by commercial fishermen to attract Skipjack. Chase boats and aerial spotter planes sometimes accompany fishing vessels to help locate schools (Bell, 1998; Gardieff, 2003).

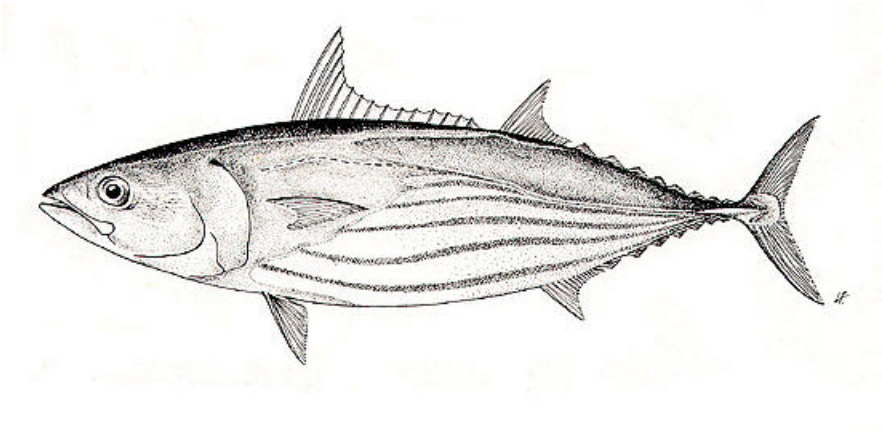

Figure 1 Skipjack tuna (*Katsuwonus pelamis*) (Collette and Nauen, 1983).

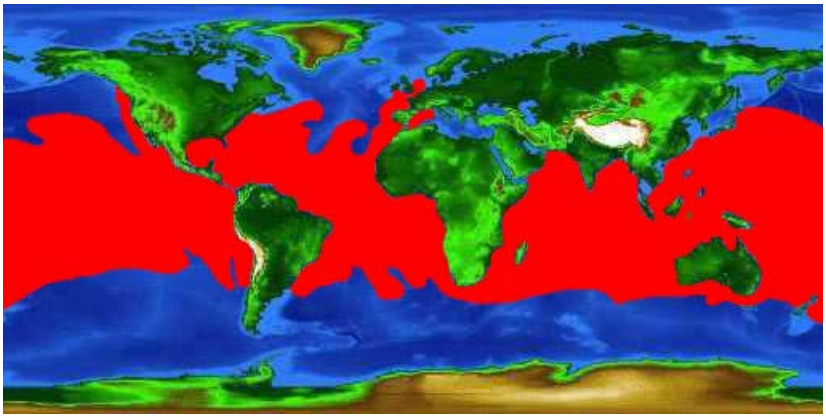

Figure 2 Skipjack tuna range, in red (Bester, 2003).

2.2 Mammal and fish muscle similarities and differences

2.2.1 Mammalian muscle structure and composition

Adult mammalian muscle tissue is primarily water (75%) and proteins (19%) (Martens et al., 1982). Figure 3 shows the structure of mammalian muscle. Beef muscle ultrastructure has been described as a collection of long cylindrical muscle fibers joined together by connective tissue (Lepetit and Culioli, 1994). Mammal muscle

consists of long, cylindrical cells called myofibers, surrounded by collagen and elastin fibers, which are located in the extracellular space surrounding the myofibers. One myofiber consists of many myofibrils. Myofibrils consist of thick (15 nm diameter) and thin (6-8 nm diameter) filaments. Myosin is the primary component of thick filaments, while actin, tropomyosin, and troponin are the primary proteins of the thin filaments. Myosin and actin are the primary structural proteins for all meat (Greaser, 1991). The sarcoplasmic proteins, mainly globular, soluble proteins found in extracellular fluid, include myoglobin, hemoglobin, globulins, albumins, and various enzymes. Stroma proteins, collagen and elastin, surround the myofibers, and are less soluble than sarcoplasmic proteins (Venugopal and Shahidi, 1996).

Approximately 90% of water contained by muscle is intracellular, located in narrow channels between thick and thin filaments contained by the myofibrils. The remaining 10% of water is distributed in extracellular compartments (Offer et al., 1989). Muscle macro and microstructure, in particular the myofibrillar proteins, are responsible for the retention of water in meat (Honikel and Hamm, 1994).

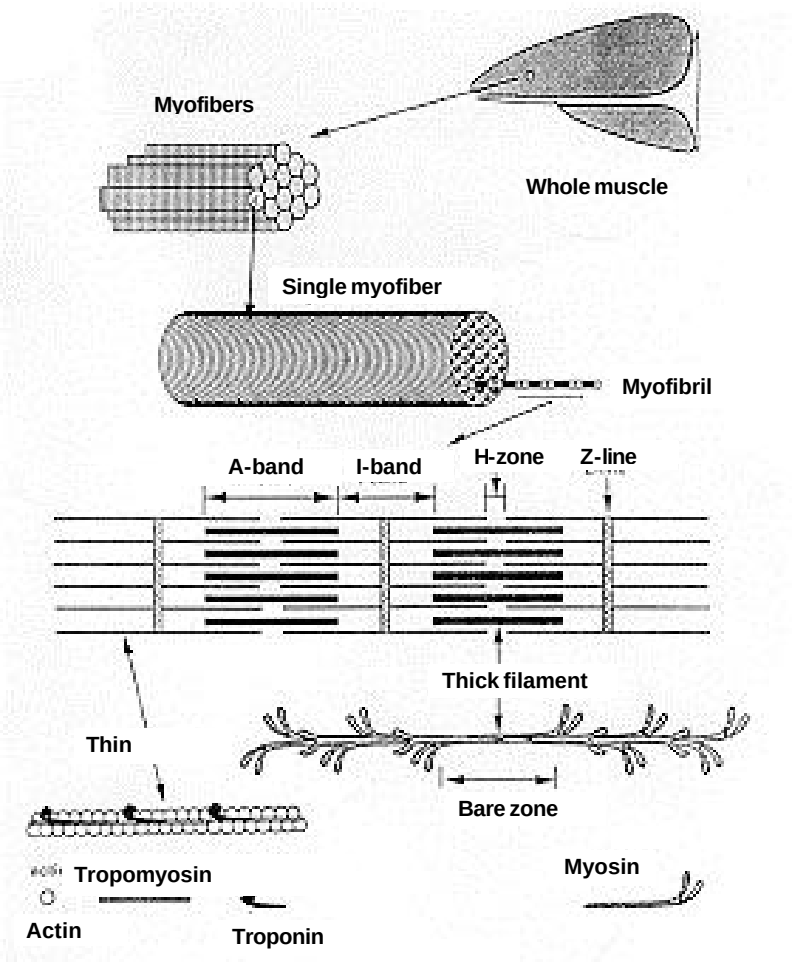

Figure 3 Diagram of mammalian muscle tissue (Greaser, 1991).

2.2.2 Fish and Skipjack tuna muscle structure and composition

Fish in general have roughly the same composition as beef, although raw Skipjack tuna has less water and more protein - approximately 71.7% water, 25.9% protein, and 0.6% fat (Venugopal and Shahidi, 1996). Fish muscle is more rudimentary than mammalian muscle, and consists of a few long sheets of muscle extending the whole length of the body (Figure 4). Fish have a metameric muscle structure, or a linear series of muscle segments, which are primitive when compared with mammalian muscle. These long sheets are transversely divided by sheets of connective tissue

called myocommata, into myotomes (Dunajski, 1979). Fish muscle cells join two adjacent myocommata, and are parallel to the long axis of the muscle. Fish muscle fibers are short relative to mammalian muscle fibers (Dunjanski, 1979), although the muscle cell structure is basically the same as mammals.

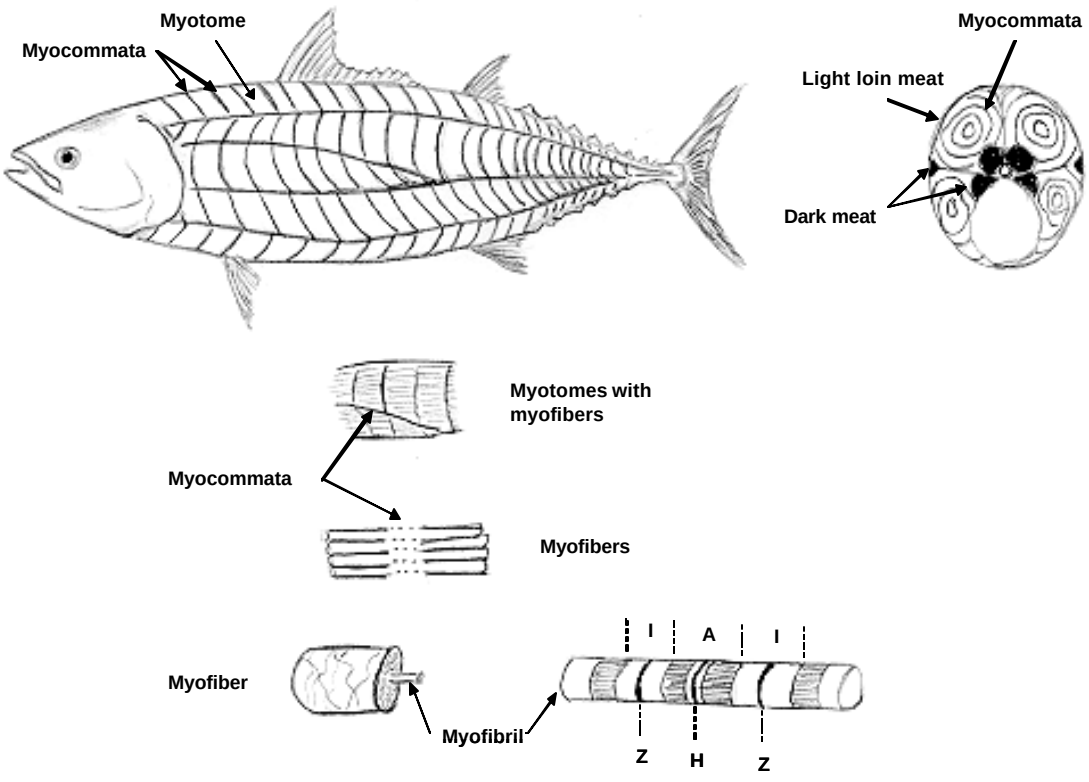

Figure 4 Skipjack tuna muscle structure.

The proteins that make up fish muscle function like mammalian proteins, although their physical properties differ slightly. Fish myosin is more heat labile than beef, although tuna myosin is almost as stable as rabbit and beef myosin (Venugopal and Shahidi, 1996). Connective tissue, mainly collagen, is more evenly distributed and is less abundant in fish than mammals, probably due to the water environment which supports their bodies (Venugopal and Shahidi, 1996). Fish collagen is less heat stable

and more soluble than beef or pork collagen (Dunajski, 1979; Venugopal and Shahidi, 1996).

Tuna have both dark (also referred to as red) and light muscle. The dark muscle is used for continuous swimming, while light muscle is used for short bursts of rapid swimming (Venugopal and Shahidi, 1996). The dark muscle is also involved in body temperature regulation, as Skipjack are capable of somewhat regulating their body temperature (Gardieff, 2003). Light muscle in fish is very uniform in composition, no matter where the muscle is located. This is not true in mammals, where muscle composition changes depending on location (Foegeding and Lanier, 1996).

2.3 Canned tuna processing

Figure 5 shows a flow diagram of a typical tuna canning process. Incoming frozen tuna are delivered to the canning plant by transport ships and sorted by size and species. Fish over 9 kg are sorted by hand while fish under 9 kg are automatically sorted by weight. Sorted fish are placed into containers called scows and stored in plant freezers until processing.

When required for processing, frozen tuna lots are selected from the freezer based on size and species and are placed into thaw tanks, usually 18 scows per thaw tank, and the thaw tanks are filled with water. The fish are thawed to an estimated -2°C backbone temperature, then progress to the butchering line for manual grading and evisceration. After grading and evisceration, tuna are placed into baskets, which are slid into racks similar to bread proofing carts. A group of 12 to 30 racks are wheeled into a batch precooker where the fish are subjected to 100 to 104°C steam for a time dependent on the size of the fish. Cook time is determined by the amount of time

required to raise the backbone temperature of the tuna to 60 to 66°C. This processing step is performed to change the texture of the fish muscle for easier hand cleaning.

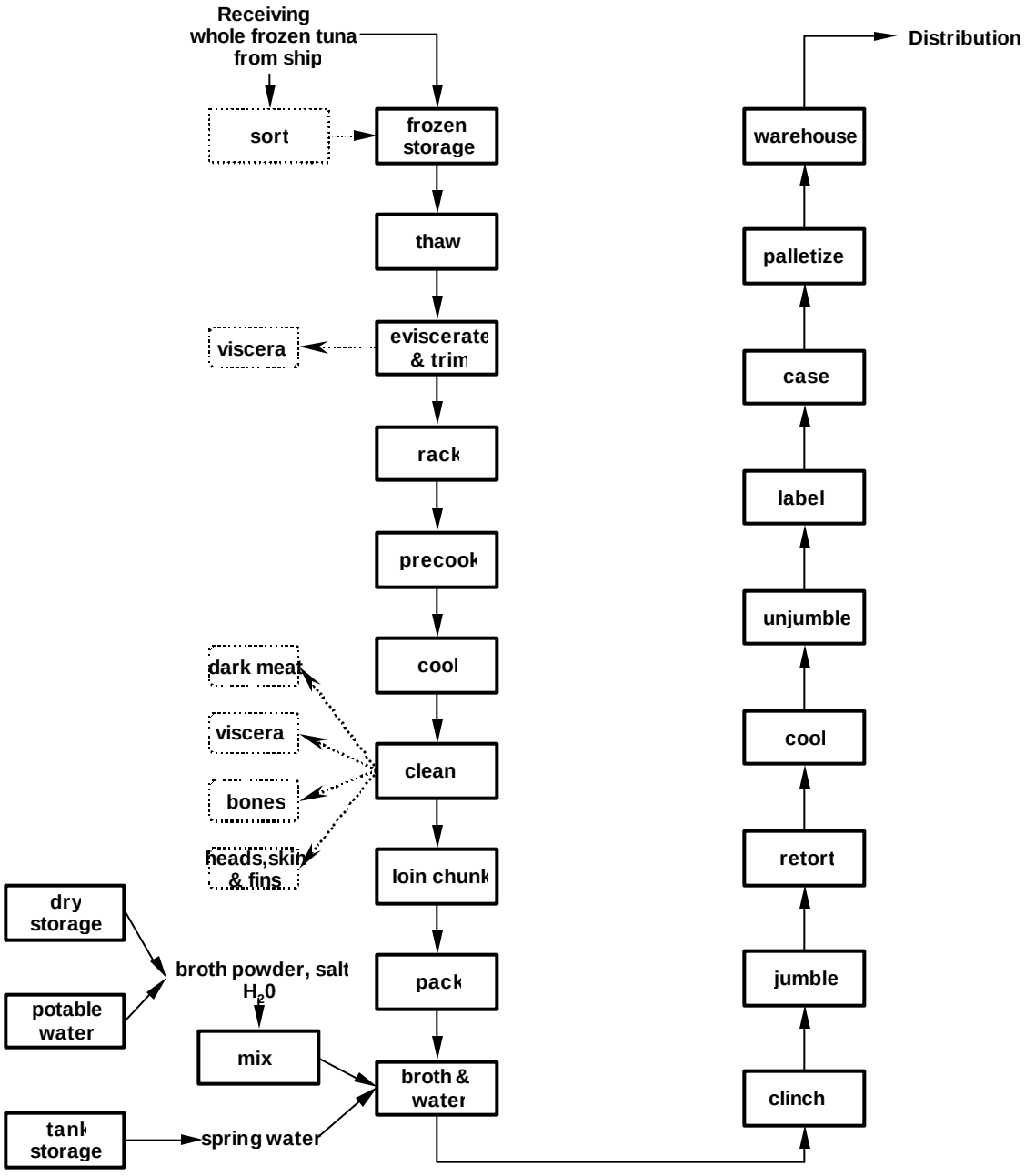

Figure 5 Tuna canning diagram.

After precooking, cooking carts are moved to a cool down area where a combination of water mist and ambient air cool the fish. Cooling firms fish flesh so that the fish carcass is less friable and more easily separated into its constituent pieces. After cooling, fish are cleaned by hand on a cleaning line. From each fish carcass four light loins are separated for canning, while dark meat is segregated and processed for cat food. Bones and heads, skin, and viscera are removed and processed into fishmeal. Figure 6 shows the location of these components in a cross section of Skipjack tuna.

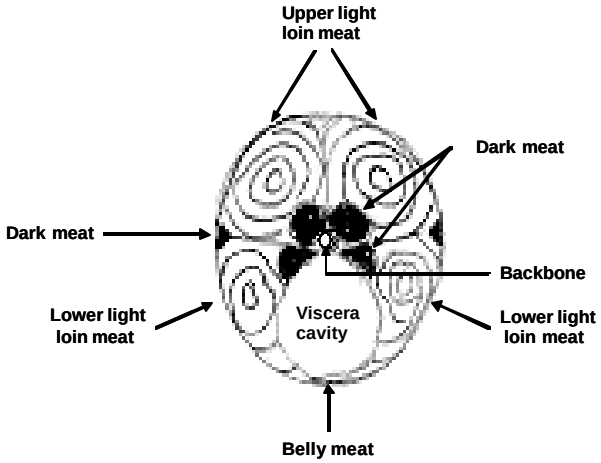

Figure 6 **Cross section of a Skipjack tuna showing upper and lower loins, dark meat, backbone, viscera cavity, and belly meat.**

From cleaning, the loins progress to a loin cutter and are cut into chunks for canning. After cutting, loin pieces are conveyed to the filling machine and placed with a piston into open cans. The open cans are topped with a combination of water and vegetable broth, a lid applied and seams are sealed, then sealed cans are randomly placed into baskets to retort. The baskets are retorted for a specific time and temperature combination dependent on can size, then cooled, unjumbled, labeled, and packaged in cases. The cases are then palletized and placed in a warehouse until distribution (Lawson, 1965; Finch, 1963; Farkas et al., 1999; Horner, 1992).

2.3.1 The impact of precooking on canned tuna

The precook step is the most important for quality and yield (Wheaton and Lawson, 1985; Lassen, 1965). A common belief in the tuna industry is that to get a "good cook" the temperature of a tuna, as measured along the upper part of the spinal column in the thickest part of the fish, must be heated to approximately 60 to 66°C during the precook operation. Further heating beyond this point is not only unnecessary, but actually reduces both yield and flavor of the tuna meat, as temperature influences weight loss, texture change, and ultimately, plant yield.

One result of higher precook temperatures is lower meat moisture content. Lassen (1965) reported an inverse linear relationship between the moisture content of precooked Yellowfin tuna and fish backbone temperature. Lower moisture contents of precooked tuna might translate into lower plant yields due to water that is lost and not recovered during the canning process. Higher precook temperatures may also change how the muscle holds water and broth during the canning operation, and cause increased friability, thereby decreasing plant yield.

Under precooking tuna makes meat more difficult to pull from the bone and reduces yield, and also might leave some enzymes active that degrade texture. These enzymes give an unacceptable, "mushy" final canned product (Lassen, 1965; Bell, 1998). The knowledge of the precooking operation is still largely empirical, with processors not sharing precooking times within the industry.

2.4 Changes occurring during tuna precooking

To describe the phenomena that occur during precooking of tuna, four areas will be addressed in the cooking of meat and fish –

- Protein denaturation, coagulation, and meat ultrastructure changes
- Moisture and protein loss
- Texture changes
- Friability changes

2.4.1 Protein denaturation, coagulation, and ultrastructure changes in meat and fish

Heat treatment of meat denatures, solublizes, and coagulates proteins, and releases water. Three major textural proteins in beef are myosin, collagen, and actin. In beef, the denaturing and coagulation of myosin and actin are thought to be responsible for toughening with cooking, while collagen solublization and gelatinization are thought responsible for tenderizing with cooking (Kramer and Szczesniak, 1973). Beef texture is influenced by all three, but fish texture is more influenced by myosin and actin, as fish have much less collagen than beef (Foegeding and Lanier, 1996; Dunajaski, 1979).

Protein denaturation is first to occur with heating. Parsons and Patterson (1986) showed raw beef had three characteristic protein denaturation peaks, located at 55°C, 66°C, and 79°C (Figure 7). These three peaks were taken to be myosin, sarcoplasmic proteins and collagen, and actin proteins, respectively. Other researchers have found similar results for denaturation temperatures, although some debate exists as to whether collagen is also represented by the second DSC peak (Bertola et al., 1994; Martens et al., 1982).

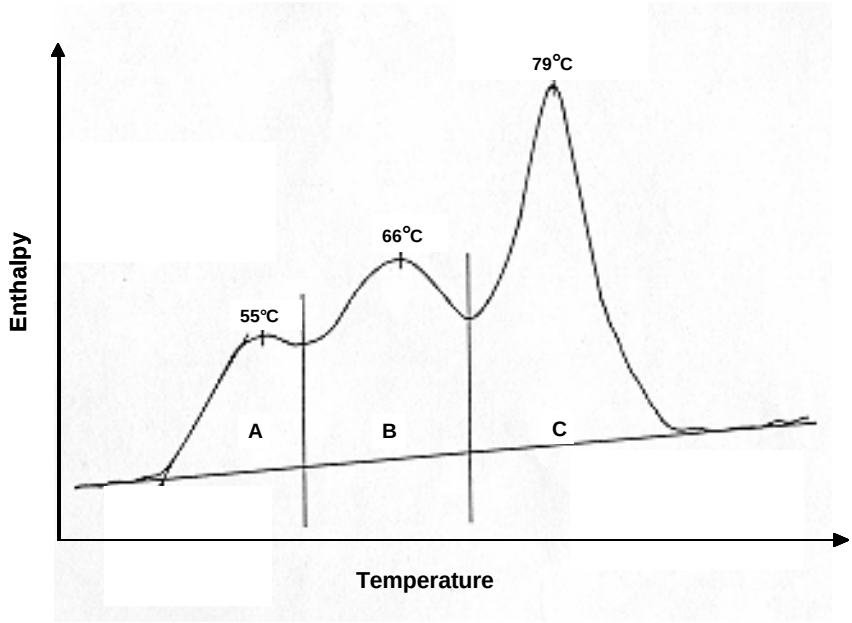

Figure 7 **DSC thermogram of raw beef muscle scanned at 10°C/min with denaturation peaks at 55°C, 66°C, and 79°C (Parsons and Patterson, 1986).**

After proteins denature, they either solubilize and/or coagulate. The mechanism for meat texture changes with heating are not well established, however some actomyosin complexes form and collagen first solublizes then gelatinizes. The main factors that affect beef texture are myofibrillar proteins, muscle cytoskeleton intramuscular connective tissue, and intrafiber water (Harris, 1976; Jones et al., 1977; Leander, 1977; Offer et al., 1989). When beef is heated, tenderizing effects have been attributed to connective tissue changes, while toughening effects have been attributed to hardening of the myofibrillar proteins (Laakkonen, 1973). With fish, with much less collagen and much shorter muscle cells, the tenderizing phenomenon does not appear to happen nearly as much as in beef.

Muscle ultrastructure is also influenced by cooking. A simple model for meat structure can be described as a collection of parallel fibers, the myofibrillar structure, bound together by a three dimensional connective tissue network (Bouton et al., 1975).

Cooking muscle tissue causes a reduction in muscle fiber diameter and sarcomere length, and a simultaneous translocation of water, lipids, and dissolved materials out of the muscle (Leander et al., 1980). According to Palka and Daun (1999), the structural changes caused by heating beef muscle tissue can be described as –

- Up to 50°C - Slight effect on structure, some denaturation of myofibrillar proteins, primarily actomyosin complex.
- 50°C - Myofibrillar protein compression
- 60°C - Thick/thin filament coagulation, additional myofibrillar shrinkage, sarcolemma granulation
- 70°C - Myofibrillar fragmentation at Z disk, total shrinkage of endomesium
- 80°C - Additional thin filament disintegration, collagen fiber gelatinization in perimysium
- 90°C - Amorphous structure, although sarcomeres can be identified.

2.4.2 Meat and fish moisture, protein, and weight loss during heating

When meat is cooked, water, soluble proteins, and fats are expelled from the tissue (Leander et al., 1980). Most water in meat is located within the myofibrils, in the narrow channels between thick and thin filaments, therefore water lost during cooking is a result of protein denaturation and coagulation (Offer, 1984; Bertola et al., 1994). Protein loss during heating is a result of proteins solubilized and expelled with the water leaving the meat.

Beef cook losses as a function of temperature have been reported by Martens et al. (1982). These researchers found losses of 5 to 35% occurred over 45 to 85°C. Similar beef cook losses have been reported by other researchers (Palka and Daun, 1999; Bouton and Harris, 1972). Weight losses in chicken have also been reported from 5 to 28% over 40 to 80°C, but these losses vary with postmortem hold time, added salt

percentage, and cooking method (Lyon et al., 1984; Lyon and Lyon, 1993). Researchers have found that total losses depend on the heating temperature and heating rate during cooking (Hearne et al., 1978).

Some research has been performed on Yellowfin and Skipjack texture and meat microstructure changes upon heating, but these experiments studied only physiological changes (Kanoh et al., 1988; Lampila and Brown, 1986). No research was performed in these studies on weight and moisture content losses with heating. Researchers have quantified moisture content changes and weight loss rate of change of Skipjack tuna fillets with steam cooking, although accompanying texture changes were not quantified (Bell et al., 2001)

2.4.3 Meat and fish texture changes due to heating

2.4.3.1 Measuring texture in meat and fish

Two types of texture measurements exist – physiological, or sensory texture testing, and instrumental texture testing. Sensory texture testing is used to quantify the acceptability of food texture. Sensory tests require a panel of trained assessors, panel size depending on the amount of difference between samples, and repetitive testing to ensure accurate results. Because of the difficulties associated with human sensory panels and the need to quantify texture measurements, instrumental texture testing is also used by researchers to measure food texture.

Meat texture can be difficult to quantify. Meat is anisotropic, and has different physical properties according to which direction is tested (Lepetit and Culioli, 1994). The textural properties of meat have not been identified as well as other foods due to sample anisotropy and the multitude of pre and post mortem factors that influence texture

(Kramer and Szczesniak, 1973). Although difficult for researchers to quantify, meat texture is important to the consumer.

A multitude of instrumental texture tests can be used to quantify meat texture. A survey of 82 public and private organizations involved in production, quality control, and processing meat showed that 78% used the Warner-Bratzler shear test for texture testing (Lepetit and Culioli, 1994). This test is an empirical technique, and researchers usually focus on one parameter, the maximum force during sample shear. Other tests for meat texture include compression tests, tensile tests, penetrometry, multi-blade shear, and bite tests (Lepetit and Culioli, 1994).

Fish texture is also important to the consumer. A market study of Norwegian salmon showed that 75% of buyers indicate texture is one of the most important attributes (Hyldig and Nielsen, 2001). The texture of fish muscle has been investigated by many researchers, and no one measurement method is preferred. Many researchers use shearing methods such as the Warner Bratzler shear test because samples are easy to prepare and tests are not difficult to perform. Although popular, this method only gives shear force perpendicular to the muscle fibers. Like beef texture methods, other fish texture measurement methods include single or double compression (Texture Profile Analysis), puncture, and shear strength (punch and die, Kramer shear cell) (Hyldig and Nielsen, 2001; Hamann and Lanier, 1986).

Researchers investigating beef and fish texture have more recently been leaning away from single point measurements and towards multipoint measurements that give multiple texture parameters (Sigurgisladottir, 1997). Texture has been defined by Szczesniak (1963a) as both the physical structure of food and the characteristics of food during mechanical treatment and Bourne (1982) has stated that texture is a group of

physical properties that derive from the structure of food, not just a single property, thus the move away from single point to multipoint texture testing.

2.4.3.2 The ITPA method

A method which gives multiple texture descriptors is the Instrumental Texture Profile Analysis (ITPA) method. This method was developed for sensory panels as a method to describe food texture (Szczesniak, 1963a; Szczesniak, 1963b), and adapted to machine testing with the invention of the General Foods Texturometer (Freidman et al., 1963). Bourne (1978) later adapted the ITPA test for Instron use.

ITPA testing subjects a sample to a double compression and the resulting data are analyzed for up to eight parameters to describe food texture. In this data, time is analogous to sample deformation as the Instron cross head speed is kept constant throughout testing. Advantages of using ITPA testing include the ability to instrumentally test samples for multipoint texture values and a relatively quick, easy, and inexpensive way to test texture compared to the sensory panel method. One disadvantage to using the ITPA test is that it is difficult to compare values from other tests due to non-standardized testing techniques, including different cross head speeds, compression heights, and sample shapes (Bourne and Comstock, 1981).

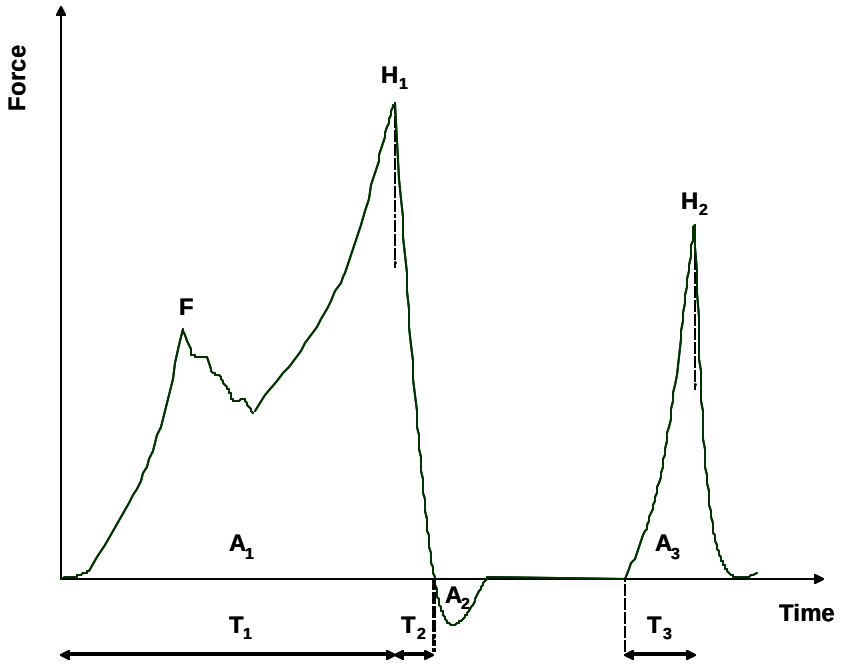

Figure 8 Hypothetical ITPA curve.

Figure 8 shows a hypothetical curve that illustrates the eight measurements from an ITPA test. The definitions of ITPA parameters calculated from data shown in Figure 8 are –

- Hardness (H_1, H_2) – Peak force during a compression cycle (Bourne, 1978). Hardness 1 (H_1) is usually reported, and is the peak force during the first compression cycle. Hardness 2 (H_2) can also be reported, and is the peak force during the second compression cycle. Hardness 1 is related to the compressive strength of a sample, defined as the maximum load during a compression test divided by the specimen's original cross sectional area (Mohsenin, 1986).

- Fracturability (F) – Force at the first significant break during the first compression cycle (Bourne, 1978). Not all samples exhibit fracturability. This measurement is analogous to a sample's bioyield point (Mohsenin, 1986).

- Cohesiveness (A_3/A_1) – Ratio of the positive force area of the second compression cycle (A_3) divided by the positive force area of the first compression cycle (A_1) (Bourne, 1978). This measurement is related to the work needed to overcome the internal bonds of a sample (Friedman et al., 1963).

- Adhesiveness (A_2) – The negative force area resulting from the first compression cycle. This area is analogous to the work necessary to pull the compression platen away from the sample (Bourne, 1978). Not all samples exhibit adhesiveness.

- Instantaneous springiness (T_2/T_1) – The height the sample recovers immediately after the first compression cycle, as measured by the time over which the load cell records a force from the sample. This measurement is related to the elasticity of a sample (Fiszman et al., 1998). Some researchers also call this measurement Resilience (Veland and Torrissen, 1999; Palka, 2000).

- Retarded springiness (T_3/T_1) – The height the sample recovers during the time between the end of the first compression cycle and start of the second compression cycle, as measured by the time over which the load cell records a force from the sample. This measurement is related to the viscosity of the sample (Fiszman et al., 1998).

- Gumminess ($H_1 \bullet A_3/A_1$) – The product of hardness and cohesiveness, and is described as the energy required to disintegrate a semisolid food product (Friedman et al., 1963). This measurement should only be reported as a characteristic of a semisolid food (Szczesniak, 1996; Bourne, 1996).

- Chewiness ($H_1 \bullet (A_3/A_1) \bullet (T_3/T_1)$) – The product of gumminess and retarded springiness, alternately the product of hardness, cohesiveness, and retarded springiness (Freidman et al., 1963). This measurement is described as the energy required to chew a solid food product, and should only be reported when testing a solid food product (Szczesniak, 1996; Bourne, 1996).

ITPA has been used extensively for fruit and vegetable texture measurements such as sweet potatoes, carrots, pears, apples, and potatoes, as these commodities have a uniform internal structure. ITPA has also been used to characterize cooked beef texture (Duizer et al., 1996; Palka and Daun, 1999; Palka, 2000), cooked poultry (Lyon and Lyon, 1990; Lyon and Lyon, 1993; Smith et al., 1988; Lyon et al., 1981; Lyon et al., 1984; Lyon and Hamm, 1984), cooked, breaded shrimp (Soo and Sander, 1977), Kamaboko (Konstance, 1991), cooked meat batter (Barbut and Mittal, 1990), dry-cured ham (Tabilo et al., 1999), cooked, restructured pork chops (Trout et al., 1990), and cooked mutton (Mahendrakar et al., 1990). This method has been used to characterize the effect of storage time and temperature on raw Atlantic salmon texture (Veland and Torrissen, 1999), the effect of hydrothermal processing temperature and time on Pacific

chum salmon texture (Bhattacharya et al., 1993), and influence of sexual maturity on the texture of canned salmon (Reid and Durance, 1992).

2.4.3.3 Texture impact of cooking meat and fish

Cooking temperature has been shown to have a significant effect on ITPA hardness, retarded springiness, cohesiveness, and chewiness for beef (Palka and Daun, 1999). These researchers saw hardness increase, retarded springiness ultimately decrease, and cohesiveness ultimately decrease with increased temperature. They attributed texture changes to protein and ultrastructure changes associated with heating.

Heating also impacts fish texture as measured by ITPA. Pacific chum salmon subjected to hydrothermal treatments exhibited increased hardness, cohesiveness, and springiness with increased heat, although hardness and springiness decreased with prolonged heating times (Bhattacharya et al., 1993). The salmon ITPA results were less complex than those of the beef researchers, and one reason might be that changes in beef texture can be attributed to two mechanisms, both tenderization due to collagen solubilization and toughening due to actin/myosin hardening. Muscle fibers are the main textural components of fish (Dunajski, 1979), hence fish texture changes are primarily due to actin/myosin hardening.

No researcher has completed a detailed study of how the texture of tuna changes during the precook unit operation. The texture change accompanying precooking is critical for plant yield, as the texture defines how efficiently tuna are cleaned. Defining the texture change associated with precooking will aid processors in making a decision about precooking temperature of tuna.

2.4.4 Meat friability

A term that combines precook yield and texture is friability. Friability is defined as the "liability of a material to break into smaller pieces when subjected to repeated handling" (ASTM, 1994). This definition can be thought of as the complement of the size stability of particles, with higher friability meaning more of a tendency for particles to disintegrate with handling. Friability has been quantified by several empirical methods for materials such as coal, and the test is done by tumbling a sample of coal for a specified time and then sizing with a series of screens. Percent friability of that sample, as referred to in method D 441 (ASTM, 1994), is calculated by

$$Friabilty = 100\frac{(S-s)}{S},\ \% \quad \text{..... (1)}$$

where S represents the average piece size before treatment, and s the average piece size after treatment.

To calculate s, a measure of the average piece size after treatment, a normalizing factor N_{screen} for screen size is first used to weight the percent of material left on the screens by size

$$N_{screen} = \frac{\frac{r_{screen} + p_{screen}}{2}}{\frac{r_{\max screen} + p_{\max screen}}{2}} \quad \text{..... (2)}$$

where r_{screen} is the smallest piece size retained on a particular screen, and p_{screen} is the largest piece size possible for that screen. The denominator of the above equation represents the average of the smallest and largest piece size on the largest screen used. The percent of material left on each screen, w_{screen}, is calculated by

$$w_{screen} = 100\left(\frac{W_{screen}}{W_{sample}}\right),\ \% \quad \text{..... (3)}$$

where W_{screen} is the weight of material on the screen, and W_{sample} is the weight of the original sample. The factor s, which represents the average piece size after treatment, is calculated from the percent of material on each screen, w_{screen} and the normalizing factor N_{screen} by

$$s = \sum N_{screen} w_{screen}, \quad \% \qquad (4)$$

S, which represents the average piece size before treatment, is calculated by normalizing the weight of the whole sample and the average piece size of that sample to 100% by

$$S = 100\left(\frac{W_{sample} N_{\max screen}}{W_{sample}}\right) = 100\% \qquad (5)$$

Very few researchers have tried to quantify the friability of food. The friability of boneless turkey roasts was quantified by sensory panelists (Cash and Carlin, 1968), and friability has been investigated as a function of extruder flow rate for soy flour (Alexandridis, 1984). Friability of air dried and freeze dried chicken white meat has been investigated with a modified ASTM method for quantifying coal friability (Farkas and Singh, 1991). These studies both concluded that no difference in friability was measured as a function of experimental treatment, however this lack of difference might be due to small sample sizes.

Friability of precooked tuna is a factor in plant yield. Tuna are cooled to “firm up” the meat prior to cleaning and to allow workers to handle the fish without sustaining burns. During cooling some proteins reassociate and coagulate, and the fish flesh becomes less friable. The degree of tuna friability is directly related to plant yield, with more friable tuna negatively impact the “cleanability” of the fish. More friable fish will result in more fines generated and more potential for meat loss due to the inability of workers to separate fine particles of edible meat from dark meat and fish meal

components. Tuna friability due to heat treatment is not well established. A difference in tuna muscle friability might be established with precooked treatment because of the low connective tissue percentage of fish and the effect of heat on muscle proteins and ultrastructure.

2.5 Linear regression data modeling

Simple linear regression is a modeling technique in which one input is mapped to one output by the linear relationship –

$$Y = b_0 + b_1 X_1 + e \quad \text{..... (6)}$$

where *Y* is the dependent variable, *X* is the independent variable, $ß_0$ and $ß_1$ are coefficients, and *e* is the error of the system. Simple linear regression is very popular with researchers due to ease of implementation and easy visualization.

Simple linear regression is a special case of multiple linear regression. Multiple linear regression (MLR) is a technique in which several dependent variables are modeled as linearly dependent on independent factors. An advantage of multiple linear regression is the simplicity of using a simple statistical model that assumes no underlying physical phenomena.

Researchers have found that MLR correlated soak time and soak temperature with drain weight and texture of cowpeas (Taiwo et al., 1998). Other researchers noted that MLR outperformed neural networks when modeling sensory color quality of tomatoes and peaches, although the neural network models were less complex than the MLR model (Thai and Shewfelt, 1991). The disadvantage of MLR is that it fails to predict nonlinear behavior. Peters and others proved that surimi quality behaved nonlinearly, and MLR proved inadequate to model this behavior. These researchers

showed that neural networks were a better choice to model surimi quality (Peters et al., 1996).

2.5.1 Multiple linear regression example

A multiple linear regression model with three independent variables consists of the following terms –

$$Y = b_0 + b_1X_1 + b_2X_2 + b_3X_3 + b_4X_1X_2 + b_5X_1X_3 + b_6X_2X_3 + b_7X_1X_2X_3 + e \quad \text{... (7)}$$

where *ß$_n$ are model coefficients, X_1*, *X_2*, and *X_3* are independent variables, *Y* is the output matrix of dependent variables, and *e* is the standard error (Littell et al., 2002). Given the manipulated independent variable matrix *X* and the measured dependent variable matrix *Y*, the matrix of coefficients can be calculated by

$$b = \left(X^T X\right)^{-1} X^T Y \quad \text{..... (8)}$$

A full multiple linear regression model of the above system for four dependent variables is represented by –

$$\begin{bmatrix} y_1 \\ y_2 \\ y_3 \\ y_4 \end{bmatrix} = \begin{bmatrix} b_{1,0} & b_{1,1}x_1 & b_{1,2}x_2 & b_{1,3}x_3 & b_{1,4}x_1x_2 & b_{1,5}x_1x_3 & b_{1,6}x_2x_3 & b_{1,7}x_1x_2x_3 \\ b_{2,0} & b_{2,1}x_1 & b_{2,2}x_2 & b_{2,3}x_3 & b_{2,4}x_1x_2 & b_{2,5}x_1x_3 & b_{2,6}x_2x_3 & b_{2,7}x_1x_2x_3 \\ b_{3,0} & b_{3,1}x_1 & b_{3,2}x_2 & b_{3,3}x_3 & b_{3,4}x_1x_2 & b_{3,5}x_1x_3 & b_{3,6}x_2x_3 & b_{3,7}x_1x_2x_3 \\ b_{4,0} & b_{4,1}x_1 & b_{4,2}x_2 & b_{4,3}x_3 & b_{4,4}x_1x_2 & b_{4,5}x_1x_3 & b_{4,6}x_2x_3 & b_{4,7}x_1x_2x_3 \end{bmatrix} \quad \text{.. (9)}$$

Usually, not all terms of an MLR model are used. In fact, the fit of the model can be improved by dropping terms. Model efficacy is usually judged by the adjusted R^2 term, which is the numeric representation of how much variability is accounted for by the model. Terms are dropped according to increases in the adjusted R^2 of the MLR model.

2.6 Fuzzy logic

Fuzzy logic has become more popular with food processors (Giese, 1993). Conventional models are often challenged by defining food processes in precise mathematical, linear terms because of the nonlinearity of these systems. Conventional modeling often assumes, simplifies, or lumps parameters to mathematically model food processes. These tweaks may result in a model that does not accurately govern the actual system. Fuzzy logic is a good choice for food processing because it can accurately describe processes that are mathematically ill defined but can be described by empirical relationships (Singh and Ou-Yang, 1994).

In fuzzy logic relations, measured variables are converted to fuzzy variables. Linguistic rules are implemented using these fuzzy variables in IF THEN relations in conjunction with a fuzzy associative memory (FAM) table to dictate model output (Zhang and Litchfield, 1992). Food processing applications of fuzzy logic models and control systems include aseptic processing (Singh and Ou-Yang, 1994), grain drying, continuous fermentation, beer brewing, vegetable oil processing (Zhang et al., 1993; Zhang and Litchfield, 1992), and corn breakage during drying (Zhang and Litchfield, 1993). Fuzzy mathematics have also been applied to product development and comparison (Zhang and Litchfield, 1991), meat chilling and malt modification (Dohnal et al., 1993), sucrose inversion by modified yeast, simulation of extrusion bioreactor control, and lactic acid fermentation (Linko, 1988), and steak doneness (Unklesbay et al., 1988).

2.6.1 Fuzzy logic theory

Researchers have traditionally used probability theory to deal with uncertainties in mathematical modeling. These uncertainties are dealt with in probability theory as

random occurrences, however not all uncertainties are random. Randomness describes the uncertainty in the occurrence of the event, however fuzziness describes the ambiguity of the event (Ross, 1995). Figure 9a illustrates this point – the geometric shape shown is a rectangle, with width w and height h. When will this shape become a square? The answer is when w = h, or w/h = 1. When w/h << 1 or when w/h >> 1, the shape clearly becomes a rectangle, and when w/h approaches infinity, a line results. By these definitions, a membership function can be developed to describe the geometric set called a "square". Any mathematical function can be used to define a membership function of a fuzzy set. A Gaussian distribution for the ratio of width to height of a rectangle,

$$m_C\left(\frac{w}{h}\right) = e^{\left(-3\left(\frac{w}{h}-1\right)^2\right)} \quad \text{..... (10)}$$

offers a good approximation of the membership function for the fuzzy set "square", denoted S.

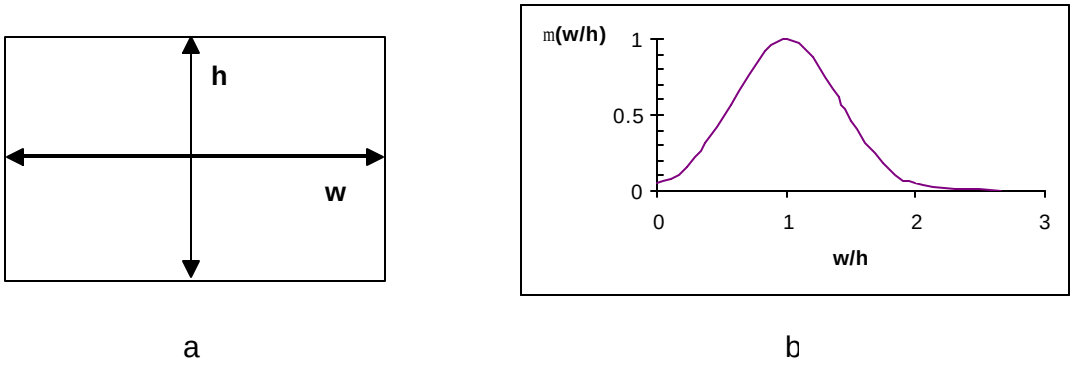

Figure 9 **The geometric shape (a) and Gaussian membership function (b) for a square.**

Figure 9b is a plot of the membership function given by the above equation. As the ratio of w/h goes to 1, the membership value approaches 1, and the membership of

that shape becomes that of a square. Conversely, when w/h goes to infinity or to 0 the shape becomes a line, and the membership for the ratio of w/h in the square set becomes smaller and smaller. Only shapes with w/h = 1 can truly be called a square, however shapes with memberships of 0.8 and 0.9 are almost square. Just like in the real world, close counts, and what constitutes a "square" shape is open for interpretation.

If a large number of generally square shapes were put into a bag, what is the probability of randomly selecting a square from the bag? To answer this question, the selector must first look at the two different types of uncertainty – ambiguity and randomness. Ambiguity can be addressed by assessing the fuzziness in the meaning of "square" by selecting the membership value above which the selector would be comfortable calling a shape a "square", for example a shape with a membership value of 0.9 or above would be considered a "square". Randomness can be addressed by the selector knowing the proportion of shapes in the bag that have a membership value equal to or greater than 0.9.

Fuzzy logic can be used to approximate nonlinear functions. Suppose the knowledge of a process could not be described by a mathematical relation, rather it was in the more complex form of measured inputs and observed outputs. Figure 10 is an example of this phenomenon, and shows observations made for the color change versus the amount of heat applied to a metal rod. The color change of the rod is distinct and predictable, however it does not appear to be easily modeled by traditional mathematics. By using fuzzy logic instead of traditional mathematics, a relationship can be developed from these measurements and observations and can be described by linguistic IF A then B rules.

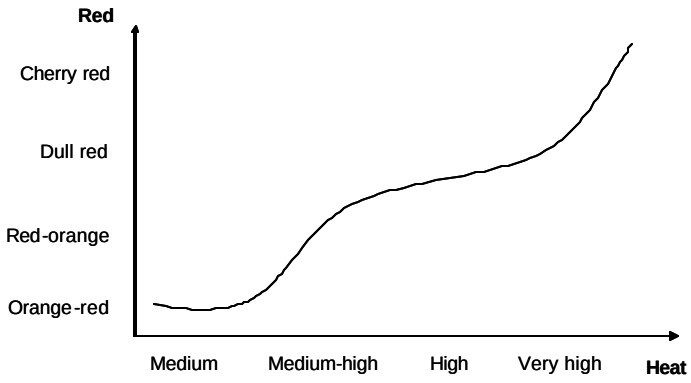

Figure 10 Nonlinear relationship of heat and red color for a metal rod.

Figure 11 shows how fuzzy logic can be used to map regions of the input space, in this example applied heat, to regions of the output space, in this case red color of the rod. We observe that when we apply "medium" heat", we get an "orange-red" color, when we apply "medium high" heat, we get "red-orange", and so on. These relationships can be represented by the following IF A THEN B rules –

IF medium heat THEN orange red color
IF medium-high heat THEN red-orange color
IF high heat THEN dull red color
IF very high heat THEN cherry red color

The inputs and outputs of Figure 11 are not points, rather they are regions of the variables in each universe. These regions represent the fuzziness by describing the variables linguistically, and can overlap, as do real world linguistic definitions. Likewise, the relationships between input and output variables can also be represented by regions, or fuzzy relations between the input and output variables of the system.

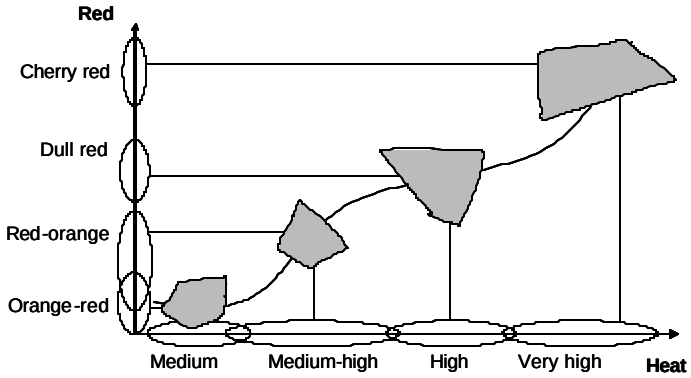

Figure 11 **A fuzzy nonlinear relation matching regions in the input space to regions in the output space for amount of heat applied to a rod and the resulting red color.**

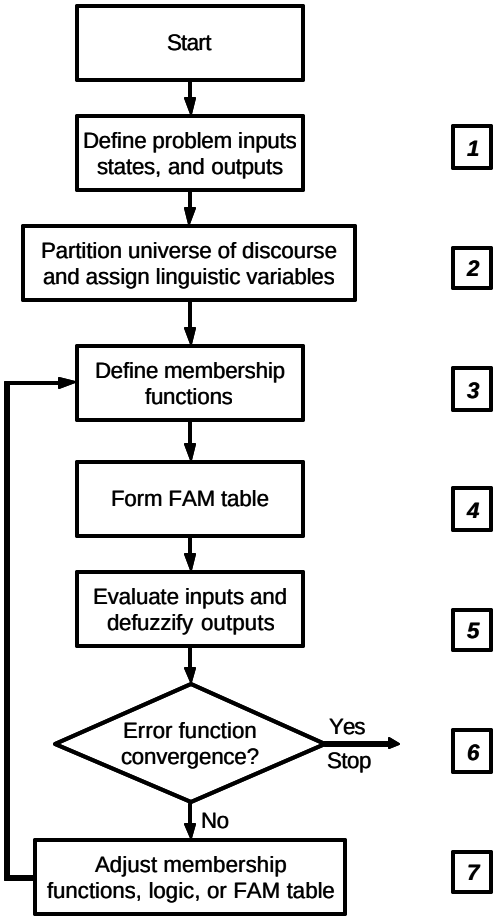

Figure 12 **Pseudocode for a fuzzy logic system, using an iterative procedure to adjust membership functions, logic, and FAM table.**

2.6.2 Fuzzy logic example

Figure 12 shows the pseudocode for modeling a problem using fuzzy logic. The following example refers to this figure, and is an illustration of how systems are modeled using fuzzy logic.

1. Problem to solve is

A small company dries sushi wrap, made of seaweed, prior to packaging. The process consists of batch drying in an oven sheets of seaweed arranged on flat trays. Sometimes the company has a big order, and runs the oven at maximum capacity. Other times the company only has a small order, and runs the oven at less than capacity. The oven is kept at a somewhat constant temperature, however adjustments need to be made when the oven temperature is out of the preset range, and for the size of the sushi wrap batch.

The problem is defined as how to relate oven temperature and sushi wrap batch size to how the operator should control the oven's thermostat.

Define inputs, states, and outputs

The inputs of the problem are sushi wrap batch size and oven temperature. The output is oven thermostat setting.

Let A = sushi wrap batch size, B = oven temperature, and Z = oven thermostat setting. A has states, or crisp values, of 1 (small), 2 (medium), and 3 (large). B has states 3 (cool), 4 (warm), and 5 (hot). Z has states 11 (turn hotter), 12 (leave alone), and 13 (turn colder).

2. Partition universe of discourse and assign linguistic variables

The universe of discourse is the set of values over which all variables range. Fuzzy subsets are defined as values around where the variables group.

Variable A universe of discourse is 0 = a = 3.5, fuzzy subsets are small (crisp value = 1, represented by x_1), medium (2, x_2), and large (3, x_{3a}) sushi wrap batches. Variable B universe of discourse is 2.5 = b = 5.5, fuzzy subsets are cool (3, x_{3b}), warm (4, x_4), and hot (5, x_5) oven temperatures. Variable Z universe of discourse is 10.5 = z = 13.5, fuzzy subsets are turn hotter (11, x_{11}), leave alone (12, x_{12}), and turn colder (13, x_{13}) thermostat adjustments.

3. Define membership functions for each fuzzy subset

For each variable, draw the membership functions that the fuzzy subset numbers represent. Any shape can be used as a membership function. In Figure 13, membership functions are triangles. From Figure 13, if A is 1 (small sushi wrap batch) it has a membership of 1 in the small variable. If A is 1.5, then it has 0.5 membership in small and 0.5 membership in medium categories.

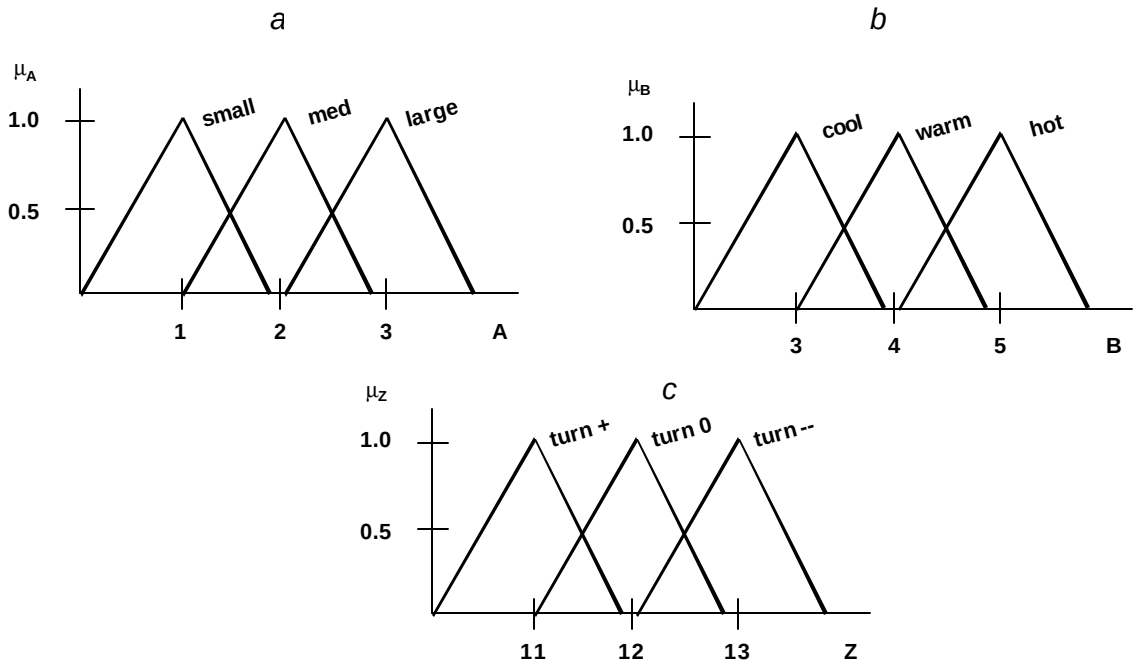

Figure 13 **Membership functions for sushi wrap batch size (*a*), oven temperature (*b*), and thermostat adjustment (*c*).**

4. Form fuzzy approximate reasoning (FAM table)

The general rule for this system, as determined by the oven operator, is written as

IF a AND b THEN z

From his familiarity with the system, the oven operator knows that specific conditions warrant actions on his part. He constructs a fuzzy associative memory (FAM) table from his experiences that relates sushi wrap batch size and oven temperature to thermostat adjustment (Figure 14).

a

A \ B	cool	warm	hot
small	+	0	--
med	0	0	0
large	+	0	--

b

A \ B	3	4	5
1	11	12	13
2	12	12	12
3	11	12	13

Figure 14 **FAM table showing fuzzy output (*a*) and crisp output (*b*) for thermostat setting.**

5. Fuzzify inputs via membership functions

The company gets a call from a customer who requests a sushi wrap shipment that is in between small and medium (A = 1.5). The plant manager tells the oven operator, who then looks to see the oven temperature, which is on the hot side of warm (B = 4.6). These system inputs are fuzzified by taking the crisp values for A and B and seeing what membership each value has in the defined fuzzy sets. In this example, A = 1.5 (medium-small sushi wrap batch size) has 0.5 membership in small and 0.5 membership in medium fuzzy sets. Likewise, B = 4.6 (hot side of warm) has 0.2 membership in warm and 0.6 membership in hot (Figure 15).

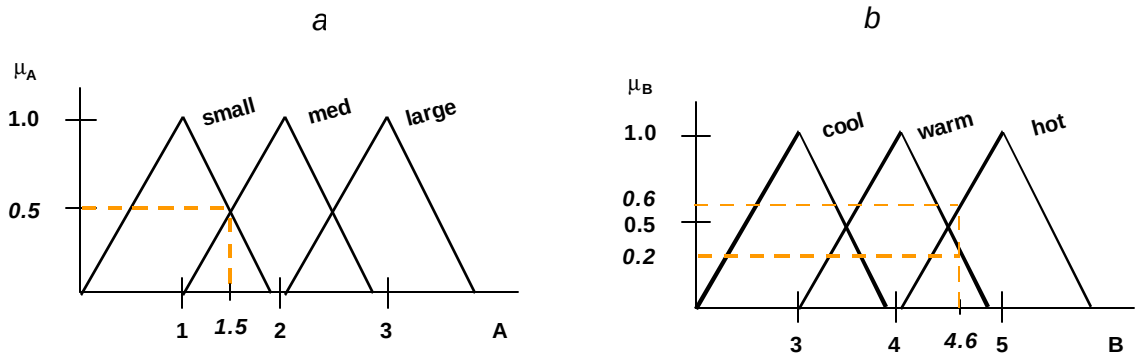

Figure 15 **Fuzzified inputs of sushi wrap batch size (a) and oven temperature (b).**

This can be related by the following notation –

$$\begin{matrix} m_{a1}(1.5) = 0.5,\ m_{a2}(1.5) = 0.5 \\ m_{b4}(4.6) = 0.2,\ m_{b5}(4.6) = 0.6 \end{matrix} \quad \text{..... (11)}$$

Alternately, a's membership in the defined fuzzy sets for sushi wrap batch size can be represented by the following fuzzy set notation -

$$\underset{\sim}{A} = \left\{ \frac{0.5}{x_1} + \frac{0.5}{x_2} + \frac{0}{x_{3a}} \right\} \quad \text{..... (12)}$$

where input a has 0.5 membership in the small (x_1) fuzzy set, 0.5 membership in the medium (x_2) fuzzy set, and 0 membership in the large (x_{3a}) fuzzy set. Likewise, the membership of input b in the B fuzzy sets are represented by

$$\underset{\sim}{B} = \left\{ \frac{0}{x_{3b}} + \frac{0.2}{x_4} + \frac{0.6}{x_5} \right\} \quad \text{..... (13)}$$

The fuzzy relation between the two input variables can be represented by Mamdami's implication, or the fuzzy cross product of the fuzzy sets A and B.

$$\underset{\sim}{Z} = \underset{\sim}{A} \times \underset{\sim}{B} = \min(x_a, x_b) = \begin{matrix} & x_{3b} & x_4 & x_5 \\ x_1 & 0 & 0.2 & 0.5 \\ x_2 & 0 & 0.2 & 0.5 \\ x_{3a} & 0 & 0 & 0 \end{matrix} \quad \text{..... (14)}$$

Apply fuzzy approximate reasoning (FAM table)

The FAM table can be used to map input values to output responses, and can also be used with Mamdami's implication (Figure 16).

FAM table logic	Mamdami's implication logic
IF (A = small) AND (B = warm) THEN (Z = leave alone)	min(0.5,0.2) = 0.2
IF (A = small) AND (B = hot) THEN (Z = turn cooler)	min(0.5,0.6) = 0.5
IF (A = med) AND (B = warm) THEN (Z = leave alone)	min(0.5,0.2) = 0.2
IF (A = med) AND (B = hot) THEN (Z = leave alone)	min(0.5,0.6) = 0.5

A \ B	cool	warm	hot
small	+	0	–
med	0	0	0
large	+	0	–

Figure 16 **FAM table logic and corresponding Mamdami's implication logic, and FAM table showing thermostat adjustment for sushi wrap batch size (A) and oven temperature (B).**

Aggregate fuzzy outputs recommended by rules

From the FAM table output of three thermostat "leave alone" and one "turn cooler" responses, one would guess that the fuzzy logic output for the a and b inputs would be to "turn a little cooler". From the above Mamdami's implication, and max/min composition of the rules, the fuzzy outputs were 0.2 and 0.5. Mapping these two outputs

onto the thermostat adjustment gives a shape made up of two trapezoids, one that intersects the leave alone and one that intersects the turn cooler membership functions of the fuzzified output. To de-fuzzify this output, the centroid of the conglomerated outputs is taken and translated into a crisp value.

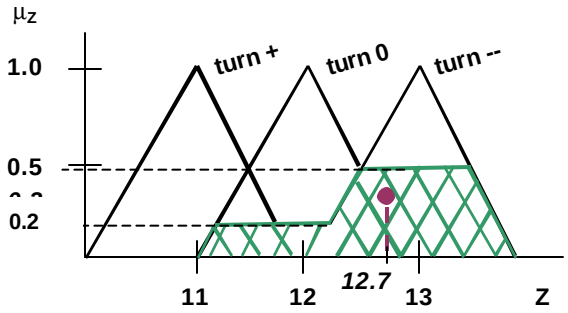

Figure 17 Defuzzification of output from system.

The defuzzified value that the operator receives is 12.7, or turn the thermostat down a little.

6. Error convergence

The operator checks to see if the adjustment to the oven thermostat resulted in the correct action, in this case cooling off of the oven temperature. If his action had the intended effect, then all is well.

7. Adjustment of the membership functions, logic, or FAM table

If the action did not result in a satisfactory result, the operator has the option of adjusting the membership functions, the logic, or the FAM table to achieve better results next time. For a function mapping problem using fuzzy logic, these corrections would be performed iteratively using training set data and need for model term adjustments would

be judged by a set error metric, such as Root Mean Square Error (RMSE). A test set would then be used to determine the goodness of fit of the model.

2.7 Neural networks

Neural networks mimic the natural learning pattern of the human brain. This approach relates inputs to corresponding outputs via a set on interconnected computing elements called neurons. The network learns by changing the importance of the connections between neurons, so that a specific input fires a certain pattern of neurons to elicit the matching output. The network is not programmed to give the correct answer initially, rather the network learns by example which output goes with what inputs (Simutis et al., 1993). A properly trained network does not memorize, rather it uses educated guesses to infer the correct output given an unseen input. Neural networks are most commonly used to solve classification and function approximation problems, but are also used for data compression, feature extraction, and statistical clustering problems (Hammerstrom, 1993).

Neural networks have been used in food processing to predict alcohol formation in production scale beer brewing (Simitus et al. 1993), computing equivalent lethality processes given temperatures, can size, thermal diffusivity, and other kinetic parameters (Sablani et al., 1995), in poultry carcass inspection (Chen et al., 1998), and other vision systems (Zhang and Litchfield, 1992). They have also been used to estimate bioprocess variables and state predictions (Linko and Zhu, 1991), identify processes and control extrusion (Eerikainen et al., 1994), predict milk shelf life (Vallejo-Cordoba et al., 1995), forecast bread loaf volume after baking (Horimoto et al., 1995), predict temperature, moisture, and fat of slab shaped foods and meatballs during deep fat frying (Mittal and Zhang, 2000a; Mittal and Zhang, 2001), and model temperature and moisture during

thermal processing of frankfurters (Mittal and Zhang, 2000b). A neural network model was superior to fuzzy logic and multiple linear regression models for predicting the biological activity surface that described the inhibiting effects of benzoic and cinnamic acids on *Listeria monocytogenes* (Ramos-Nino et al., 1997). A neural network model also was superior to both fuzzy logic and first order kinetic models for predicting texture changes of peas cooked a long time (Xie et al., 1998).

2.7.1 Neural network neurons

A neural network is made up of neurons. A single neuron is pictured in Figure 18. Neurons work when an input *p* is multiplied by a scalar weight term *w*, and the bias (usually set at one) is multiplied by a scalar weight term *b*. Both *wp* and *b1* are summed to form *n*, the input to the transfer function *f* of the neuron. The output *a* of the neuron depends on how the transfer function maps the input onto output space. For example, if the neuron has a linear transfer function, the output of the neuron will be

$a = f(n) = f(wp + b) = n = (wp + b)$ ..... (15)

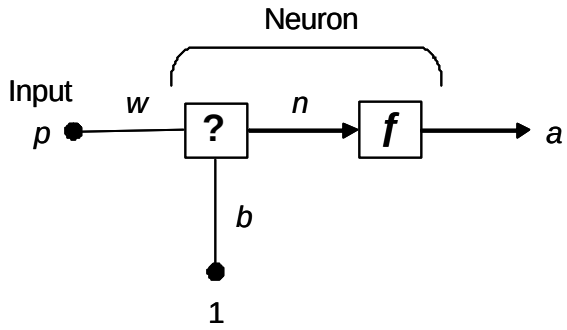

Figure 18 **Single neuron consisting of input *p*, weight *w*, bias *b*, and output *a* (adapted from Hagan et al., 1996).**

For the single neuron shown in Figure 18, both *w* and *b* are adjustable scalars, and weight, or influence, the importance of input *p*. These weight values represent the connection strength between nodes. The bias node can be thought of as a threshold value that must be reached before any neuron activity can take place.

The transfer function *f* can be any function that relates an input value to an output value. Typical transfer functions used in neural networks are pictured in Figure 19, and include the hard limit which sets neuron output *a* to 0 if *n* is less than 0 and 1 if *n* is greater or equal to 0, the linear, which sets output *a* of neuron equal to it's input *n*, and the log-sigmoid, which relates the neuron output *a* to input *n* by the equation

$$a = \frac{1}{1+e^{-n}} \quad \text{..... (16)}$$

Hard limit transfer functions are typically used when threshold logic, or a 0 or 1 output, is needed, as in classical logic. Linear transfer functions are used when a direct mapping is needed. Log sigmoid transfer functions are used to transform inputs into nonlinear outputs. Log sigmoid transfer functions are commonly used in networks that model nonlinear behavior, are differentiable, and also squash the neuron output within the range of 0 to 1.

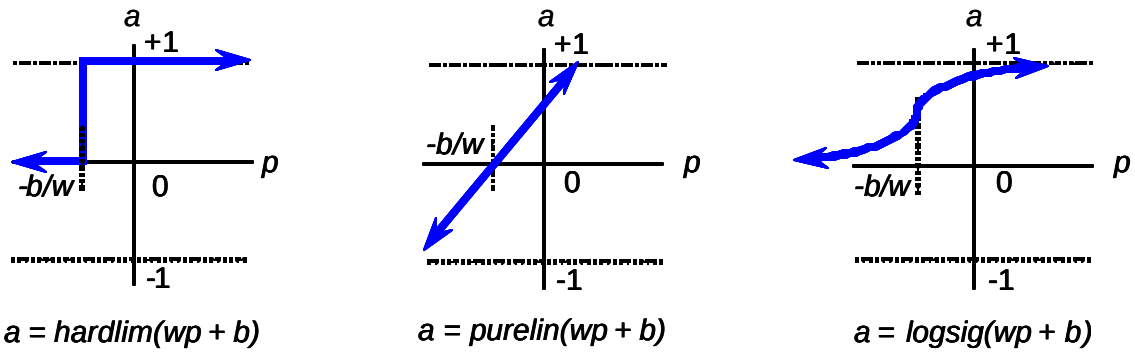

Figure 19 **Hard limit (hardlim), pure linear (purelin), and log sigmoid (logsig) transfer functions (adapted from Hagan et al., 1996).**

2.7.2 Neural network architecture

Neural networks can be engineered in a variety of architectures. Feed forward architecture is commonly used, which consist of adjacent layers of nodes with complete interconnection of nodes between adjacent layers. No nodes are connected within a layer (Figure 20). The input layer to the network has input terminals, and feeds examples, or training patterns, to the network. The output layer is the final layer fed by the network, and gives the results of the network processing on the inputted examples. Between the input and output layers are one or more hidden layers. The hidden layers only connection to the outside world is by inputs from the input layer, and only influence is the output layer. For a network with multiple hidden layers, each layer node sums all inputs from nodes in the preceding layer and passes this signal through neuron transfer functions to every node in the following layer. Neural networks are used for many types of problems, including pattern recognition and function approximation. A neural network that has three layers, input, hidden with nonlinear neural transfer functions, and output with linear transfer functions can approximate any function (Hagan et al., 1996).

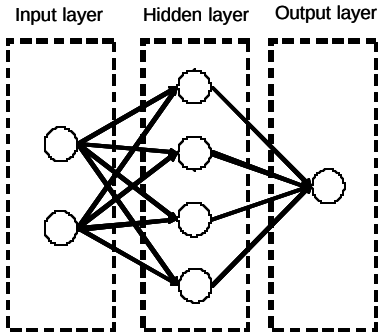

Figure 20 **Neural network consisting of an input layer of two nodes, a hidden layer of four nodes, and an output layer of one node. Bias nodes are not shown.**

2.7.3 How neural networks find solutions

Neural nets are trained to give a specific response given an input set. This action can be described as a search for the ideal set of weights in the network that represent the solution set to a specific problem with defined inputs and outputs. The learning process for a neural net can be described as a search in multidimensional weight space for this solution set.

An analogy to multidimensional weight space can be described as flattening the multidimensional weight space, thereby creating a two dimensional plane, or the multidimensional weight plane. A measure of the network's error output can be mapped over this weight plane, and is called the error topology for a problem. The solution space is described by a deep valley, also referred to as the global minimum of the problem. The path that the neural network takes to find the global minimum is analogous to the error metric shown with training epoch, as the error metric chosen by the researcher defines the error topology in the multidimensional weight space. Figure 21 shows a representation of error versus weight space in graphical form. This figure was generated by graphing the nonlinear function

$$f(x,y) = 3(1-x)^2 e^{-x^2-(y+1)^2} - 10\left(\frac{x}{5} - x^3 - y^5\right)e^{-x^2-y^2} - \frac{1}{3}e^{-(x+1)^2-y^2} \quad \text{..... (17)}$$

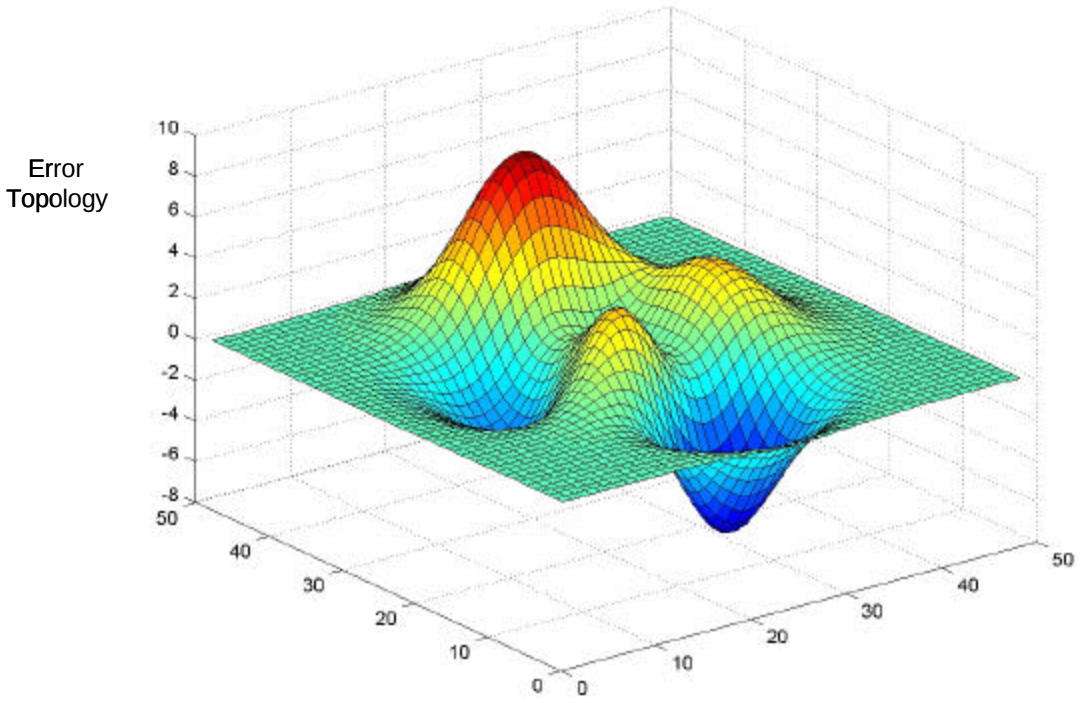

Figure 21 **A representation of the multidimensional weight plane for a hypothetical problem with a global minimum solution.**

2.7.4 Backpropagation

Neural networks that use backpropagation as their learning algorithm are common for function approximation problems. This algorithm is a popular method for training neural networks because it is widely applicable to a multitude of problems and it generalizes well. Backpropagation neural networks are constructed with at least three layers. The input layer is passive, and receives input from the problem, and the number of input nodes equals the number of input variables. The second, or hidden layer, usually has nonlinear transfer functions due to their ability to model nonlinear functions. The output layer typically contains linear neurons to map network responses because of their capacity to express any value given by the sum of the hidden layer neuron outputs.

The backpropagation algorithm chooses a path through the error topology for the problem by iteratively predicting and choosing the direction of the greatest negative slope at every point on the path. Backpropagation is a supervised learning method, as network outputs are compared to a known answer during training, and the error between the known answer, or target, and the network output is fed back through the network, thereby altering connection weights so as to minimize this error (Hammerstrom, 1993). Backpropagation requires that transfer functions be differentiable to propagate backwards error to change weights and bias matrices.

Backpropagation originated from the Gradient Descent method for traversing a surface. The Gradient Descent method chooses a route down the error topology by predicting the direction of maximum gradient at any point by specifying the weight changes required for each weight *w* for the network to move in the direction of maximum error gradient, or

$$\Delta w \propto \frac{dE}{dw} \quad \text{..... (18)}$$

where *E* is the error of the network and *w* represents a weight in the network. The maximum amount of weight increase or decrease will be prescribed for the weight dimension that shows the greatest error gradient at that point in training.

The Widrow-Hoff rule is an approximate steepest descent algorithm for which mean square error is used as the performance index. This algorithm uses gradient descent to train single layer networks, and gives the absolute weight change ? w_{ij} for any weight change w_{ij} between nodes *i* and *j* by

$$\Delta w_{ij} = hO_i d_j \quad \text{..... (19)}$$

where d_j is the backpropagated error of node *j*, O_i is the output of node *i*, and *?* is the learning rate. The learning rate *?* defines the step sizes the algorithm takes when

descending the error surface. If the learning rate is too small, the time for finding a solution will be long, but too large a step size might cause the network to oscillate around a solution or give a solution that is not generalized for the given problem.

The Generalized Delta Rule generalizes the Widrow-Hoff rule for multilayered networks. The error measure of a node in a hidden layer is a function of outputs of nodes of following layers. Error measurements are propagated backwards through the network, layer by layer, in the opposite direction of network inputs by the equation

$$\Delta w = -h \frac{dE}{dw} \quad \text{..... (20)}$$

Backpropagation learns through the generalized delta rule, in which weights are changed in order to minimize the error of the network. Error is defined as the difference between the network outputs and targets, and is defined in backpropagation algorithms as Mean Square Error (MSE)

$$e = \sum_{i=1}^{N_{train}} \left\{ \frac{1}{N} \sum_{j=1}^{J} \left(t_{ij} - a_{ij} \right)^2 \right\} \quad \text{..... (21)}$$

where *i* is the number of training patterns presented to the network, *j* is the number of inputs in a network, *t* is the target, and *a* is the neural network output (Hagan et al., 1996; Haykin, 1999).

2.7.5 Backpropagation neural network example

Figure 22 shows the pseudocode for a neural network that employs backpropagation as the learning algorithm. An example of one iteration through the backpropagation algorithm follows this figure.

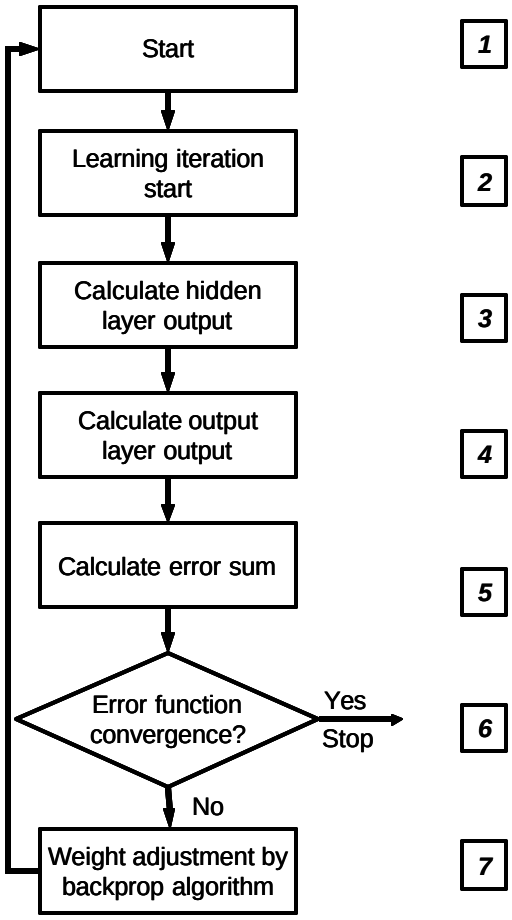

Figure 22 **Pseudocode for neural network with backpropagation algorithm, using early stopping technique.**

Figure 23 shows the details of a one input layer, two log sigmoid neuron hidden layer, and one linear output layer neuron network for the example that follows.

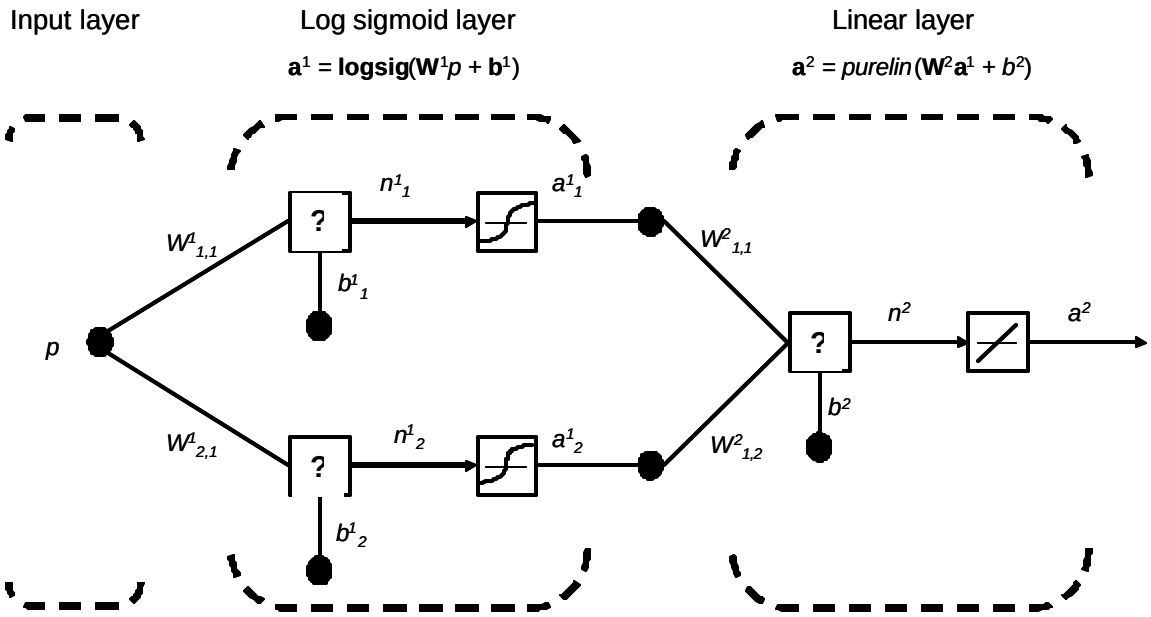

Figure 23 **Neural network example with one input, two log sigmoid neurons in one hidden layer, and one linear neuron in the output layer (adapted from Hagan et al., 1996).**

For Figure 23 the following notation applies –

- p = network input
- $\mathbf{W}^1$ = weight matrix of layer 1, for this example includes $w^1_{1,1}$ (weight in layer 1, to neuron 2 in layer 1, from input 1), and $w^1_{2,1}$.
- $\mathbf{W}^2$ = weight matrix of layer 2, for this example includes $w^2_{1,1}$ (weight in layer 2, to neuron 1 in layer 2, from neuron 1 in layer 1), and $w^2_{1,2}$.
- $\mathbf{b}^1$ = bias matrix of layer 1, for this example includes b^1_1 (bias in layer 1, to neuron 1) and b^1_2.
- $\mathbf{b}^2$ = bias matrix of layer 2, for this example is b^2 (bias in layer 2).
- n^1_1, n^1_2, and n^2 = sums of inputs to individual neurons, according to $n = wp + b(1)$.
- a^1_1, a^1_2, and a^2 = outputs of neurons. For hidden layer, log sigmoid neuron, output is $a = \frac{1}{1+e^{-n}}$. For output layer, linear neuron, $a = n$.

From the flowchart of Figure 22, the following steps are used by the backpropagation network shown in Figure 23 –

1. Problem to solve is

$$g(p) = 1 + \cos(\frac{p}{2} p)$$, for -2 = *p* = 2 ..... (22)

2. Initialize all weights and biases –

$$W^1(0) = \begin{bmatrix} -0.33 \\ -0.40 \end{bmatrix}$$ ..... (23)

$$b^1(0) = \begin{bmatrix} 0.51 \\ 0.25 \end{bmatrix}$$ ..... (24)

$$W^2(0) = \begin{bmatrix} 0.05 & 0.35 \end{bmatrix}$$ ..... (25)

$$b^2(0) = \begin{bmatrix} -0.41 \end{bmatrix}$$ ..... (26)

3. Calculate hidden layer output –

Input $a^0 = p(0) = 2$,

$$a^1 = f^1(W^1 a^0 + b^1) = \log sig\left(\begin{bmatrix} -0.33 \\ -0.40 \end{bmatrix}[2] + \begin{bmatrix} 0.51 \\ 0.25 \end{bmatrix}[1]\right)$$

$$a^1 = \log sig\left(\begin{bmatrix} -0.15 \\ -0.55 \end{bmatrix}\right) = \begin{bmatrix} \frac{1}{1+e^{-(-0.15)}} \\ \frac{1}{1+e_{-(-0.55)}} \end{bmatrix} = \begin{bmatrix} 0.4626 \\ 0.3659 \end{bmatrix}$$ ..... (27)

4. Calculate output layer output –

$$a^2 = f^2(W^2 a^1 + b^2) = purelin\left(\begin{bmatrix} 0.05 & 0.35 \end{bmatrix} \begin{bmatrix} 0.4626 \\ 0.3659 \end{bmatrix} + \begin{bmatrix} -0.41 \end{bmatrix} \begin{bmatrix} 1 \end{bmatrix} \right) \quad \text{..... (28)}$$

$$a^2 = purelin(\begin{bmatrix} 0.1512 \end{bmatrix} + \begin{bmatrix} -0.41 \end{bmatrix}) = \begin{bmatrix} -0.2588 \end{bmatrix}$$

5. Calculate error sum –

Error = *e*, target = *t*

$$e = t - a$$

$$t = 1 + \cos\left(\frac{2p}{2}\right) = 0 \quad \text{..... (29)}$$

$$e = 0 - (-0.2588) = 0.2588$$

6. Error function convergence check

Error limit is 0.001

Error calculated by mean square error is

$$MSE = (t-a)^2 = (0 - 0.2588)^2 = 0.0670$$

$$0.0670 > 0.001, \ \therefore \ MSE > target\ error \quad \text{..... (30)}$$

MSE greater than target, therefore continue with iteration.

7. Backpropagate error through the network

Derivatives of hidden and output layer neurons –

$$f'^1(n) = \frac{d}{dn}\left(\frac{1}{1+e^{-n}}\right) = \frac{e^{-n}}{\left(1+e^{-n}\right)^2}$$

$$f'^1(n) = 1 - \frac{1}{\left(1+e^{-n}\right)}\left(\frac{1}{1+e^{-n}}\right) = \left(1-a^1\right)a^1 \quad \text{..... (31)}$$

$$f'^2(n) = \frac{d}{dn}(n) = 1$$

Calculate sensitivities to adjust weights and biases –

$$s^2 = -2F'^2(n^2)e = -2[1](0.2588) = [-0.5176]$$

$$s^1 = F'^1(n^1)(W^2)^T s^2 = \begin{bmatrix} (1-a^1)(a^1) & 0 \\ 0 & (1-a^2)(a^2) \end{bmatrix}(W^2)^T s^2$$

$$s^1 = \begin{bmatrix} (1-0.5374)(0.5374) & 0 \\ 0 & (1-0.6341)(0.6341) \end{bmatrix}\begin{bmatrix} 0.05 \\ 0.35 \end{bmatrix}[-0.5176] = \quad \text{..... (32)}$$

$$\begin{bmatrix} -0.0064 \\ -0.0420 \end{bmatrix}$$

Update weights, using learning rate a = 0.2

$$W^2(1) = W^2(0) - as^2(a^1)^T = [0.05 \quad 0.35] - 0.2(-0.5176)\begin{bmatrix} 0.4626 \\ 0.3659 \end{bmatrix} =$$

$$[0.0979 \quad 0.3879]$$

$$b^2(1) = b^2(0) - as^2 = [-0.41] - 0.2[-0.5176] = -0.3065 \quad \text{..... (33)}$$

$$W^1(1) = W^1(0) - as^1(a^0)^T = \begin{bmatrix} -0.33 \\ -0.40 \end{bmatrix} - 0.2\begin{bmatrix} -0.0064 \\ -0.0420 \end{bmatrix}[2] = \begin{bmatrix} -0.3274 \\ -0.3832 \end{bmatrix}$$

$$b^1(1) = b1(0) - as^1 = \begin{bmatrix} 0.51 \\ 0.25 \end{bmatrix} - 0.2\begin{bmatrix} -0.0064 \\ -0.0420 \end{bmatrix} = \begin{bmatrix} 0.5113 \\ 0.2584 \end{bmatrix}$$

8. Go back to step 1, select another input and target set for estimation by the neural network equipped with new weights and biases.

2.7.6 Backpropagation enhancements

The backpropagation algorithm is susceptible to local minima embedded in the error surface which increases the time needed for the algorithm to find a global solution. In addition, the curvature of the error space can vary widely between regions of the defined space which can make the solution search oscillate greatly. To overcome these weaknesses, several techniques are used to enhance backpropagation learning.

As has been presented, the learning rate constant *a* is the step length that the search algorithm takes per iteration. This constant is an enhancement to

backpropagation, in that the learning is controlled in a stepwise manner. Learning rates affect the speed at which the network learns. A learning rate that is too small will take a long time to converge to a solution. A learning rate too large will cause network error to oscillate around the solution, and if this constant is very large, will cause increased oscillation and divergence of the network to a solution (Hagan et al., 1996). An adaptive learning rate is one in which the learning rate is not constant, and adapts to the error surface of the problem by measuring the performance of the algorithm. There are many techniques used for varying the learning rate, however one that illustrates this technique in a simple manner has been described by Vogl et al. (1988).

1) If the squared error (MSE) increases by more than a set percentage (usually one to five percent) after a weight update, the weight update is discarded, the learning rate is multiplied by a factor (usually between zero and one), and the momentum coefficient is set to zero. This causes the network to go back, “slow down”, and reuse weights found to be adequate for that particular point in error space to find a better descent path.
2) If the MSE decreases after a weight update, the weight update is kept and the learning rate is multiplied by a factor greater than one. If momentum was previously set to zero, it is reset to its original value. This causes the network to “speed up” through that particular region of error space.
3) If the MSE increases by less than some set percentage (again, usually one to five percent) after a weight update, then the weights are kept but the learning rate and the momentum coefficient are unchanged. This causes the network to investigate that particular region of error space for a better descent path.

Momentum is another technique used to enhance the backpropagation algorithm. Momentum operates like a low pass filter, and smoothes oscillations in the error

trajectory. Momentum makes the trajectory of the search algorithm continue in the same direction it was going, and accelerates convergence to a solution when the error trajectory is moving in a consistent direction. Larger values of momentum make the trajectory continue along the direction. Momentum lessens backpropagation's sensitivity to small details in the error surface, and helps the algorithm out of local minima.

To apply momentum to the backpropagation algorithm, a low pass filter is first presented –

$$\begin{aligned} &y(k) = g\,y(k-1) + (1-g)w(k),\ given \\ &w(k) = \ filter\ input \\ &y(k) = \ filter\ output \\ &g = momentum\,coefficient,\ 0 \le g < 1 \end{aligned} \quad \text{..... (34)}$$

The analog for this low pass filter in a backpropagation algorithm to update weights and biases would be –

$$\begin{aligned} &\Delta W^m(k) = g\Delta W^m(k-1) - (1-g)as^m(a^{m-1})^T \\ &\Delta b^m(k) = g\Delta b^m(k-1) - (1-g)as^m \end{aligned} \quad \text{..... (35)}$$

The momentum term is always between 0 and 1. Momentum values closer to 1 makes a network slower to respond to changes in the error surface, however error oscillations are reduced. An additional benefit to using this technique is that a network can learn with a larger learning rate when using momentum and still maintain algorithm stability. The momentum term tends to dampen the response of the network to small changes in the error surface (Bishop, 1997).

Batch training is another technique used to enhance backpropagation learning. Sequential training, or presenting one input/output pair out of a set of training examples and then updating weights and biases, can cause the error to oscillate due to rapidly changing error gradients. Batch training accumulates the errors over the whole training set and only updates the weights and biases after the whole training set has been

presented. The error gradients for each example are averaged together over the whole training set, which makes for a more accurate estimate of the error gradient (Demuth and Beale, 2002).

Input and output scaling is another technique that can enhance backpropagation learning. In theory, neural networks can estimate any nonlinear function when equipped with log sigmoid neurons in hidden layers and linear neurons in output layers. In practice, if some inputs and outputs are numerically much greater than others, they can dominate the effects of smaller inputs and outputs by inordinately influencing weight and bias changes. Normalization of input and output data to within the same range of values, say between 0 and 1, will remove the influence of numerically large data from overshadowing other inputs and outputs of the neural network (Kennedy et al., 1995).

2.8 REFERENCES

Alexandridis, N.A., 1984. Effects of process variables on the physical and chemical properties of extrusion cooked soy flour. Ph. D. dissertation, Virginia Polytechnical Institute and State University, Blacksburg, Virginia.

ASTM, 1994. Standard test method for tumbler test for coal. American Society for Testing and Materials, D 441 – 86.

Barbut, S. and Mittal, G.S., 1990. Effects of heating rate on meat batter stability, texture and gelation. Journal of Food Science, 55 (2), 334-337.

Bell, J.W., Farkas, B.E., Hale, S.A., and Lanier, T.C., 2001. Effect of thermal treatment on moisture transport during steam cooking of Skipjack tuna (*Katsuwonas pelamis*). Journal of Food Science, 66 (2), 307-313.

Bell, J. 1999. Unpublished data. North Carolina State University, Department of Food Science, Raleigh, North Carolina.

Bell, J. 1998. Personal communication. North Carolina State University, Dept. of Food Science, Raleigh, North Carolina.

Bertola, N.C., Bevilacqua, A.E., and Zaritzky, N.E., 1994. Heat treatment effect on texture changes and thermal denaturation of proteins in beef muscle. Journal of Food Processing and Preservation, 18, 31-46.

Bester, C., 2003. Distribution of Skipjack tuna from NOAA location data. Florida Museum of Natural History. http://www.flmnh.ufl.edu/fish/Gallery/Descript/SkipjackTuna/SkipjackTuna.html.

Bhattacharya, S., Choudhury, G.S., and Studebaker, S., 1993. Hydrothermal processing of Pacific chum salmon: effects on texture and in-vitro digestibility. Journal of Food Quality, 16, 243-251.

Bishop, C.M., 1997. Neural Networks for Pattern Recognition. Bookcraft Ltd., Midsomer Norton, Avon, England.

Bourne, M.C. and Comstock, S.H., 1981. Effect of degree of compression on texture profile parameters. Journal of Texture Studies, 12, 201-216.

Bourne, M.C., 1996. In support of methodology clarification. Journal of Texture Studies, 27, vii.

Bourne, M.C., 1982. Food texture and viscosity: concept and measurement. Academic Press, New York, NY.

Bourne, M.C., 1978. Texture profile analysis. Food Technology, July 62-66, 72.

Bouton, P.E. and Harris, P.V., 1972. The effects of cooking temperature and time on some mechanical properties of meat. Journal of Food Science, 37, 140-144.

Bouton, P.E., Harris, P.V., and Shorthose, W.R., 1975. Possible relationships between shear, tensile, and adhesion properties of meat and meat structure. Journal of Texture Studies, 6 (3), 297-314.

Cash, D. B., and Carlin, A. F. 1968. Quality of frozen boneless turkey roasts precooked to different internal temperatures. Food Technology, v 22 Nov 1968, p 143-146.

Chen, Y.R., Park, B., Huffman, R.W., and Nguyen, M., 1998. Classification of on-line poultry carcasses with backpropagation neural networks. Journal of Food Process Engineering, 21 (1), 33-48.

Code of Federal Regulations, 1998. Canned tuna; Title 21, Volume 2, Parts 100 to 169. Food and Drug Administration, Department of Health and Human Services, US Government. 21CFR161.190, p. 489-496.

Collette, B.B. and Nauen, C.E., 1983. FAO Species Catalog, Vol. 2: Scombrids of the world. An annotated and illustrated catalog of tunas, mackerels, bonitos, and related species known to date. FAO Fisheries Synopsis (125), vol. 2, 137 p.

Demuth, H. and Beale, M., 2002. Neural Network Toolbox for use with MatLab, Users guide, version 4, release 13. The MathWorks, Natick, MA.

Dohnal, M., Vystrcil, J., Dohnalova, J., Marecek, K., Kvapilik, M., and Bures, P., 1993. Fuzzy food engineering. Journal of Food Engineering, 19, 171-201.

Duizer, L.M., Gullett, E.A., and Findlay, C.J., 1996. The relationship between sensory time-intensity, physiological electromyography, and instrumental texture profile analysis measurements of beef tenderness. Meat Science, 42 (2), 215-224.

Dunajski, E., 1979. Texture of fish muscle. Journal of Texture Studies, 10, 301-318.

Eerikainen, T., Zhu, Y.H., and Linko, P., 1994. Neural networks in extrusion process identification and control. Food Control, 5 (2), 111-119.

Farkas, B.E., and Singh, R.P. 1991. Physical properties of air-dried and freeze dried chicken white meat. Journal of Food Science, v 56 no 3 p 611-615.

Farkas, B.E., Stewart, H.E., Bell, J.B., Zhang, J., and Webb, E.L. 1997. Unpublished data. North Carolina State University, Raleigh, North Carolina.

Finch, R., 1963. The tuna industry. Ch 7 in *Industrial Fishery Technology*, M. E. Stansby and J. A. Dassow, Eds. Reinhold Publishing Corp., New York.

Fiszman, S.M., Pons, M., and Damasio, M.H., 1998. New parameters for instrumental texture profile analysis: instantaneous and retarded recoverable springiness. Journal of Texture Studies, 29, 499-508.

Foegeding, E.A. and Lanier, T.C., 1996. Characteristics of edible muscle tissues. In Food Chemistry, Fennema, O. (ed). Marcel Dekker, New York, NY.

Friedman, H.H., Whitney, J.E., and Szczesniak, A.S., 1963. The Texturometer – a new instrument for objective texture measurement. Journal of Food Science, 28, 390-396.

Gardieff, S. 2003. Biological profiles: Skipjack tuna. Florida Museum of Natural History. http://www.flmnh.ufl.edu/fish/Gallery/Descript/SkipjackTuna/SkipjackTuna.html.

Giese, J. 1993. Processing trends: sensors, safety, and fuzzy logic. Food Technology Sept. 1993: 144.

Greaser, M.L., 1991. An overview of the muscle cell cytoskeleton. 44th Annual Reciprocal Meats Conference Proceedings, June 9-12, 1991, Kansas State University, Manhattan, KS, 44, 1-5.

Hagan, M.T., Demuth, H.B., Beale, M., 1996. Neural Network Design. PWS Publishing Co., Boston, MA.

Hamann, D.D. and Lanier, T.C., 1986. Instrumental methods for predicting seafood sensory texture quality. In Seafood Quality Determination, Kramer, D.E. and Liston, J., (eds). Proceedings of an international symposium coordinated by the University of Alaska Sea Grant College Program, Anchorage, Alaska, 10-14 Nov 1986. Elsevier Science Publishers, B.V., Amsterdam, the Netherlands.

Hammerstrom, D., 1993. Neural networks at work. IEEE Spectrum, June 1993, 26-32.

Harris, P.V., 1976. Structural and other aspects of meat tenderness. Journal of Texture Studies, 2, 49-63.

Haykin, S., 1999. Neural Networks: a Comprehensive Foundation, 2nd ed. Prentice Hall, Upper Saddle River, NJ.

Hearne, L.E., Penfield, M.P., Goertz, G.E., 1978. Heating effects on bovine semitendinosus: shear, muscle fibre measurements and cooking losses. Journal of Food Science, 43, 10-12, 21.

Honikel, K.O. and Hamm, R., 1994. Measurement of water-holding capacity and juiciness. In Quality Attributes and their Measurement in Meat, Poultry, and Fish Products, Advances in Meat Research, Volume 9, Pearson, A.M. and Dutson, T.R. (eds). AVI Publishing Company, Westport, CT.

Horimoto, Y., Durance, T., Nakai, S., and Lukow, O.M., 1995. Neural networks versus principal component regression for prediction of wheat flour loaf volume in baking tests. Journal of Food Science, 60 (3), 429-433.

Horner, W. F. A., 1992. Canning fish and fish products. Ch 5 in *Fish Processing Technology*, G. M. Hall, Ed. Blackie Academic and Professional, published in North American by VCH Publishers, New York, NY.

Hyldig G. and Nielsen, D., 2001. A review of sensory and instrumental methods used to evaluate the texture of fish muscle. Journal of Texture Studies, 32, 219-242.

Jones, S.B., Carrol, R.J., Cavanaugh, J.R., 1977. Structural changes in heated bovine muscle: a scanning electron microscope study. Journal of Food Science, 42, 125-131.

Joseph, J., 2003. Managing fishing capacity of the world's tuna fleet. FAO Fisheries Circular No. 982.

Kanoh, S., Polo, J.M.A., Kariya, Y., Kaneko, T., Watabe, S., and Hashimoto, K., 1988. Heat-induced textural and histological changes of ordinary and dark muscles of Yellowfin tuna. Journal of Food Science, 53 (3), 673-678.

Kennedy, R., Lee, Y., Reed, C., and Van Roy, B., 1995. Solving Pattern Recognition Problems. Unica Technologies Inc., Brighton, MA.

Konstance, R.P., 1991. Axial compression properties of Kamaboko. Journal of Food Science, 56 (5), 1287-1291.

Kramer, A. and Szczesniak, A.S., 1973. Texture Measurements of Foods, 68-69. D. Reidel Publishing Co., Boston, MA.

Laakkonen, E., 1973. Factors effecting tenderness during heating of meat. In Advances in Food Research, Chichester, C.O., Mrak, E.M., Stewart, G.F. (Eds.), 20, 257-323. Academic Press, NY.

Lampila, L.E. and Brown, W.D., 1986. Changes in the microstructure of Skipjack tuna during frozen storage and heat treatment. Food Microstructure, 5, 25-31.

Lassen, Sven 1965. Tuna Canning and the Preservation of the Raw Material through Brine Refrigeration. Ch. 4 in *Fish as Food*, v 4, part 2, G. Borgstrom (Ed.) p. 207-245, Academic Press, New York and London.

Leander, R.C., 1977. Effect of heating on the ultrastructure of bovine muscle. Proceedings of the 30th Annual Reciprocal Meat Conference of the American Meat Science Association, p 99-115.

Leander, R.C., Hedrick, H.B., Brown, M.F., and White, J.A., 1980. Comparison of structural changes in bovine longissimus and semitendinosus muscles during cooking. Journal of Food Science, 45(1):1-6, 12.

Lepetit, J. and Culioli, J., 1994. Mechanical properties of meat. Meat Science, 36, 203-237.

Linko, P. and Zhu, Y., 1991. Neural network programming in bioprocess variable estimation and state prediction. Journal of Biotechnology, 21, 253-270.

Linko, P., 1988. Uncertainties, fuzzy reasoning, and expert systems in bioengineering. Annals of the New York Academy of Science, 542, 83-101.

Littell, R.C, Stroup, W.W., and Freund, R.J. 2002. SAS for Linear Models, 4th ed. SAS Institute, Cary, NC.

Lyon, C.E. and Hamm, D., 1984. Effects of age and sex on the texture profile analysis of hot stripped broiler breast meat. Poultry Science, 63, 2508-2510.

Lyon, C.E., Lyon, B.G., Hamm, D., and Thomson, J.E., 1984. The effects of postmortem holding and salt addition on the cooked yield and texture of broiler breast meat patties. Poultry Science, 63, 502-506.

Lyon, C.E., Lyon, B.G., and Hudspeth, J.P., 1981. Effects of using mechanically deboned meat from broiler breast frames and isolated soy protein on objective and sensory characteristics of poultry rolls. Poultry Science, 60, 584-590.

Lyon, B.G. and Lyon, C.E., 1990. Texture profile of *Pectoralis major* as influenced by post-mortem deboning time and heat method. Poultry Science, 69 (2), 329-340.

Lyon, B.G. and Lyon, C.E., 1993. Effects of water cooking in heat sealed bags versus conveyor belt grilling on yield, moisture, and texture of broiler breast meat. Poultry Science, 72 (11), 2157-2165.

Kennedy, R., Lee, Y., Reed, C., and Van Roy, B., 1995. Solving Pattern Recognition Problems. Unica Technologies Inc., Brighton, MA.

Mahendrakar, N.S., Dani, N.P., Ramesh, B.S., and Amla, B.L., 1990. Effect of post-mortem conditioning of ewe carcasses on instrumental texture profile of cooked thigh muscles. Meat Science 28 (3), 195-202.

Martens, H., Stabursvik, E., Martens, M., 1982. Texture and colour changes in meat during cooking related to thermal denaturation of muscle proteins. Journal of Texture Studies, 13, 291-309.

Mohsenin, N.N., 1986. Some basic concepts of rheology. Ch. 4 in Physical Properties of Plant and Animal Materials, Gordon and Breach, Science Publishers, Inc., New York, NY.

Mittal, G.S. and Zhang, J., 2000a. Use of artificial neural network to predict temperature, moisture, and fat in slab-shaped foods with edible coatings during deep-fat frying. Journal of Food Science, 65 (6), 978-983.

Mittal, G.S. and Zhang, J., 2000b. Prediction of temperature and moisture content of frankfurters during thermal processing using neural network. Meat Science, 55, 13-24.

Mittal, G.S. and Zhang, J., 2001. Artificial neural network for the prediction of temperature, moisture, and fat contents in meatballs during deep-fat frying. International Journal of Food Science and Technology, 36, 489-497.

Offer, G., Knight, P., Jeacocke, R., Almond, R., Cousins, T., Elsey, J., Parsons, N., Sharp, A., Starr, R., Purslow, P., 1989. The structural basis of the water-holding, appearance, and toughness of meat and meat products. Food Microstructure, 8, 151-170.

Offer, G., Restall, D., and Trinck, J., 1984. Water-holding in meat. In Recent advances in Chemistry of Meat, Bailey, A.J. (ed). 71-83, The Royal Society of Chemistry, London, England.

Palka, K., 2000. Roasting induced changes in texture and fibre microstructure of bovine *M. semitendinosus* muscle. Polish Journal of Food and Nutrition Sciences, 50 (2), 41-45.

Palka, K., and Daun, H., 1999. Changes in texture, cooking losses, and myofibrillar structure of bovine *M. semitendinosus* during heating. Meat Science, 51, 237-243.

Parsons, S.E., and Patterson, R.L.S., 1986. Assessment of the previous heat treatment given to meat products in the temperature range 40°-90°C. Part 2: Differential scanning calorimetry, a preliminary study. Journal of Food Technology, 2, 123-131.

Peters G, Morrissey MT, Sylvia G, and Bolte J. 1996. Linear regression, neural network, and induction analysis to determine harvesting and processing effects on surimi quality. Journal of Food Science 61 (5) 876-880.

Ramos-Nino, M.E., Ramirez-Rodriguez, C.A., Clifford, M.N., and Adams, M.R., 1997. A comparison of quantitative structure-activity relationships for the effect of benzoic and cinnamic acids on *Listeria monocytogenes* using multiple linear regression, artificial neural network and fuzzy systems. Journal of Applied Microbiology, 82, 168-176.

Reid, R.A. and Durance, T.D., 1992. Textural changes of canned chum salmon related to sexual maturity. Journal of Food Science, 57 (6), 1340-1342.

Ross, T. J., 1995. *Fuzzy Logic with Engineering Applications*, McGraw Hill Inc., New York, NY.

Sablani, S.S., Ramaswamy, H.S., and Prasher, 1995. A neural network approach for thermal processing applications. Journal of Food Processing and Preservation, 19, 283-301.

Simutis, R., Havlik, I., Luebbert, A., 1993. Fuzzy-aided neural network for real-time state estimation and process prediction in the alcohol formation step of production-scale beer brewing. Journal of Biotechnology, 27 (2), 203-215.

Singh, R. K., and Ou-yang, F. 1994. Knowledge-based fuzzy control of aseptic processing. Food Technology June 1994: 155-161.

Smith, D.P., Lyon, C.E., and Fletcher, D.L., 1988. Comparison of the Allo-Kramer shear and texture profile analysis methods of broiler breast meat texture analysis. Poultry Science, 67, 1549-1556.

Soo, H.M. and Sander, E.H., 1977. Prediction of sensory response to textural parameters of breaded shrimp shapes using Instron texture profile analysis. Journal of Food Science, 42, 163-167.

Szczesniak, A.S., 1963a. Classification of textural characteristics. Journal of Food Science, 28, 385-389.

Szczesniak, A.S., 1963b. Objective measurements of food texture. Food Technology, 28, 410-420.

Szczesniak, A.S., 1996. Texture profile analysis – methodology interpretation clarified. Journal of Texture Studies, 27, vi.

Tabilo, G., Flores, M., Fiszman, S.M., and Toldra, F., 1999. Postmortem meat quality and sex affect textural properties and protein breakdown of dry cured ham. Meat Science, 51, 255-260.

Taiwo, K.A., Akanbi C.T., and Ajibola O.O., 1998. Regression relationships for the soaking and cooking properties of two cowpea varieties. Journal of Food Engineering, 37, 331-344.

Thai, C.N. and Shewfelt, R.L., 1991. Modeling sensory color quality of tomato and peach: neural networks and statistical regression. Transactions of the ASAE, 950-955.

Trout, G.R., Chen, C.M., and Dale, S., 1990. Effect of calcium carbonate and sodium alginate on the textural characteristics, color and color stability of restructured pork chops. Journal of Food Science, 55 (1), 38-42.

Unklesbay, K., Keller, J., Unklesbay, N., and Subhangkasen, D., 1988. Determination of doneness of beef steaks using fuzzy pattern recognition. Journal of Food Engineering, 8, 79-90.

Vallejo-Cordoba, B., Arteaga, G.E., and Nakai, S., 1995. Predicting milk shelf-life base don artificial neural networks and headspace gas chromatograph data. Journal of Food Science, 60 (5), 885-888.

Veland, J.O. and Torrissen, O.J., 1999. The texture of Atlantic salmon (*Salmo salar*) muscle as measured instrumentally using TPA and Warner-Bratzler shear test. Journal of Science in Food and Agriculture, 79, 1737-1746.

Venugopal, V. and Shahidi, F., 1996. Structure and composition of fish muscle. Food Review International, 12(2), 175-197.

Vogl, T.P., Mangis, J.K., Zigler, A.K., Zink, A.K., and Alkon, D.L., 1988. Accelerating the convergence of the backpropagation method. Biological Cybernetics, 59, 256-264.

Wheaton, F.W. and Lawson, T.B., 1985. Heat processing and canning: canning of tuna. In Processing Aquatic Food Products, John Wiley and Sons, New York, NY.

Xie, G., Xiong, R., and Church, I., 1998. Comparison of kinetics, neural network and fuzzy logic in modeling texture changes of dry peas in long time cooking. Lebensm.-Wiss. u.-Technol., 31, 639-647.

Zhang, Q and Litchfield, J.B., 1991. Applying fuzzy mathematics to product development and comparison. Food Technology, July 1991, 108-115.

Zhang, Q. and Litchfield, 1993. Fuzzy logic control for a continuous crossflow grain dryer. Journal of Food Process Engineering, 16, 59-77.

Zhang, Q., and Litchfield, J. B. 1992. Advanced process controls: applications of adaptive, fuzzy and neural control to the food industry. Food Processing Automation II, Proceedings of the 1992 Conference, May 4-6, Food and Process Engineering Institute: p. 169-176.

Zhang, Q., Litchfield, B., and Bentsman, J. 1993. Fuzzy logic control for food processes. Food Dehydration, AIChE Symposium Series 89 (297): 90-97.

3.0 MANUSCRIPT 1

Relating texture and protein changes of Skipjack tuna (*Katsuwonas pelamis*) loin meat to different time and hydrothermal treatments by Instrumental Texture Profile Analysis and Differential Scanning Calorimetry

ABSTRACT

Skipjack tuna was hydrothermally treated to 40, 55, 70, 85, and 100°C for 0, 3, 5, 10, 20, 30, 45, 60, 90, and 120 minutes. Instrumental Texture Profile Analysis (ITPA) was used to measure changes in texture parameters. Sample weight loss, moisture content, and remaining native protein were also measured. Three native protein peaks were observed for raw Skipjack tuna. Increased temperature caused more rapid native protein denaturation, increased hardness, retarded springiness, and increased instantaneous springiness for all but 55°C samples. Cohesiveness was similar for all treatments but 55°C samples.

Native protein denaturation and aggregation, muscle structure changes, and auto proteolysis influenced ITPA parameters. Temperature, not time, was a primary influence of ITPA parameters for all except the 55°C treatment. Proteolysis was suspected in the 55°C treatment because values for cohesiveness, instantaneous springiness, and retarded springiness declined as treatment time increased. Sample weights and moisture contents were influenced by water and protein migration, although these changes minimally affected ITPA measurements.

Key Words – Skipjack, tuna, Instrumental Texture Profile Analysis, Differential Scanning Calorimetry, protein, hydrothermal temperature treatment

INTRODUCTION

The commercial tuna canning process uses precooking, a unit operation where whole fish are cooked prior to canning to change fish texture for a more efficient cleaning and separation of consumable meat from the rest of the fish. The texture change that occurs in precooking may result from both thermal treatment time and temperature. Precooked fish texture directly affects yield and product quality, therefore precooking is arguably the most important unit operation for a cannery (Wheaton and Lawson, 1985; Lassen, 1965).

The texture of muscle tissue is related to its structure. The structure of muscle tissue has been described as a two component system comprised of bundles of parallel fibers bound by a connective tissue network (Bouton et al., 1975; Lepetit and Culioli, 1994; Bailey 1987). The parallel fibers are myofibers or muscle cells, and are made up of many myofibrils. Myofibrils contain thick and thin filaments, and water. Thick filaments are primarily myosin and thin filaments are primarily actin. Collagen, the major connective tissue protein in meat, is present in the sarcoplasm where it binds myofibrils to one another (Foegeding et al., 1996).

Fish and beef muscles are similar. The same major myofibrillar proteins in beef are present in fish and are thought to have similar purposes (Schwimmer 1981a; Schwimmer 1981b). Like mammalian muscle, fish myosin and actin are considered the major structural proteins (Venugopal and Shahidi, 1996), while collagen is the major connective tissue protein (Dunajski, 1979). The fundamental structure of fish muscle can be compared to that of cross-striated mammalian muscles; however fish muscle cells are shorter and smaller in diameter than those of mammals. Fish connective tissue is more evenly disbursed, less abundant, and less thermally stable than that of beef (Dunajski, 1979). Because of these differences, fish collagen has a minimal effect on

cooked muscle texture (Foegeding et al., 1996). Fish myosin is also less thermally stable than mammalian myosins, although tuna myosin appears almost as stable as rabbit or beef myosins (Venugopal and Shahidi, 1996).

Meat texture changes during cooking primarily as a result of both native protein thermal denaturation and degree of aggregation between denatured protein molecules. The cooked muscle may soften or toughen depending on whether the native muscle structure or the cooked, aggregated protein structure is mechanically stronger (Martens et al., 1982). Protein thermal denaturation and aggregation produces muscle ultrastructure alterations that relate to texture changes. Phase contrast microscopy revealed increased muscle fiber disintegration in beef with increased thermal treatment from 40 to 70°C. Similarly, scanning electron microscopy found increased myofibrillar fragmentation, increased intermyofibrillar spaces, and sarcomere shortening with increased thermal treatment of beef (Hearne et al., 1978). Other researchers have shown that beef muscle fiber length decreased when heated from 50 to 121°C (Palka and Daun, 1999). It appears tuna muscle ultrastructure changes parallel those of beef. Electron micrographs of precooked Skipjack tuna have shown that muscle fiber shrinkage and erosion can be attributed to thermal processing (Lampila and Brown, 1986). Other researchers reported non linear increases in shear force that correlated with muscle ultrastructure changes when yellowfin tuna was heated (Kanoh et al., 1988).

Auto proteolysis during heating affects cooked meat texture. Cathepsins, a class of proteases active at temperatures up to 70°C at an optimal pH of 4 to 5, have been implicated in myofibrillar deterioration of raw mammalian muscle tissues (Porter et al. 1996; Kirschke and Barrett 1987). Fish cathepsins are ten times more active than mammalian cathepsins, are linked to myosin and actin degradation, and are thermally stable up to 70°C (Siebert 1958; Reddi et al., 1972). These enzymes have been

implicated in the textural softening during cooking of whole fish muscle and the setting of surimi pastes (Wasson, 1992). Cathepsins, a class of auto proteolitic enzymes have been implicated in the proteolytic degradation of Skipjack tuna processed at 55°C (Stagg, 1999). Skipjack samples processed at 55°C exhibited more autolysis and less remaining myosin compared with others heated from 40°C to 80°C, and Kramer shear force measurements were also lower for tuna cooked at 55°C than either 40°C or 70°C (Stagg, 1999).

Instrumental Texture Profile Analysis (ITPA) subjects materials to a double compression, relating force-time data to textural attributes scored by a sensory panel (Freidman et al., 1963; Bourne, 1978). ITPA is a widely used test because up to eight different texture characteristics can be defined with one experiment. This method has been used to describe texture in apples, cheese, and sweet potatoes (Anantheswaran et al., 1985; Lazos et al., 1996; Truong et al., 1997; Drake et al., 1999). ITPA has also been used to characterize cooked beef texture (Duizer et al., 1996; Palka and Daun, 1999; Palka, 2000), cooked poultry (Lyon and Lyon, 1990; Lyon and Lyon, 1993; Smith et al., 1988; Lyon et al., 1984; Lyon and Hamm, 1984), cooked, restructured pork chops (Trout et al., 1990), and cooked mutton (Mahendrakar et al., 1990). This method has quantified the effect of storage time and temperature on raw Atlantic salmon texture (Veland and Torrissen, 1999), hydrothermal processing temperature and time on Pacific chum salmon texture (Bhattacharya et al., 1993), and sexual maturity on the texture of canned salmon (Reid and Durance, 1992).

The influences of thermal treatment and time on Skipjack tuna muscle texture changes have not been defined with more than one texture parameter. Defining how different texture parameters change with time/temperature treatment combinations can help processors make decisions about precook treatments for processed tuna.

The objectives of this research were:

1) Analyze the influence of native protein denaturation, coagulation, and auto proteolysis of Skipjack tuna on ITPA parameters.
2) Determine the impact of time and thermal treatment combinations on the texture of Skipjack tuna using ITPA analysis.
3) Assess the impact of sample weight loss and final moisture content on ITPA texture parameters.

MATERIAL AND METHODS

One lot of twenty five 4 kg Western Pacific Skipjack tuna (*Katsuwonas pelamis*) was shipped frozen from a Puerto Rico cannery to North Carolina State University, Raleigh NC. Fish were weighed, tagged, and placed into a –40°C freezer for storage prior to slicing. Fish were sliced while still frozen using a meat band saw oriented perpendicular to the backbone of the fish into four 3.8 cm steaks, with the first sample slice beginning 1.3 cm behind the start of the dorsal fin. Steaks were vacuum packed and returned to the –40°C freezer until needed.

Hydrothermal treatment

For each experiment, steaks were tempered in 28°C water for 15 minutes to prepare the muscle for sampling. Care was taken to prevent over thawing as this produced a muscle texture which made sample cutting difficult. Cylindrical samples (c 15.7 mm diameter x 38 mm) were cut from each steak parallel to the muscle fiber. Only light loin meat was sampled. Although the exact number of samples varied because of steak size and condition, approximately three samples were taken from each upper loin and two from each lower loin per steak.

Hydrothermal treatment experiments encompassed 5 temperature levels (40, 55, 70, 85 and 100°C) and 10 time levels (0, 3, 5, 10, 20, 30, 45, 60, 90, and 120 minutes). Three fish were represented in each hydrothermal level with 4 replicates from each fish being sampled per time level (n = 12). For each hydrothermal treatment, samples were weighed and placed into 25 mm X 100 mm vials. The center temperatures of four randomly selected samples were monitored using a 30 gage type T thermocouple (Omega Engineering Inc., Stamford, CT), ADAM 4018M data acquisition modules, an ADAM 4520 RS232 to RS422/RS485 converter module, and GENIE v. 2.12 data acquisition and control software (American Advantech Co., Sunnyvale, CA). Vials were filled with water at the treatment temperature and then placed into a water bath at treatment temperature. Groups of twelve samples were pulled at 0, 3, 5, 10, 20, 30, 45, 60, 90, and 120 minutes. After hydrothermal treatment, specimens were chilled at 0°C for 5 minutes with ice water, dried, weighed, placed on a sample dish, covered with aluminum foil, and stored at 4°C until further testing. All samples, with the exception of the 100°C treatment, equilibrated with the water bath temperature after 10 minutes. The 100°C samples reached 90°C after 10 min and equilibrated with the water bath temperature after 30 minutes.

Differential scanning calorimetry

Separate samples were taken from the same lot of fish and hydrothermally processed as previously described prior to analysis in a differential scanning calorimeter (DSC). DSC samples were prepared for analysis using 50 to 60 mg of meat from the center portion of the sample. The extent of protein denaturation was recorded using a Perkin Elmer DSC 7 equipped with an Intracooler II refrigeration unit and dry box with nitrogen flush (Perkin Elmer Corp., Norwalk, CT). Nitrogen gas at 40 ml/min was

circulated around the sample holder. Samples were scanned from 4°C to 100°C at a 10°C/min heating rate. Enthalpy changes exhibited by the samples during DSC testing were calculated using Pyris ® software (Perkin-Elmer Corp., Norwalk, CT). Three replicates were performed for each thermal treatment temperature and time combination, and data are reported as averages (n = 3). Testing for each hydrothermal treatment either continued for the entire experiment time, or stopped when no protein remained. DSC tested was not done for the 85 and 100°C treatments due to the rapid protein denaturation at these higher treatments.

Instrumental Texture Profile Analysis

Instrumental Texture Profile Analysis (ITPA) was performed on samples with an Instron 1122 Universal Testing Instrument (Instron Corp., Canton, MA) equipped with a 5.8 cm diameter x 3.8 cm piston and an 890 N compression load cell. Samples were taken from the refrigerator and allowed to equilibrate to room temperature for 35 minutes, then cut to 1.6 cm length to ensure the length to diameter ratio fell between 1.0 and 1.5 to eliminate sample buckling, and weighed to check that all samples were within ± 15% of the average sample weight. ITPA was done using 20 mm initial platen separation, 80% compression, 50 mm/min crosshead speed, and 400 N full scale load. Both Instron piston and platen were wiped with non stick cooking spray prior to each test to eliminate sample adhesion. Testing parameters were selected based on review of other ITPA methods used on meats, and an unpublished pretest that showed tuna tissue did not exhibit fracture at high compressions. Data collection began when the load cell sensed the platen had applied a 0.0981 N pre load to the sample. MTS TestWorks v. 4.02 software (MTS Systems Corp., Eden Prairie, MN) was used to operate the Instron,

record data, and calculate ITPA parameters of hardness, cohesiveness, instantaneous springiness, and retarded springiness.

Weight loss and moisture content

Samples were weighed before and after hydrothermal treatments to determine weight loss (n = 12). Weight loss was calculated as a percentage of initial sample weight. Moisture content determination was performed after ITPA sampling was completed (n = 5) using AOAC air drying method 950.46B, modified by substituting 100°C as the drying temperature to minimize case hardening of the sample surface (AOAC, 1995).

Statistics

Data were analyzed using SAS 8.01 statistical analysis software (SAS, Cary NC). Whole fish and upper/lower loin measurements did not differ significantly as determined by analysis of variance (ANOVA), thus data were averaged by fish and between upper and lower loin samples. An analysis of variance was performed with the General Linear Models procedure specifying fish, hydrothermal temperature, and time as variables. A test of hypothesis using Type III mean square error showed that means of fish between hydrothermal temperature treatments were significantly different for all variables tested. Results are reported as the means and standard errors by fish for each time/hydrothermal temperature treatment (n=3).

ANOVA was performed on all data to assess temperature, time, weight loss, and moisture content influences on ITPA texture values. A Pearson correlation analysis was performed to determine the strength of correlation between temperature, time, weight loss, moisture content, and percent denatured protein and ITPA texture parameters. All

data was used for this analysis (n = 50), except for percent denatured protein, where results from 40, 55, and 70°C experiments were used (n = 30). A Pearson correlation analysis was also performed on ITPA parameters to determine inter-correlation (n = 50).

RESULTS AND DISCUSSION

Differential scanning calorimetry results

Differential scanning calorimetry (DSC) for raw Skipjack tuna samples scanned at 10°C/min revealed three major native protein denaturation peaks at 50.1, 64.7, and 73.5°C (Figure 1). These peaks most likely represent myosin (peak I), collagen and other sarcoplasmic proteins (peak II), and actin (peak III) (Findlay and Barbut, 1990). Zhang et al. (2001) similarly found three protein denaturation peaks for raw Skipjack at slightly lower temperatures of 49°C, 59°C, and 68°C, caused by a slower scan rate. At slower heating rates, such as occur during commercial cooking, meat proteins may be denatured at temperatures even lower than these.

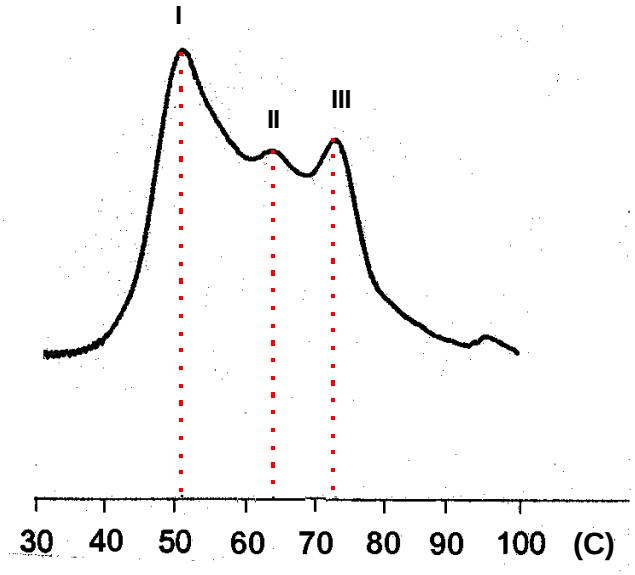

Figure 1 **Raw Skipjack tuna DSC thermogram at 10°C/min scan rate showing peak I, peak II, and peak III protein denaturation peaks.**

Differential scanning calorimetry for tuna heated at 40°C over time revealed peak I elimination from 0 to 30 minutes, slight reduction in peak II, and no reductions in peak III up to 120 minutes of treatment (Figure 2). At 55°C peak I and peak II disappeared by 10 minutes, and a gradual elimination of peak III occurred up to 45 minutes of treatment. All peaks were eliminated after 60 minutes of treatment. At 70°C all peaks had disappeared after 10 minutes of heating. Percent of native protein denatured with treatment time was calculated from the enthalpy recorded from DSC analyses (Figure 3).

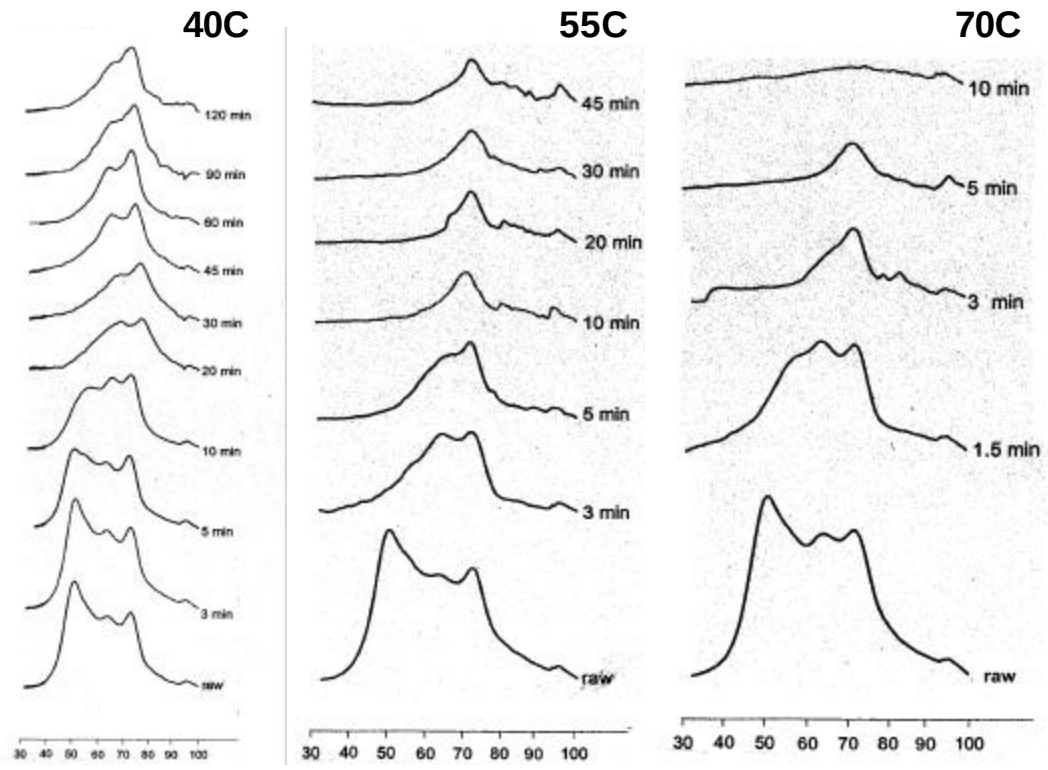

Figure 2 **DSC thermograms at 10°C/min scan rate of Skipjack tuna light loin muscle after 40°C, 55°C, and 70°C hydrothermal treatments.**

.

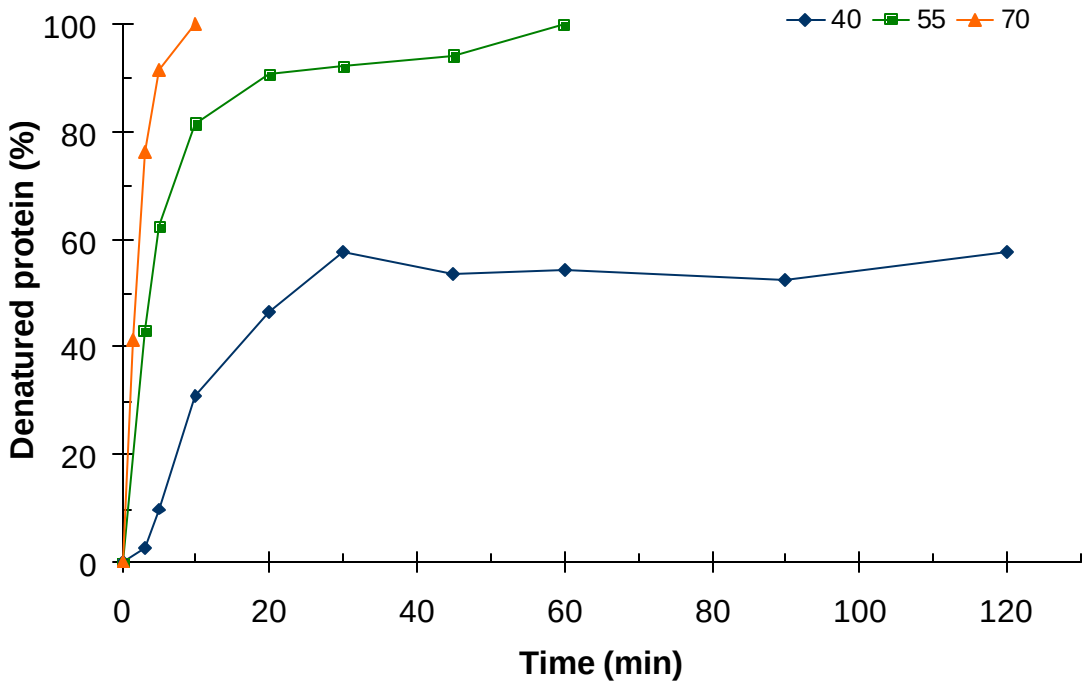

Figure 3 **Amount of protein denatured versus time as measured by enthalpy changes from DSC thermograms of Skipjack tuna light loin muscle proteins after 40°C, 55°C, and 70°C hydrothermal treatments.**

Influence of meat characteristics on Instrumental Texture Profile Analysis parameters

ANOVA for the influence of temperature, time, weight loss, moisture content, and denatured protein on ITPA parameters indicated that all ANOVA models had good success accounting for model error when using all parameters (Table 1). Temperature was a factor for all ITPA parameters. Time and weight loss were factors only for cohesiveness and retarded springiness. Moisture content did not influence any ITPA parameters.

Table 1 **R^2 and a values from ANOVA analysis, type III sum of squares results for the effect of temperature, time, weight loss, and moisture content on ITPA parameters of Skipjack tuna light loin meat for all temperature treatments.**

ITPA parameter	ANOVA model a / R^2	Temperature	Time	Weight loss	Moisture content
Hardness	< 0.0001 [a] 0.94	< 0.0001 [a]	0.3593	0.2758	0.0993
Cohesiveness	< 0.0001 [a] 0.94	0.0045 [a]	< 0.0001 [a]	< 0.0001 [a]	0.0889
Instantaneous Springiness	< 0.0001 [a] 0.87	< 0.0001 [a]	0.3233	0.4274	0.9475
Retarded Springiness	< 0.0001 [a] 0.93	< 0.0001 [a]	0.0001 [a]	0.0031 [a]	0.1974

Values of a marked with [a] indicate statistical significant influence of measured variable on model or ITPA parameter (a = 0.05, or 95% confidence).

Pearson correlation analysis between temperature, time, weight loss, moisture content, percent of denatured protein, and ITPA parameters revealed weight loss, percent denatured protein, and temperature had positive correlations with most ITPA variables (Table 2). Cohesiveness positively correlated with time and weight loss. Moisture content only correlated with instantaneous springiness, and this correlation was weakly negative.

Table 2 **R and a values from Pearson correlation analysis results to examine the relationships between temperature, time, weight loss, and moisture content on ITPA parameters of Skipjack tuna light loin meat.**

ITPA parameter	Temperature (a / R)	Time (a / R)	Weight loss (a / R)	Moisture content (a / R)	Denatured protein (a / R)
Hardness	< 0.0001 [a] 0.75	0.0268 [a] 0.31	< 0.0001 [a] 0.67	0.0668 -0.26	< 0.0001 [a] 0.87
Cohesiveness	0.3437 0.14	0.0160 [a] 0.34	< 0.0001 [a] 0.84	0.2720 0.16	< 0.0001 [a] 0.74
Instantaneous Springiness	< 0.0001 [a] 0.83	0.5051 0.10	0.0016 [a] 0.44	0.0118 [a] -0.35	0.0015 [a] 0.55
Retarded Springiness	< 0.0001 [a] 0.68	0.1183 0.22	< 0.0001 [a] 0.68	0.2596 -0.16	< 0.0001 [a] 0.87

Values of a marked with [a] indicate statistical significant influence of measured variable on model or ITPA parameter (a = 0.05, or 95% confidence), (n = 50 for all variables, except denatured protein, where n = 30).

All ITPA parameters were interdependent with one another, and were positively correlated (Table 3). Hardness was highly correlated with instantaneous and retarded springiness, cohesiveness with retarded springiness, and instantaneous springiness with retarded springiness. Interdependence of ITPA parameters indicated the same general mechanism of protein denaturation, coagulation, and muscle ultrastructure changes are responsible for texture changes in Skipjack tuna muscle.

Table 3 **R and a values from Pearson correlation analysis results to examine the relationships between ITPA parameters of Skipjack tuna light loin meat.**

	Hardness (a / R)	Cohesiveness (a / R)	Instantaneous Springiness (a / R)	Retarded Springiness (a / R)
Hardness	1	< 0.0001 [a] 0.65	< 0.0001 [a] 0.90	< 0.0001 [a] 0.96
Cohesiveness	--	1	0.0017 [a] 0.43	< 0.0001 [a] 0.75
Instantaneous Springiness	--	--	1	< 0.0001 [a] 0.89
Retarded Springiness	--	--	--	1

Values of a marked with [a] indicate statistical significant influence of measured variable on model or ITPA parameter (a = 0.05, or 95% confidence).

Instrumental Texture Profile Analysis results

ITPA parameter trends were similar for most measurements as indicated by Figures 4-7 and by Pearson correlation analysis (Table 3). These parameters changed the greatest when temperatures were not steady state, and most increased with temperature but not with time. The ITPA parameters hardness, instantaneous springiness, and retarded springiness appear to reflect the same phenomena occurring during hydrothermal treatment – denaturation, coagulation, and macrostructure changes in muscle tissue. Changes in ITPA parameters at 70°C and above were due only to protein coagulation and muscle ultrastructure changes because percent denatured protein ceased to be a factor during steady state heating at 70°C and higher. Not all ITPA parameters increased with temperature. ITPA cohesiveness, except for 55°C samples, did not change with increased temperature treatment.

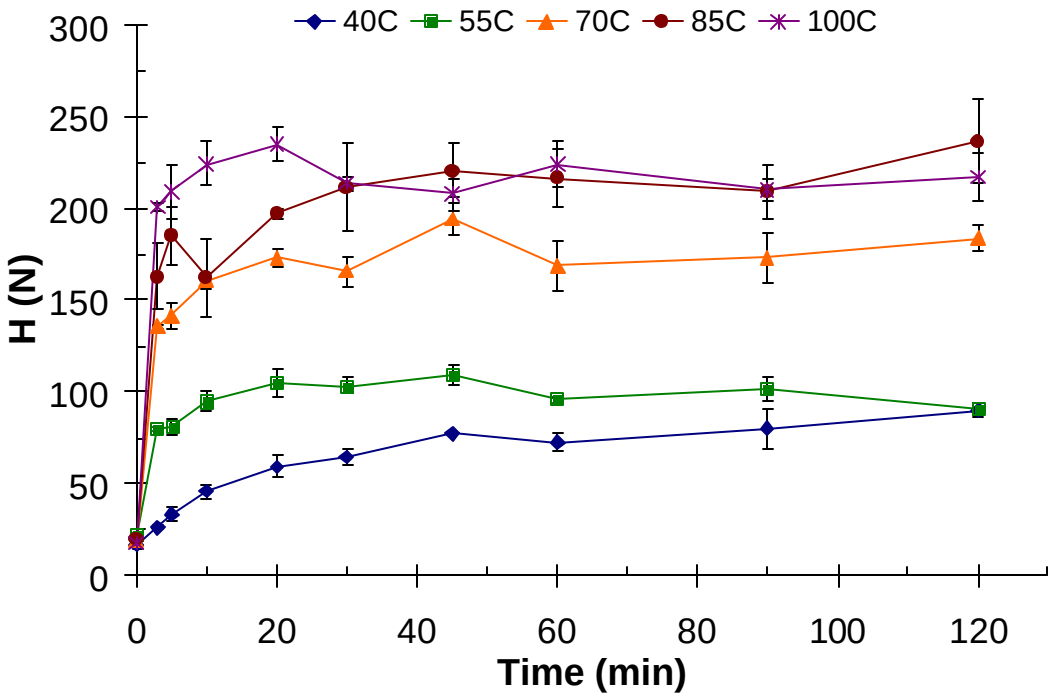

Figure 4 **ITPA hardness versus time for Skipjack tuna light loin meat at different hydrothermal treatment temperatures. Error bars indicate standard error about the mean of three fish (n = 3).**

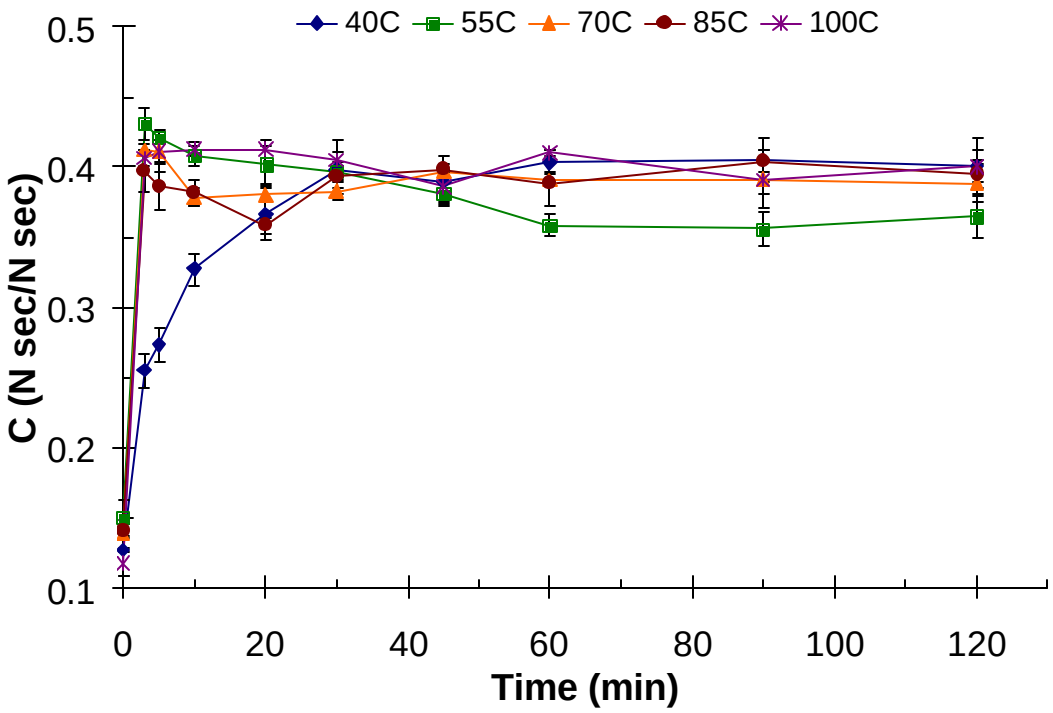

Figure 5 **ITPA cohesiveness versus time for Skipjack tuna light loin meat at different hydrothermal treatment temperatures. Error bars indicate standard error about the mean of three fish (n = 3).**

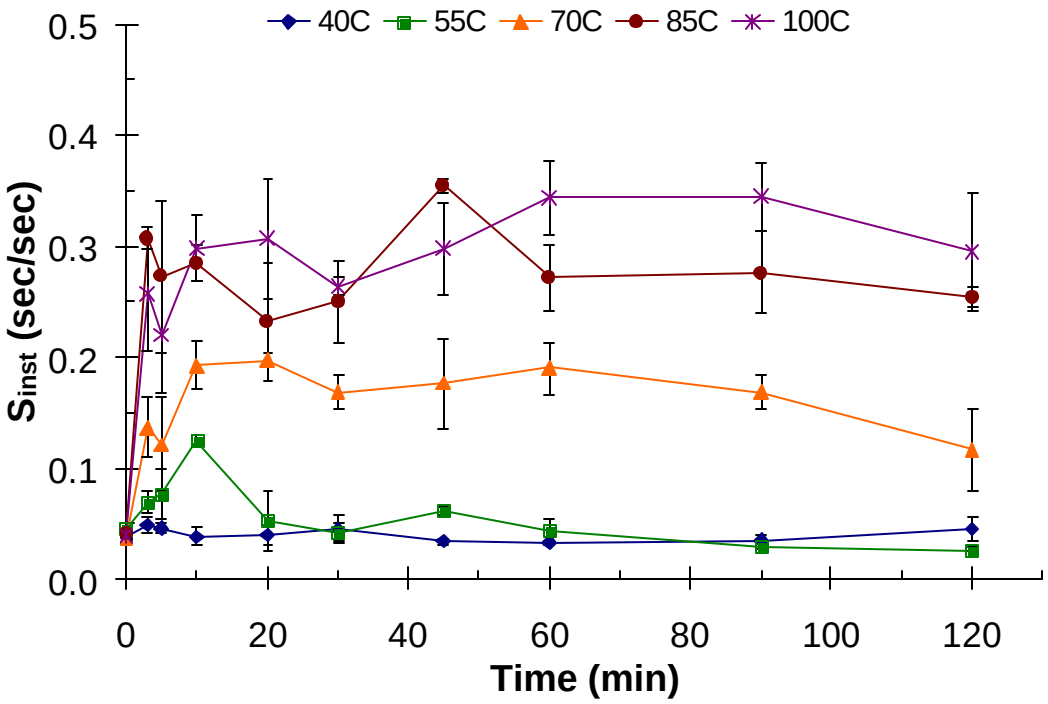

Figure 6 **ITPA instantaneous springiness versus time for Skipjack tuna light loin meat at different hydrothermal treatment temperatures. Error bars indicate standard error about the mean of three fish (n = 3).**

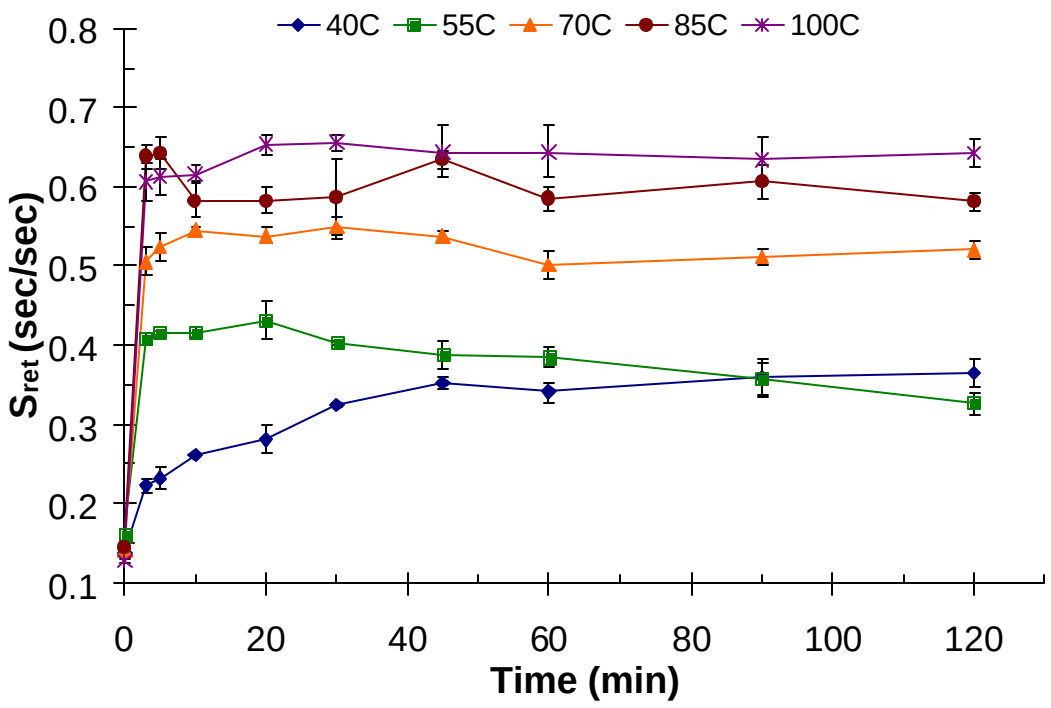

Figure 7 **ITPA retarded springiness versus time for Skipjack tuna light loin meat at different hydrothermal treatment temperatures. Error bars indicate standard error about the mean of three fish (n = 3).**

ITPA texture measurements of 55°C samples appeared to indicate enzyme auto proteolysis. These samples exhibited decreased cohesiveness from 5 to 60 minutes (Figure 5), decreased retarded springiness after 30 minutes (Figure 7), and an abrupt instantaneous springiness decline after 10 minutes treatment time to levels recorded for 40°C samples (Figure 6). These ITPA parameter declines are likely due to cathepsin L, a protease active at thermal treatments up to 70°C which attacks a wide variety of muscle proteins (Porter et al., 1996; Matsukura et al., 1981). Catheptic activity has been observed in Skipjack tuna, and is reported to be most evident at 55°C (Stagg, 1999). DSC results for the 55°C treatment show all native proteins were denatured after 45 minutes. Therefore, both native and heat coagulated proteins are attacked by cathepsin L. The 55°C treatment hardness was mostly constant with time, as were all treatments hardness values. Hardness did not appear to be sensitive to catheptic activity (Figure 4), possibly because the macrostructure of the muscle is still intact. Sample microstructure, including native and coagulated proteins might be weakened by catheptic attack, with declined cohesiveness (reduced strength of internal bonds in the sample), instantaneous springiness (reduced elasticity of muscle fibers), and retarded springiness (increased viscous behavior of the muscle) as indicators. Time does appear to be a factor in 55°C samples, contrary to Dunajski (1979), who stated thermal treatment time effects on fish texture were not very important.

Samples appeared more friable at higher hydrothermal treatments, as indicated by observation and also larger standard errors for hardness, instantaneous springiness, and retarded springiness measurements with higher temperatures. Other researchers have reported increased muscle fiber disintegration in beef with increased thermal treatment from 40°C to 70°C (Hearn et al., 1978), and increased muscle fiber disintegration of precooked versus raw Skipjack tuna (Lampila and Brown, 1986).

Friability is difficult to quantify for temperature treatments however, as other researchers did not find a temperature effect when measuring friability defined by sensory panelists for precooked boneless turkey roasts (Cash and Carlin, 1968).

ITPA hardness increased with increased hydrothermal treatment, and the most change occurred between 55°C and 70°C treatments (Figure 4). The 40°C treatment hardness increased in parallel with peak I and peak II protein denaturation. Hardness values for 85 and 100°C treatments were similar and reflect lack of further protein coagulation and collagen gelatinization. Palka and Daun (1999) reported similar ITPA hardness results in analyzing beef. These researchers reported that ITPA hardness increased with increasing thermal treatments from 50°C to 80°C, and reached maximum hardness from 80°C to 100°C. They also showed that muscle structure became more compact and sarcomere length decreased with increased thermal treatment. ITPA hardness results were also in agreement with recorded shear force values versus temperature for yellowfin tuna (Kanoh et al., 1988). Yellowfin tuna exhibited an increase in shear force from raw to 70°C, then a shear force plateau or slight decrease from 70°C to 100°C. These researchers attributed the increased shear force values from raw to 70°C to myofibrillar protein denaturation and coagulation masking collagen denaturation. Hydrothermally processed pacific chum salmon did not show the same ITPA hardness trend as Skipjack tuna (Bhattacharya et al., 1993). For this fish, ITPA hardness increased for all heating times from 0 to 40 minutes, while increased temperature did not cause increased hardness. Over temperatures, hardness increased from 60°C to an 80°C treatment maximum, while 90°C and 100°C treatments fell to the 70°C level.

Increases in cohesiveness occurred mainly during the first 5 minutes of hydrothermal treatment then reduced to a lower value (Figure 5). Cohesiveness was not generally affected by treatment temperature, although values for 40°C samples differed

from all other samples from 0 through 20 minutes ($P > 0.002$). Two separate mechanisms are proposed for cohesiveness behavior. For the 40°C treatment peak I and some peak II denaturation and subsequent coagulation paralleled increased cohesiveness. For all other treatments the coagulation due to denaturation and gelatinization of collagen between muscle fibers might be reflected in cohesiveness. Lampila and Brown (1986) reported that rapid heating of Skipjack tuna to both 60°C and 111°C caused muscle fibers to appear congealed and homogeneous with minimal myofibrillar fragmentation, and attributed granules seen between myofibrils to gelatinized collagen. Cohesiveness of pacific chum salmon mostly paralleled those found for Skipjack, with temperature not affecting this measurement (Bhattacharya et al., 1993). Cohesiveness results for beef differed from Skipjack, in that a maximum was found at 70°C (Palka and Daun, 1999). These results indicate the amount and quality of collagen in beef, and the lack thereof in fish, could impact cohesiveness.

Time reduced 55°C treatment cohesiveness after 60 minutes, and might indicate cathepsin L activity on gelatinized collagen. Cathepsin L is thought to be a major factor in muscle structure breakdown because it attacks a variety of proteins (Ogata et al. 1998), and has been implicated in reduced shear force measurements of Skipjack tuna thermally treated at 55°C (Stagg 1999).

Instantaneous springiness increased with increased hydrothermal treatment for 70, 85, and 100°C, but not for 40 and 55°C treatments (Figure 6). Means of 40°C and 55°C treatments, and likewise 85°C and 100°C treatment means were not significantly different from one another ($P>0.0005$). The 40°C treatment was not affected by time, thus peak I and slight peak II protein denaturation did not affect this variable, and peak III denaturation is necessary for instantaneous springiness response. The 55°C samples rose sharply for 10 minutes, the time at which samples reached steady state heating.

After 10 minutes, instantaneous springiness of the 55°C samples fell to the same level as the 40°C treatment. Instantaneous springiness values for 70, 85, and 100°C samples all dipped slightly at 5 minutes, the time at which samples were probably experiencing 55°C temperature. Both of these results suggest that ITPA instantaneous springiness is most likely affected by cathepsin L activity.

Retarded springiness increased with increased hydrothermal treatments (Figure 7). All treatments were significantly different ($P>0.05$). The 40°C retarded springiness values increased gradually from 0 to 30 minutes, however all other treatment values increased sharply to a nearly constant level by 3 minutes. These behaviors implicate a peak I protein mechanism for this ITPA parameter. The 55°C treatment showed a gradual decrease in retarded springiness after 20 minutes, and might indicate cathepsin L activity on the peak I protein. Increased temperature also generally increased springiness for Pacific chum salmon, although 90 and 100°C treatments had the same effect and the difference was not as great as Skipjack (Bhattacharya et al., 1993). In beef, springiness reached a maximum between 70 and 80°C, then fell to below 50 – 60°C levels (Palka and Daun, 1999). These results indicate that fish protein might coagulate more than beef or might suffer more microstructure damage during compression.

The ratio of retarded to instantaneous springiness showed two distinct trends dependent on hydrothermal treatment (Figure 8), with the 40°C and 55°C treatments grouped together, and the 70°C, 85°C, and 100°C treatments grouped together. Retarded springiness was greater than instantaneous springiness for all hydrothermal treatments, and the ratio of retarded to instantaneous springiness generally decreased with increased hydrothermal treatment. Fiszman et al. (1998) has shown retarded springiness is linked to viscous response and instantaneous springiness is associated

with the elastic response of a sample. These researchers reported significant viscous sample response where retarded springiness is appreciably greater than instantaneous springiness. The higher retarded/instantaneous ratios for 40°C and 55°C samples indicate less viscous responses than 70, 85, and 100°C samples. Grouped ratios of higher temperature treatments infer further protein coagulation, up to a point, above 55°C.

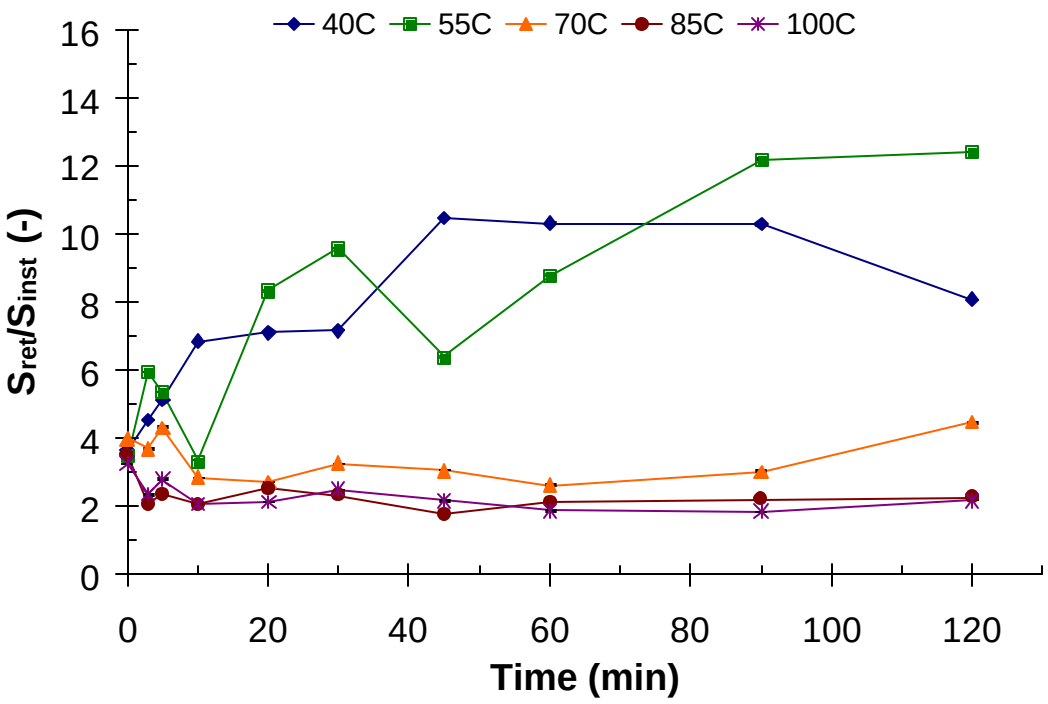

Figure 8 **Ratio of ITPA retarded to instantaneous springiness versus time for Skipjack tuna light loin meat at different hydrothermal treatment temperatures.**

Moisture content and weight loss results

Weight loss did not correlate with cooking temperature due to mass transfer of water into and soluble proteins out of the samples (Figure 9). Cloudy water surrounding the samples was also observed, and further indicated soluble protein migration. Weight losses at 5 minutes showed an expected trend of 40, 70, 55, 85, and 100°C. These results are typical of increasing muscle weight loss with increasing hydrothermal treatments. As a comparison, weight losses at 120 minutes ordered 55, 70, 100, 40, and 85°C. Weight loss results for the experiment show all samples were within 3% of each other, and were slightly less than steam cooked loin data from Bell (2001) which showed an approximate 17% weight loss at 40 minutes. ANOVA results show weight loss did have an impact on texture parameters.

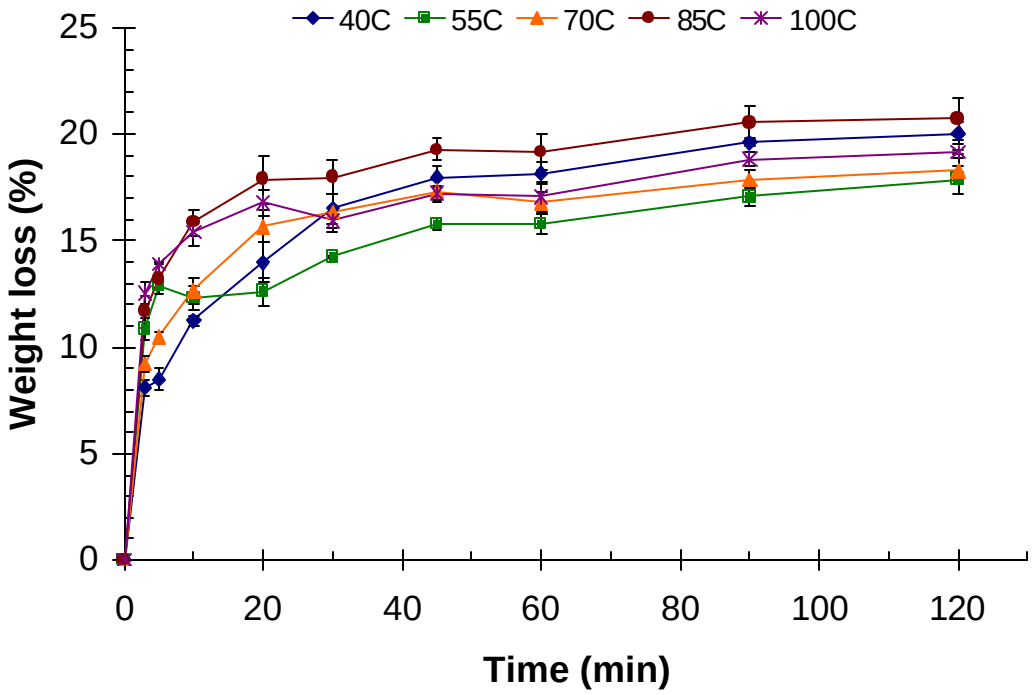

Figure 9 **Weight loss versus time for Skipjack tuna light loin meat at different hydrothermal treatment temperatures. Error bars indicate standard error about the mean of three fish (n = 3).**

Samples absorbed water, as measured by moisture content (Figure 10), and by other work by Bell et al. (2001) which showed moisture content decreased in whole steamed Skipjack tuna with increased temperature. Moisture content of the samples was influenced by pressing, however samples at 5 minutes show the expected trend decreasing moisture trend of 100, 85, 70, 55, and 40°C, which indicated water migration had probably not yet begun. Moisture contents performed at 120 minutes indicated samples absorbed water, as moisture contents at that time were ordered 85, 70, 40, 100, and 55°C. Moisture contents for all samples including raw ranged from 69.5% to 72.3%, and at no time did the difference in moisture contents exceed 2%. These minimal moisture content differences and ANOVA analysis results show water uptake did not significantly affect texture measurements.

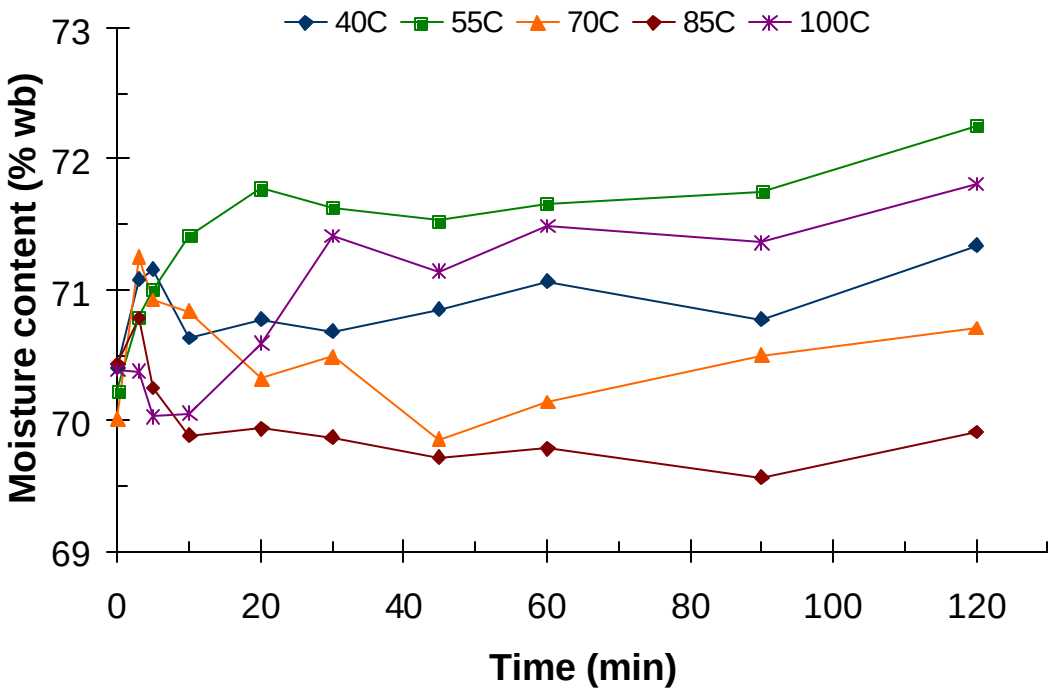

Figure 10 **Moisture content versus time for Skipjack tuna light loin meat at different hydrothermal treatment temperatures.**

CONCLUSIONS

Three native protein denaturation peaks were observed for Skipjack tuna. The 40°C treatment caused peak I protein to completely denature within 30 minutes, and peak II protein to partially denature. The 55°C treatment caused peak I and II proteins to denature completely in 10 minutes, and peak III protein to denature after 45 minutes. The 70°C treatment caused all peak proteins to completely denature after 10 minutes.

Changes in texture resulted from the degree of native protein denaturation and aggregation, muscle structure changes, and proteolysis. Hardness and retarded springiness increased with increased hydrothermal treatment. Instantaneous springiness generally increased with increased hydrothermal treatment, with the exception of the 55°C treatment. Cohesiveness after 30 minutes was similar for all except the 55°C treatment.

Hydrothermal treatment affected texture more than time, except for the 55°C treatment. For the 55°C treatment, proteolysis is suspected because values for cohesiveness, instantaneous springiness, and retarded springiness lessened as treatment time increased. For the 40°C treatment, peak I and partial peak II protein denaturation influenced hardness, cohesiveness, and retarded springiness, but not instantaneous springiness. Sample weight losses and moisture contents were influenced by bidirectional mass transfer. Weight loss did affect, but moisture content did not appear to affect ITPA measurements.

ACKNOWLEDGMENTS

This work was supported by a grant from the StarKist Seafood Company and the USDA National Needs Fellowship program. The authors would also like to thank Tim Seaboch, Den Truong, and Penny Amato for their guidance and assistance in this work.

REFERENCES

AOAC, 1995. Official Methods of Analysis, 16th ed. Association of Official Analytical Chemists, 39.1. Washington, DC.

Anantheswaran RC, McLellan MR, Bourne MC. 1985. Thermal degradation of texture in apples. J Food Sci 50:1136-1138.

Bailey AJ. 1987. Connective tissue and meat quality. In: Blanshard JMV, Lillford P. Food structure and behavior. London. Academic Press Harcourt Brace Jovanovich. p 152-160.

Bell, J.W., Farkas, S.A., Hale, S.A., and Lanier, T.C., 2001. Effect of thermal treatment on moisture transport during steam cooking of Skipjack tuna (*Katsuwonas pelamis*). Journal of Food Science, 66 (2), 307-313.

Bhattacharya, S., Choudhury, G.S., and Studebaker, S., 1993. Hydrothermal processing of Pacific chum salmon: effects on texture and in-vitro digestibility. Journal of Food Quality, 16, 243-251.

Bourne MC. 1978. Texture profile analysis. Food Tech July 62-66, 72.

Bouton PE, Harris PV; Shorthose WR. 1975. Possible relationships between shear, tensile, and adhesion properties of meat and meat structure. J Text-Studies 6(3):297-314.

Cash, D. B., and Carlin, A. F. 1968. Quality of frozen boneless turkey roasts precooked to different internal temperatures. Food Technology, v 22 Nov 1968, p 143-146.

Drake MA, Gerard PD, Truong VD, Daubert CR. 1999. Relationship between instrumental and sensory measurements of cheese texture. J Text Studies 30:451-476.

Duizer, L.M., Gullett, E.A., and Findlay, C.J., 1996. The relationship between sensory time-intensity, physiological electromyography, and instrumental texture profile analysis measurements of beef tenderness. Meat Science, 42 (2), 215-224.

Dunajski E. 1979. Texture of fish muscle. J Text Studies 10:301-318.

Findlay CJ, Barbut S. 1990. Thermal analysis of meat. In: Harwalkar VR, Ma CY. Thermal analysis of foods. UK: Elsevier Science Publishers Ltd. p 92-125.

Fiszman SM, Pons M, Damasio MH. 1998. New parameters for instrumental texture profile analysis: instantaneous and retarded recoverable springiness. J Text Studies 29:499-508.

Foegeding A, Lanier TC, Hultin HO. 1996. Characteristics of edible muscle tissues. In: Fenema OR, editor. Food Chemistry. 3rd ed. New York: Marcell Dekker. p 879-942.

Friedman, H.H., Whitney, J.E., and Szczesniak, A.S., 1963. The Texturometer – a new instrument for objective texture measurement. Journal of Food Science, 28, 390-396.

Hearne LE, Penfield MP, Goertz GE. 1978. Heating effects of bovine semitendinsus: phase contrast microscopy and scanning electron microscopy. J Food Sci 43:13-16.

Kanoh, S, Polo, JMA, Kariya, Y, Kaneko, T, Watabe, S, and Hashimoto, K. 1988. Heat-induced textural and histological changes in ordinary and dark muscles of yellowfin tuna. J Food Sci 53(3):673-678.

Kirschke H, Barrett AJ. 1987. Chemistry of lysosomal protienases. In: Glaumann H, Ballard FJ. Lysosomes: their role in protein breakdown. London: Academic Press. p 193-238.

Lassen, Sven 1965. Tuna Canning and the Preservation of the Raw Material through Brine Refrigeration. Ch. 4 in *Fish as Food*, v 4, part 2, G. Borgstrom (Ed.) p. 207-245, Academic Press, New York and London.

Lampila LE, Brown WD. 1986. Changes in the microstructure of Skipjack tuna during frozen storage and heat treatment. Food Microstructure 5:25-31.

Lazos ES, Servos DC, Parliaros D. 1996. Kinetics of texture degradation in apples during thermal processing. Chimika Chronika 25:11-28.

Lepetit J, Culioli J. 1994. Mechanical properties of meat. Meat Sci 36:203-237.

Lyon, C.E. and Hamm, D., 1984. Effects of age and sex on the texture profile analysis of hot stripped broiler breast meat. Poultry Science, 63, 2508-2510.

Lyon, C.E., Lyon, B.G., Hamm, D., and Thomson, J.E., 1984. The effects of postmortem holding and salt addition on the cooked yield and texture of broiler breast meat patties. Poultry Science, 63, 502-506.

Lyon, B.G. and Lyon, C.E., 1990. Texture profile of *Pectoralis major* as influenced by post-mortem deboning time and heat method. Poultry Science, 69 (2), 329-340.

Lyon, B.G. and Lyon, C.E., 1993. Effects of water cooking in heat sealed bags versus conveyor belt grilling on yield, moisture, and texture of broiler breast meat. Poultry Science, 72 (11), 2157-2165.

Mahendrakar, N.S., Dani, N.P., Ramesh, B.S., and Amla, B.L., 1990. Effect of post-mortem conditioning of ewe carcasses on instrumental texture profile of cooked thigh muscles. Meat Science 28 (3), 195-202.

Martens H, Stabursvik E, Martens M. 1982. Texture and colour changes in meat during cooking related to thermal denaturation of muscle proteins. J Text Studies 13:291-309.

Matsukura U, Okitani A, Nishimuro T, Kato H. 1981. Mode of degradation of myofibrillar proteins by an endogenous protease, cathepsin L. Biochim Biophys Acta 662:41.

Ogata H, Aranishi F, Hara K, Osatomi K, Ishihara T. 1998. Proteolytic degradation of myofibrillar components by carp cathepsin L. J Sci Food Agric 76:499-504.

Palka K, Daun H. 1999. Changes in texture, cooking losses, and myofibrillar structure of bovine M. semitendinosus during heating. Meat Sci 51:237-243.

Porter R, Koury B, Stone F. 1996. Comparison of cathepsin B, D, H, and L activity in four species of pacific fish. J Food Biochem 19:429-442.

Reddi P, Constantinides S, Dymsza H. 1972. Catheptic activity of fish muscle. J Food Sci 37:643-648.

Reid, R.A. and Durance, T.D., 1992. Textural changes of canned chum salmon related to sexual maturity. Journal of Food Science, 57 (6), 1340-1342.

Schwimmer-S. 1981a. Enzyme action and food texture: muscle to meat. In: Schwimmer S. Source book of food enzymology. Westport Connecticut: AVI Publishing Co Inc. p 461-480.

Schwimmer-S. 1981b. Roles of enzymes in fish texture and transformation. In: Schwimmer S. Source book of food enzymology. Westport,-Connecticut: AVI Publishing Co Inc. p 497-510.

Siebert G 1958. Protein-splitting enzyme activity of fish flesh. Experientia 14:65.

Smith, D.P., Lyon, C.E., and Fletcher, D.L., 1988. Comparison of the Allo-Kramer shear and texture profile analysis methods of broiler breast meat texture analysis. Poultry Science, 67, 1549-1556.

Stagg N. 1999. Response of Skipjack tuna muscle protein to thermal processing [MSc thesis]. Raleigh NC: North Carolina State University. 128 p.

Trout, G.R., Chen, C.M., and Dale, S., 1990. Effect of calcium carbonate and sodium alginate on the textural characteristics, color and color stability of restructured pork chops. Journal of Food Science, 55 (1), 38-42.

Truong VD, Walter WM, Hamann DD. 1997. Relationship between instrumental and sensory parameters of cooked sweet potato texture. J Text Studies 28:163-185.

Wasson DH. 1992. Fish muscle proteases and heat-induced myofibrillar degradation: a review. Journal of Aquatic Food Product Technology 1(2)23-41.

Wheaton, F.W. and Lawson, T.B., 1985. Heat processing and canning: canning of tuna. In Processing Aquatic Food Products, John Wiley and Sons, New York, NY.

Veland, J.O. and Torrissen, O.J., 1999. The texture of Atlantic salmon (*Salmo salar*) muscle as measured instrumentally using TPA and Warner-Bratzler shear test. Journal of Science in Food and Agriculture, 79, 1737-1746.

Venugopal V, Shahidi F. 1996. Structure and composition of fish muscle. Food Rev Int 12(2)175-197.

Zhang J, Farkas BE, Hale SA. 2001. Thermal properties of skipjack tuna (Katsuwonis pelamis). International Journal of Food Properties 4(1):81-90.

4.0 MANUSCRIPT 2

Instrumental Texture Profile Analysis parameters, weight loss, and moisture content comparisons of Skipjack tuna (*Katsuwonus pelamis*) cooked by different methods

ABSTRACT

Skipjack tuna was cooked by three different methods – conventional steaming of a whole fish, steaming small loin samples, and hydrothermally cooking small loin samples. Sample temperature, weight loss, moisture content, and Instrumental Texture Profile Analysis (ITPA) parameters were measured. Whole fish had the greatest measurement variability due to fish to fish variation, however linear fit models for small and whole fish samples showed similar slope trends.

Weight loss increased and moisture content decreased, and ITPA hardness, instantaneous springiness, and retarded springiness increased with increased temperature for all treatments. Cohesiveness did not vary with temperature, but did vary with treatment. Because small sample measurements trended similarly to whole fish samples, linear equations were developed which used small steamed and small hydrothermal ITPA, weight loss, and moisture content data to predict whole steamed fish ITPA, weight loss, and moisture values. These linear equations can be used to predict texture, weight, and moisture content changes of whole fish from small samples treated by the two listed methods.

Key Words – Tuna, texture profile analysis, weight loss, moisture content, steam, hydrothermal, cooking

INTRODUCTION

Skipjack tuna (*Katsuwonus pelamis*) has become the most popular raw material for chunk light tuna, and represents 60% of fish used for this product (Wheaton and Lawson, 1985; Bell, 1998). During processing, tuna is precooked before canning to change muscle texture so that edible meat can be efficiently separated from the rest of the fish (Figure 1). After precooking, cooling, and cleaning, loins are chopped and packed in cans with water and broth. Cans are then seamed and retorted (Figure 2).

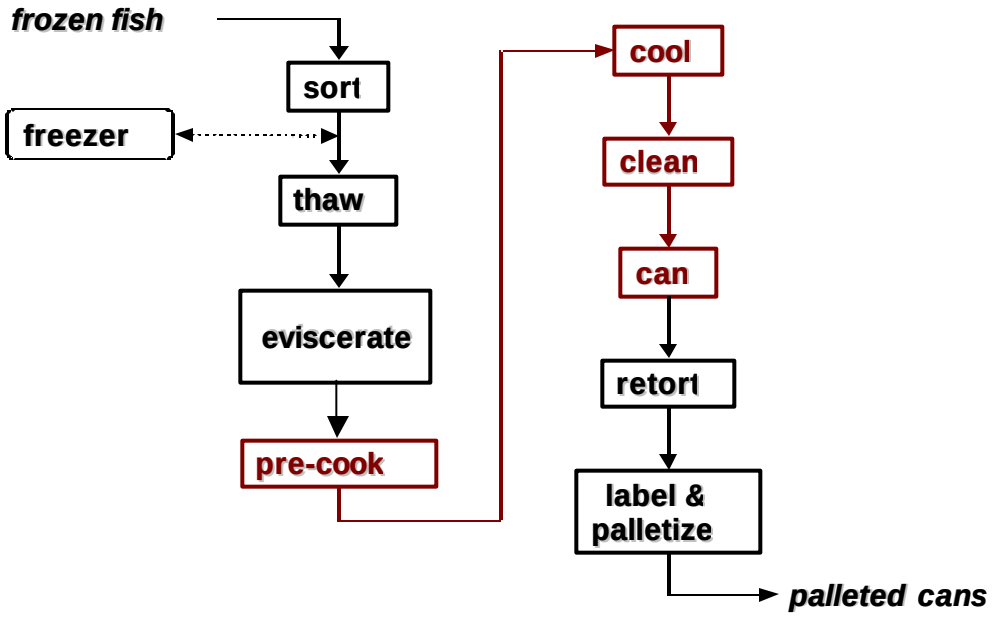

Figure 1 **Tuna processing unit operation diagram.**

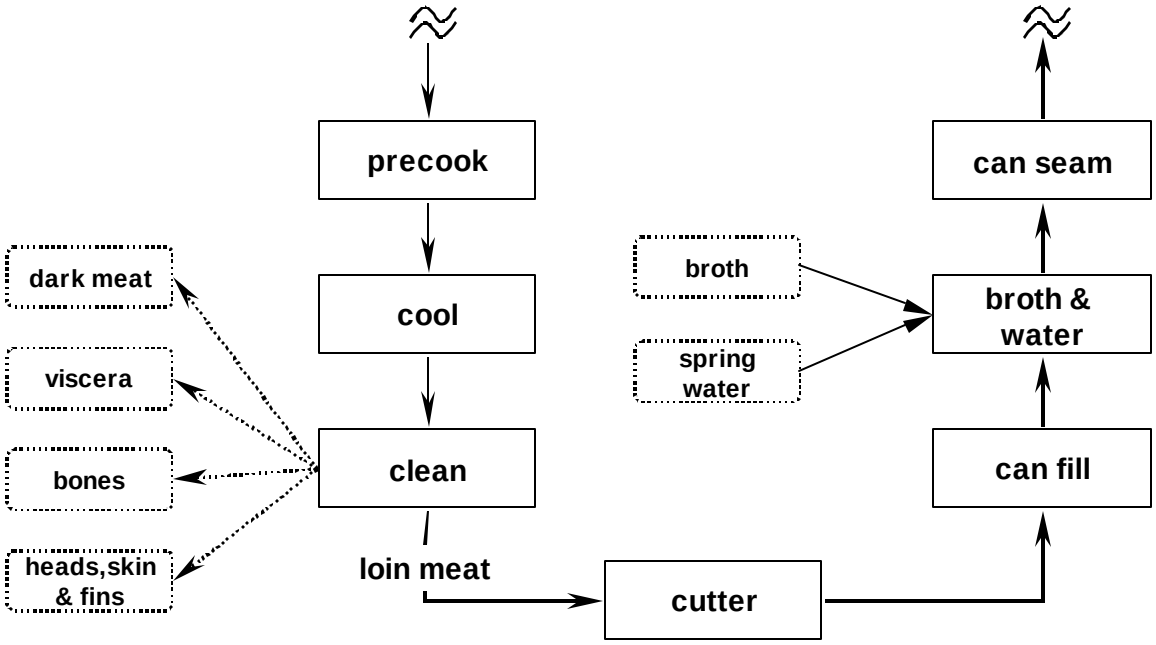

Figure 2 **Tuna precooking and canning process.**

Precooking is the most important step in tuna canning, and has the greatest influence on final product texture, yield, and flavor (Lawson, 1965). The texture change resulting from precooking is important to canners because fish texture influences carcass cleaning efficiency, cannery yield, and overall processing efficiency. Weight loss and moisture content of the fish are also important to processors, as excessive weight loss or moisture loss both translate into more tuna required to fill a can prior to broth addition and hence decreased revenue.

Past studies have used small, representative samples of meat for heating experiments to measure weight, moisture, and texture studies (Bhattacharya et al., 1993; Palka and Daun, 1998; Segars and Johnson, 1986; Bouton and Harris, 1972; Califano et al., 1997; Bertola et al., 1994; Mathevon et al., 1995; Duizer et al., 1996; Bouton et al., 1975; Webb et al., 2003). Advantages of using small samples include ease of handling, relatively quick processing time, and more rapid achievement of an isothermal system when compared to whole cuts of meat and fish. However, applying

heat treatment to small samples might not be indicative of the results obtained when cooking large cuts of meat or whole fish, as different cook methods might affect the rate of protein denaturation and agglomeration, and hence texture, weight loss, and moisture content results.

Data on texture changes of raw and cooked fish has been studied (Bhattacharya et al., 1993; Segars and Johnson, 1986; Hyldig and Nielsen, 2001; Veland and Torrissen, 1999; Dunajski, 1979; Hamann and Lanier, 1986). Past studies have focused on Yellowfin and Skipjack texture and meat microstructure changes upon heating (Kanoh et al., 1988; Lampila and Brown, 1986). All of these studies focused on physiological changes of the meat, and did not detail weight and moisture content changes. Bell et al. (2001) studied the effects of steaming whole Skipjack on loin meat moisture content, and the rate of weight loss of Skipjack fillets, but this data is not linked to meat texture change.

Tuna processors require data on how moisture content, weight loss, and texture attributes change with steam cooking of whole fish. Since small samples are easier to work with, knowledge of how measured variables of small samples relate to whole fish would be helpful for processors. This data would aid processors in making decisions about precooking variables and process design.

The objectives of this research were to –

1. Investigate temperature, weight loss, and moisture content influences on three different sample treatment ITPA texture parameters
2. Compare temperature influences on weight loss, moisture content, and ITPA parameters of the three different sample treatments
3. Relate measured variables of the two small sample methods to measured variables of whole fish.

MATERIALS AND METHODS

Whole fish steam treatment

Thirty five whole cannery grade Western Pacific Skipjack tuna (*Katsuwonas pelamis*), weighing from 2.8 kg to 5.3 kg and originating from five different lots of Skipjack tuna were used for sample selection. Fish were weighed, tagged, and placed into a –40°C freezer for storage prior to experimentation. For the experiment, fish were thawed in water to -2°C center temperature prior to cooking, as monitored by a standard meat thermometer placed next to the backbone at the thickest part of the fish. A 28 ga. type T thermocouple coated with Teflon heat shielding was inserted into one of the upper loins and placed next to the backbone at the thickest part of the fish after thawing. Thermocouple location was approximately 2.54 cm back from the start of the dorsal fin, and 15° to 20° from vertical, towards one of the two pectoral fins. One to three fish were steam cooked for each experiment with 100 – 104°C steam in a pilot plant retort. Fish, steam, and process temperatures were recorded at 1 minute intervals with ADAM 4018M data acquisition modules, ADAM 4520 RS232 to RS422/RS485 converter module, and GENIE v. 2.12 data acquisition and control software (American Advantech Co., Sunnyvale, CA). During cooking, individual fish were suspended in wire baskets and not allowed to touch each other. Fish were cooked until a predetermined "pull" temperature, defined as the temperature at which fish were removed from the retort to cool. "Pull" temperatures ranged from 57.2°C to 73.9°C, and cook times ranged from 1.08 to 2.47 hours. Final temperatures, obtained after fish were removed from the retort, ranged from 63.7°C to 80.0°C. Fish were moved from steam at the predetermined "pull" temperature and allowed to cool in ambient air by free convection. At ca. 35°C, fish were transferred to a 4°C walk in cooler, and chilled to ca. 25°C prior to cleaning. After

chilling, fish were taken from the walk in cooler, weighed, and cleaned. Skin was scraped off with a small blunt knife and head and fins were removed. The meat surrounding the visceral cavity was recovered. The fish were then split in half along the upper dorsal line and pulled apart. The spine was removed in one piece, and small bones that protect the visceral cavity were removed from the lower loins. The upper and lower loins from each half were then separated, and red meat was cleaned from the loins. Constituents of each fish were then weighed. Upper and lower loins were wrapped in plastic film and returned to the 4°C cooler prior to texture testing.

Small sample hydrothermal treatment

One lot of twenty five 4 kg Western Pacific Skipjack tuna (*Katsuwonas pelamis*) was used for sample selection. Fish were weighed, tagged, and placed into a –40°C freezer for storage prior to experimentation. Fish were sliced while still frozen using a meat band saw perpendicular to the backbone into four 3.8 cm steaks, with the first sample slice beginning 1.3 cm behind the start of the dorsal fin. Steaks were vacuum packed and returned to the –40°C freezer until required for experimentation.

For the experiment, vacuum packed steaks were tempered in 28°C water for 15 minutes to prepare the muscle for sample cutting. Care was taken to only temper the samples before cutting, as intact samples could not be cut from completely thawed steaks. Steaks were unpackaged and cylindrical samples (c 15.7 mm dia x 38 mm) were cut from each steak parallel to the muscle fiber. Only light loin meat was sampled. Although the exact number varied because of steak size and condition, approximately three samples from each upper loin and two samples from each lower loin per steak were taken for the experiment.

Hydrothermal treatment of samples encompassed five temperature levels (40, 55, 70, 85 and 100°C) and ten treatment time levels (0, 3, 5, 10, 20, 30, 45, 60, 90, and 120 minutes). Three fish were represented in each thermal treatment, with four replicates from each fish being sampled per time level. Eighty-four samples were averaged for each temperature level. For each experiment, water bath temperatures were held constant at 40, 55, 70, 85, or 100°C. Samples were weighed and placed into 25 mm X 100 mm vials and center temperatures of four samples were monitored using a 30 gage type T thermocouple (Omega Engineering Inc., Stamford, CT), ADAM 4018M data acquisition modules, an ADAM 4520 RS232 to RS422/RS485 converter module, and GENIE v. 2.12 data acquisition and control software (American Advantech Co., Sunnyvale, CA). Vials were filled with water at the treatment temperature and quickly placed into a water bath of the same temperature. Time for each experimental treatment started when the vials were placed into the water bath. Groups of twelve samples were removed at 0, 3, 5, 10, 20, 30, 45, 60, 90, and 120 minutes. All samples, with the exception of the 100°C treatment, equilibrated to the water bath temperature after 10 minutes. The 100°C samples reached 90°C after 10 min and 100°C at 30 minutes. After hydrothermal treatment, specimens were chilled in ice water at 0°C for 5 minutes, dried and weighed, placed on a sample tray and wrapped in aluminum foil, and stored in a 4°C refrigerator until needed for analysis.

Small sample steam treatment

Vacuum packed steaks were prepared from one lot of fish, thawed, and 15.7 mm dia x 38 mm cylindrical samples of light loin meat were cut parallel to the muscle fiber as described in the small hydrothermal sample method section. Twelve samples, four replicates from three different fish, were used for each thermal treatment. After thawing,

a 30 gage type T thermocouple (Omega Engineering Inc., Stamford, CT), was placed in the center of one sample, and samples were placed on a sample tray. Non-stick vegetable oil spray was used on the sample trays to prevent sticking. Samples were placed in a steamer for thermal treatment. Texture samples were steamed to 49.2, 60.5, 68.2, or 82.6°C endpoint temperature, defined as the maximum temperature the sample achieved. Weight loss and moisture content samples were steamed to endpoint temperatures that ranged from 44 to 95°C. ADAM 4018M data acquisition modules, ADAM 4520 RS232 to RS422/RS485 converter module, and GENIE v. 2.12 data acquisition and control software (American Advantech Co., Sunnyvale, CA) were used to take temperature measurements. All samples had cook times of less than 10 minutes. After steaming, samples were allowed to cool in ambient air by free convection, covered with aluminum foil, and placed in a 4°C refrigerator prior to further experimentation.

Instrumental Texture Profile Analysis

For Instrumental Texture Profile Analysis (ITPA) testing of whole fish, one upper and one lower loin were selected from each fish. Loins, at ca. 4°C, were cut with an electric knife into a 2.54 cm X 2.54 cm X loin length rectangular slab, and then cut into 2.54 cm cube samples. Twelve samples per fish were prepared for testing. Small hydrothermal and small steamed samples were prepared by cutting each cylindrical sample, at 4°C, to 1.6 cm length to ensure sample length to diameter ratios fell between 1.0 and 1.5 to prevent sample buckling. All samples were check weighed to eliminate under and oversized samples, and then allowed to equilibrate to room temperature for approximately 35 minutes prior to testing. One representative sample from each ITPA test was monitored by a 30 gage type T thermocouple (Omega Engineering Inc., Stamford, CT), to assure ambient (ca. 25°C) temperature prior to the ITPA test. ADAM

4018M data acquisition modules, ADAM 4520 RS232 to RS422/RS485 converter module, and GENIE v. 2.12 data acquisition and control software (American Advantech Co., Sunnyvale, CA) were used to record temperature data.

Instrumental Texture Profile Analysis samples were tested using an 1122 Instron Universal Testing Machine (Instron Corp., Canton, MA), equipped with a 5.8 cm dia x 3.8 cm piston and an 890 N compression load cell. The piston and load cell platen were coated with non-stick vegetable oil spray prior to each sample so that samples would not adhere and cause erroneous test results. Samples were oriented with the muscle fibers perpendicular to the Instron platen in order to simulate how individual muscle fibers react to cleaning and handling during processing. For small hydrothermal and small steamed samples tests, the Instron was programmed to provide 80% compression and 50 mm/min crosshead speed. For whole fish, testing was performed using 70% compression and 50 mm/min crosshead speed due to limitations of the load cell. Testing parameters were selected based on review of other ITPA methods used on meats for destructive testing and an unpublished pretest that showed tuna tissue did not exhibit fracture at high compressions. MTS TestWorks v. 4.02 software (MTS Systems Corp., Eden Prairie, MN) was used to operate the Instron, record data, and calculate ITPA parameters. ITPA parameters recorded included hardness (H) and cohesiveness (C) as defined by Bourne (1978), and instantaneous springiness (S_{inst}) and retarded springiness (S_{ret}), as defined by Fiszman et al. (1998). Instantaneous springiness data was not recorded for the small steamed samples. Whole fish ITPA testing used 12 replicates per fish, and data were averaged (n = 12). Small hydrothermal ITPA parameters were averaged over 10 to 120 minutes due to sample thermal equilibrium at 10 minutes (n = 84) as previous research showed ITPA parameters were mainly affected

by temperature (Webb, 2003). Small steamed ITPA testing used two samples from four fish for the reported data (n = 8).

Weight loss and moisture content

All whole fish were weighed before and after thermal treatments, and weight loss was calculated as a percentage of initial fish weight (n = 1). Small hydrothermal (n = 84) and small steamed samples (n = 5) were weighed before and after treatment, and weight loss calculated as a percentage of initial sample weight. Moisture contents for whole fish (n = 6) and small hydrothermal samples (n = 84) used a composite sample gathered from meat tested by ITPA analysis. For small steamed samples, each samples from each thermal treatment were tested individually for moisture content after cooking (n = 5). All moisture contents were performed using AOAC air drying method 950.46B, modified by using 100°C as the drying temperature to lessen case hardening (AOAC, 1995).

Statistics

Data were analyzed by SAS 8.01 statistical analysis software (SAS, Cary NC). For the all experiments, upper/lower loin ITPA, moisture, and weight measurements did not differ significantly as determined by an ANOVA, therefore data were averaged between upper and lower loin samples. For small hydrothermal and small steamed samples, individual fish was not a factor over the treatment temperatures as determined by an ANOVA. Error bars in all graphs report a 95% confidence interval about the mean of the sample. An ANOVA was performed to see if weight loss, moisture content, and ITPA texture values were statistically different between experiment treatments. An ANOVA was also performed to gage the effect of temperature, weight loss, and moisture

content on ITPA texture parameters. For this analysis, data were grouped by experiment treatment.

RESULTS AND DISCUSSION

Treatment influence on weight loss, moisture content, and Instrumental Texture Profile Analysis parameters

Weight loss, moisture content, hardness, cohesiveness, and instantaneous springiness values measured by the three experiments were statistically different; however retarded springiness values were not statistically significant between experiments (Table 1). When data was grouped by experiment, temperature appears as the primary influence on texture parameters (Table 2). Cohesiveness was the only parameter that was not influenced by temperature. Weight loss was a factor in hardness and cohesiveness. The true influence of moisture content on ITPA parameters cannot be gauged due to the different experimental treatments between small hydrothermal and whole fish (heating, pressing) and small steamed (heating only) samples. From these statistics, temperature was considered to be the primary influence for texture parameters for all cooking methods. Data from whole fish varied more that small steamed and small hydrothermal samples (Figures 3-9), and is due to fish to fish variability, shown to be a factor in Skipjack tuna (Webb et al., 2003).

Table 1 **P values from ANOVA type III sum of squares for the effect of experiment treatment on weight loss, moisture content, and ITPA parameters of Skipjack tuna light loin meat.**

Variable	Experiment treatment
Weight loss (%)	<0.0001[a]
Moisture content (% wb)	0.012[a]
Hardness (N)	<0.0001[a]
Cohesiveness (N s/N s)	<0.0001[a]
Instantaneous Springiness (s/s)	0.0301[a]
Retarded Springiness (s/s)	0.1629

Values marked with [a] indicate statistical significance between experiment treatments at a = 0.05.

Table 2 **P values from ANOVA type III sum of squares for the effect of temperature, weight loss, and moisture loss on ITPA parameters of Skipjack tuna light loin meat grouped by whole fish, small steamed, and small hydrothermal samples.**

Variable	Sample Temperature (°C)	Weight Loss (%)	Moisture Loss (%)
Hardness (N)	0.0348[a]	0.0019[a]	0.0195[a]
Cohesiveness (N s/N s)	0.4058	<0.0001[a]	0.6365
Instantaneous Springiness (s/s)	0.0004[a]	0.6284	0.4656
Retarded Springiness (s/s)	0.0003[a]	0.1196	0.8501

Values marked with [a] indicate statistical significance between experiment treatments at a = 0.05.

Weight loss and moisture content comparison

Weight loss increased and moisture content decreased with increased temperatures for all experiment methods (Figure 3, Figure 4). Both variables were represented by linear models with temperature as the independent variable (Table 3). Weight loss and moisture content of small steamed samples were adequately represented by linear models, however whole steamed and small hydrothermal samples did not have as good of a fit for these variables. For small hydrothermal samples, measurements for weight loss and moisture content could be reflecting data non linearity, as samples were experiencing bidirectional mass transfer, evidenced by cloudy cooking water (protein out) and overall increased moisture content (water in) compared with small steamed samples, even after pressing. For whole fish moisture content samples, the lack of fit could be due a confounding effect from pressing the sample prior to moisture content analysis.

Table 3 **Linear prediction equations of weight loss and moisture content for temperature (°C) as the independent variable for Skipjack tuna small steamed, whole steamed, and small hydrothermal samples.**

Dependent variable	Small steamed	Whole steamed	Small hydrothermal
Weight loss (%)	$y = 0.25x - 5.56$ $R^2 = 0.94$	$y = 0.21x + 5.40$ $R^2 = 0.11$	$y = 0.03x + 14.75$ $R^2 = 0.29$
Moisture content (%)	$y = -0.079x + 74.88$ $R^2 = 0.88$	$y = -0.009x + 70.30$ $R^2 = 0.003$	$y = -0.009x + 71.45$ $R^2 = 0.10$

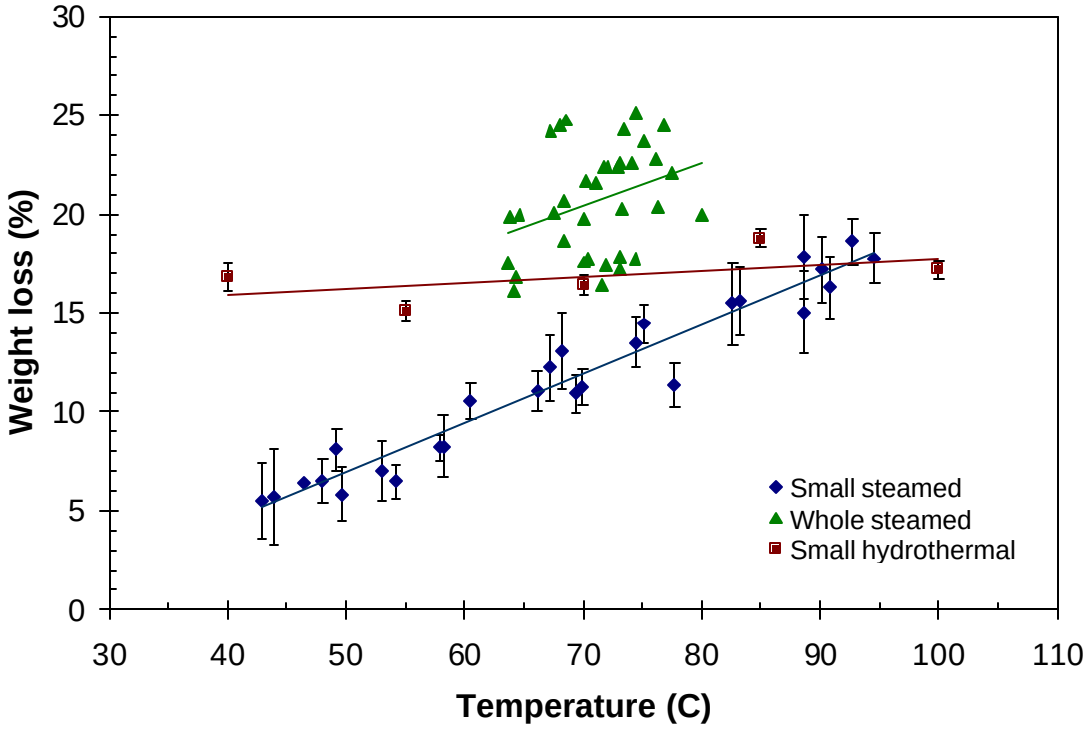

Figure 3 **Weight loss versus temperature for Skipjack tuna light loin meat small steamed, whole steamed, and small hydrothermal cooked samples. Error bars show 95% confidence of the sample mean.**

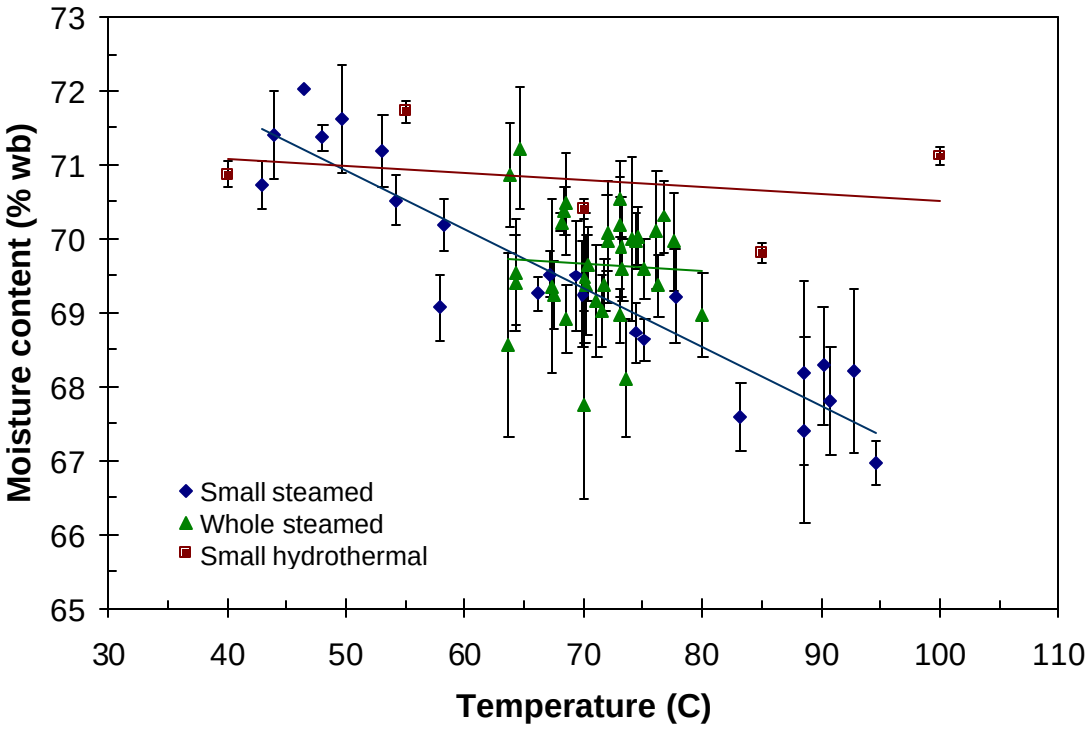

Figure 4 **Moisture content versus temperature for Skipjack tuna light loin meat small steamed, whole steamed, and small hydrothermal cooked samples. Error bars show 95% confidence of the sample mean.**

Whole fish weight loss paralleled small steamed samples weight loss (Figure 3). Higher weight loss and comparable moisture content loss, even after pressing, of whole fish versus small steamed samples could indicate whole fish lost more soluble protein or lost mass from the head and viscera of the fish. Skipjack tuna weight loss differs from beef weight loss. A comparison of retorted beef samples to Skipjack tuna treated by the three listed treatments shows that the beef had more weight loss and at a more rapid rate than Skipjack. Retorted beef sample weight loss ranged from 7.8% to 40.3% over 50 to 100°C. The beef weight loss data were better fit by a polynomial (R^2 = 0.99) than a linear (R^2 = 0.86) model (Palka and Daun, 1999). These authors attributed weight loss to actin and collagen denaturation which caused structural changes in the beef muscle which contracted and expelled water. Other researchers found similar results (Bouton and Harris, 1972; Bertola et al., 1993; Martens et al. 1982), although their data was better fit with linear models. Actual weight losses in Skipjack tuna were less and more gradual than that of beef, with a maximum weight loss of approximately 25% at 74°C for whole steamed fish. Bell et al. (2001) showed comparable data from Skipjack loin fillets which calculated to approximately 17% loss at 80°C. The weight loss difference between Skipjack and beef might be due differences in the degree of contraction and state of proteins after heating.

Bell et al. (2001) reported data for backbone moisture content of Skipjack tuna closely resembles small steamed sample data reported here (Figure 4). The moisture content relationship of Yellowfin tuna muscle to temperature was reported to be linear by Lassen (1965), and was almost parallel to small steamed sample moisture content, although values were approximately 1 to 1.5% lower than Skipjack.

Instrumental Texture Profile Analysis results

Hardness (H), instantaneous springiness (S_{inst}), and retarded springiness (S_{ret}) increased with increased temperature for all experiment treatments (Figures 5, 8, and 9). Cohesiveness (C) did not change with temperature during any experiment (Figure 7). All small hydrothermal ITPA parameters were adequately represented by linear models (Table 4). Small steamed ITPA hardness and retarded springiness were also adequately modeled by linear equations, however ITPA cohesiveness was not, and might indicate nonlinear behavior. Whole steamed samples ITPA parameters were not modeled accurately by linear equations. Like weight loss and moisture content loss for this treatment method, ITPA results show a good deal of data scatter. Large confidence intervals were also reported for all whole fish measurements. The variability of whole fish could be attributed to the variability of Skipjack tuna (Webb et al., 2003), or could be caused by difficulty in handling the whole fish samples thereby increasing sample friability and deterioration.

Table 4 **Linear prediction equations of listed texture dependent variables for temperature (°C) as the independent variable for Skipjack tuna small steamed, whole steamed, and small hydrothermal samples.**

Dependent variable	Small steamed	Whole steamed	Small hydrothermal
H (N)	$y = 3.08x - 53.54$ $R^2 = 0.97$	$y = 3.02x + 46.96$ $R^2 = 0.07$	$y = 2.70x - 35.23$ $R^2 = 0.94$
C (N s/N s)	$y = -0.0004x + 0.50$ $R^2 = 0.17$	$y = -0.0004x + 0.37$ $R^2 = 0.01$	$y = 0.0003x + 0.36$ $R^2 = 0.89$
S_{inst} (s/s)	--	$y = 0.005x - 0.09$ $R^2 = 0.09$	$y = 0.005x - 0.19$ $R^2 = 0.95$
S_{ret} (s/s)	$y = 0.0041x + 0.29$ $R^2 = 0.85$	$y = 0.003x + 0.27$ $R^2 = 0.03$	$y = 0.006x + 0.11$ $R^2 = 0.97$

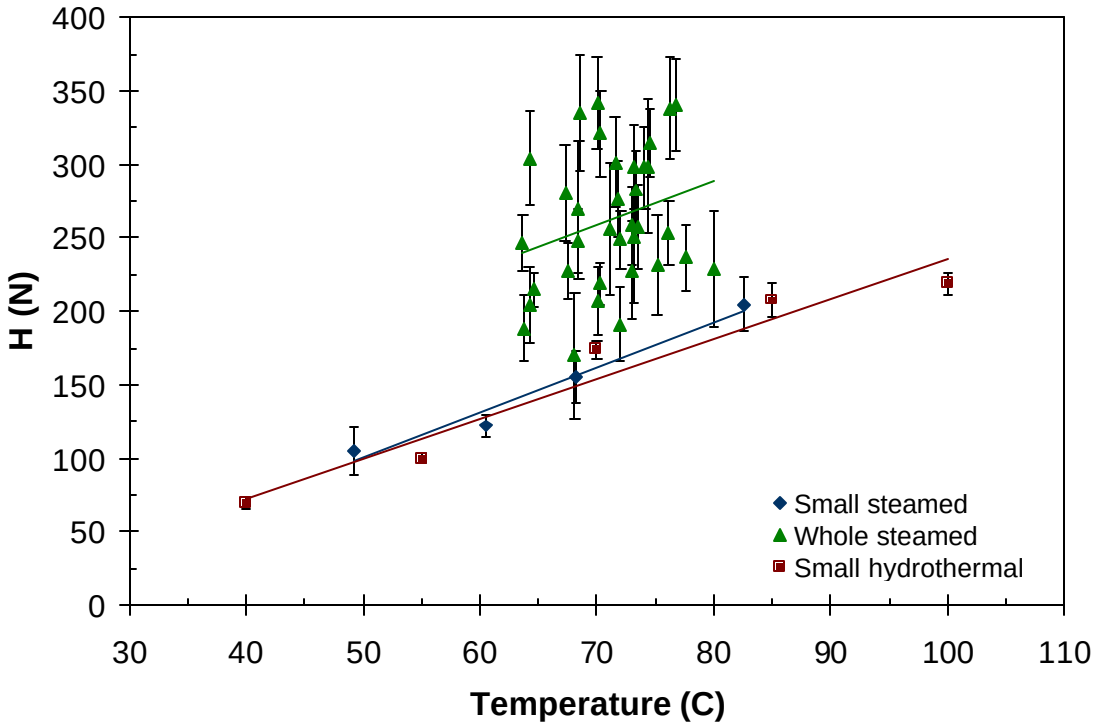

Figure 5 **ITPA hardness versus temperature for Skipjack tuna light loin meat small steamed, whole steamed, and small hydrothermal cooked samples. Error bars show 95% confidence from the sample mean.**

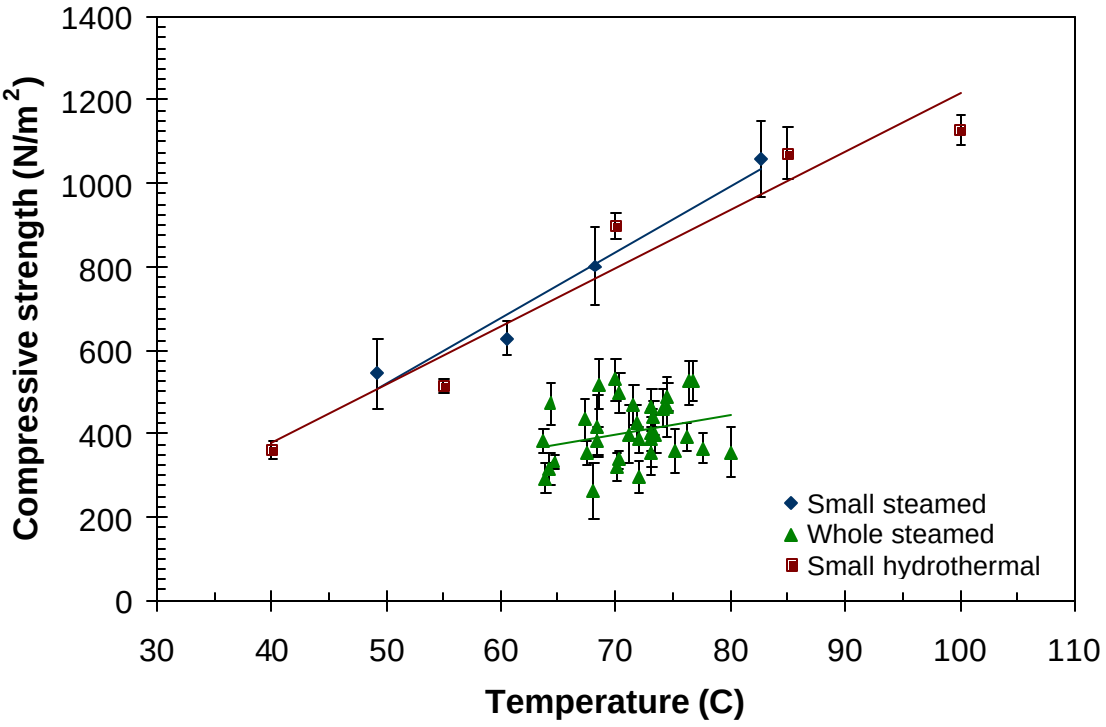

Figure 6 **Compressive strength versus temperature for Skipjack tuna light loin meat small steamed, whole steamed, and small hydrothermal cooked samples. Error bars show 95% confidence from the sample mean.**

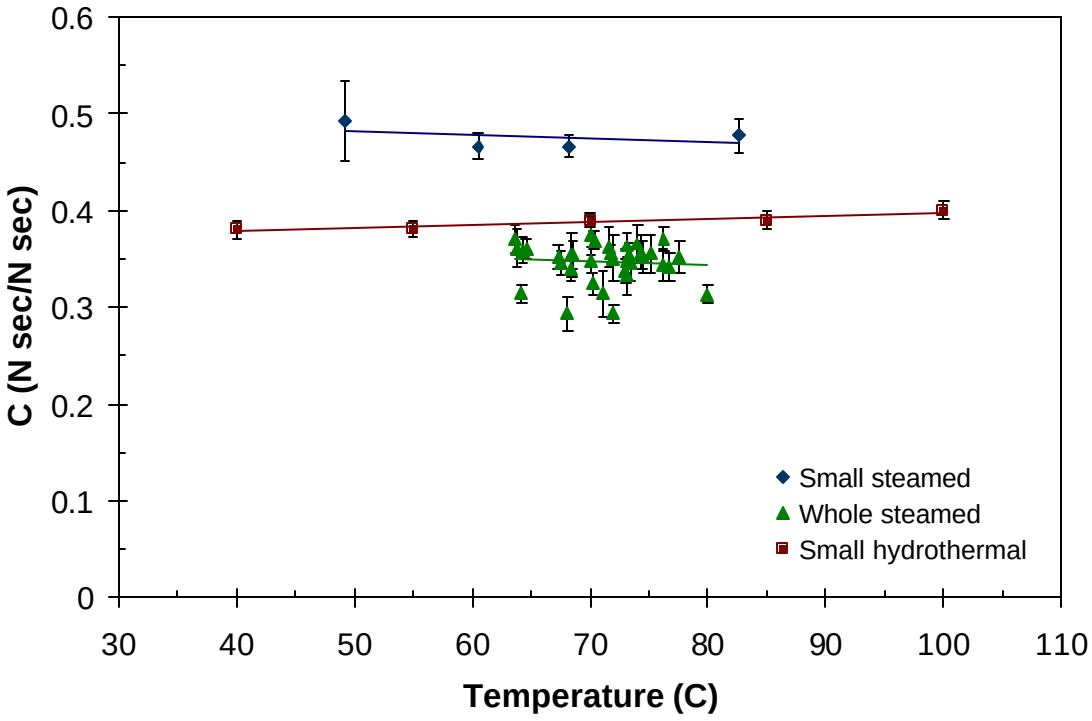

Figure 7 **Cohesiveness versus temperature for Skipjack tuna light loin meat small steamed, whole steamed, and small hydrothermal cooked samples.**

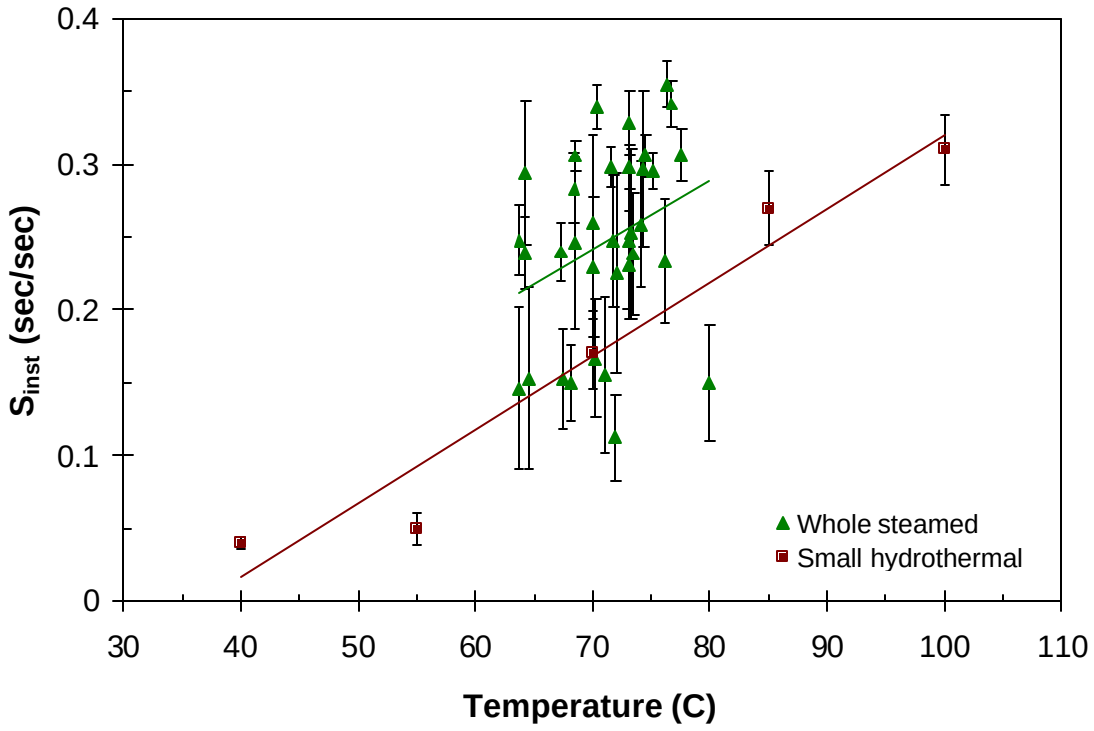

Figure 8 **Instantaneous springiness versus temperature for Skipjack tuna light loin meat small steamed, whole steamed, and small hydrothermal cooked samples.**

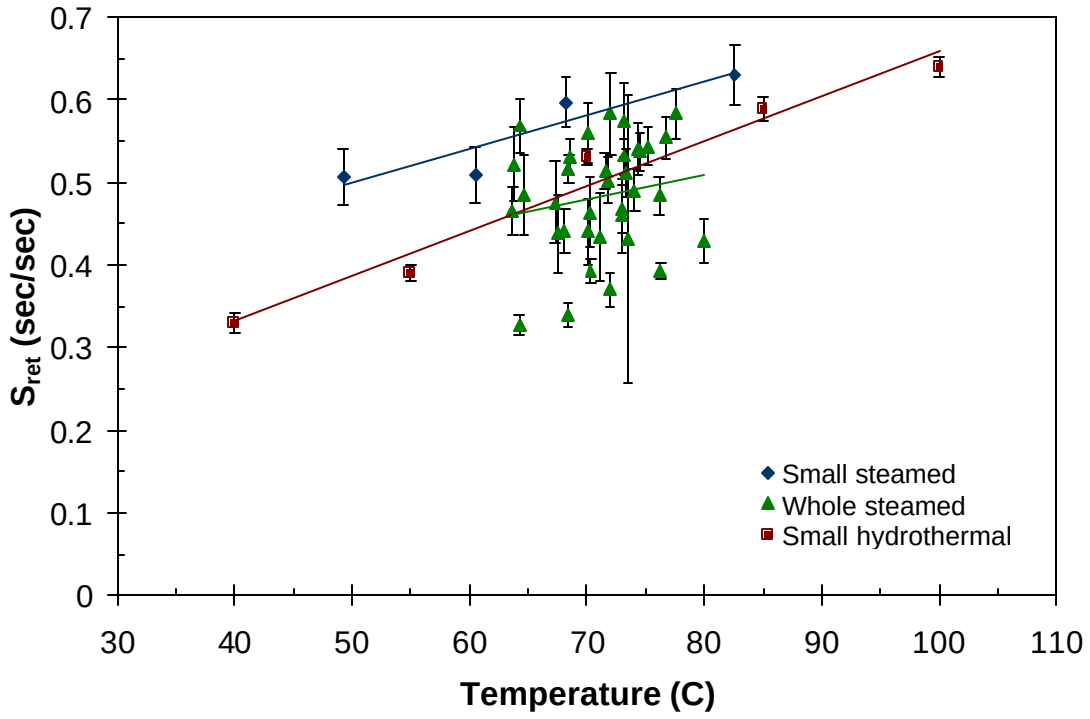

Figure 9 **Retarded springiness versus temperature for Skipjack tuna light loin meat small steamed, whole steamed, and small hydrothermal cooked samples.**

Hardness increased with increased temperature for all samples, and whole fish had higher hardness than small steamed and small hydrothermal samples (Figure 5). Hardness of small steamed and small water hydrothermal samples could be represented by one line, and paralleled whole fish samples. A linear increase in hardness with increased temperature was not reflected when small samples of chum salmon were hydrothermally treated. Average hardness values in this experiment increased from 60°C to 80°C, then decreased from 80°C to 100°C (Bhattacharya et al., 1993). Small samples of beef retorted in pouches showed hardness values more similar to data reported here. In this experiment, hardness increased from 50°C to 80°C, then plateaued from 80°C to 100°C (Palka and Daun, 1999). Hardness values of tuna samples were influenced by the characteristics of their myosin, collagen, and actin, and the agglomerates formed upon heating. Although fish myosins are generally more unstable than beef, tuna myosin has been found to be almost as stable as those found in beef (Venugopal and Shahidi, 1996). The increase in hardness shown by tuna from 80°C to 100°C might be attributed to a stronger agglomeration complex formed by tuna myosin, collagen, and actin, specifically the actin/myosin complex, upon protein denaturation. If the strength of denatured protein aggregates is mechanically stronger than native protein aggregates, the muscle will toughen (Martens et al., 1982). This toughening is related to the hardness measured from the three experiments performed in this study.

If sample geometry is taken into consideration, compressive strength, represented by the equation (Mohsenin, 1986) –

$$Compressive\ Strength = \frac{F}{A_0}$$

of whole steamed is roughly half that of small steamed and small hydrothermal samples (Figure 6). Larger hardness values for whole fish reflect larger area of applied force of whole fish samples. Heating times for small steamed and whole fish were similar, as small hydrothermal samples were heated a maximum of 2 hours and whole fish were heated from 1.08 to 2.05 hours. Increased small steamed and small hydrothermal compressive strength, as compared to whole fish, could be caused by a greater force on whole fish due to sample weight during cooking. This larger force could affect muscle macrostructure and microstructure, and lessen compressive strength.

Cohesiveness values did not change with temperature for all cook methods (Figure 7). Small steamed samples had higher cohesiveness than small hydrothermal and whole steamed samples. Small steamed samples probably retained more collagen than hydrothermal samples, because small steamed samples experienced less heating time and hydrothermal samples were subjected to the collagen hydrolyzing effect of water. Cooking muscle in water hydrolyzes collagen (Hedrick et al., 1989). Collagen surrounds muscle fiber bundles, and when hydrolyzed might not be available for agglomeration with other denaturing proteins, or might exit the sample. Lack of collagen might lessen the cohesiveness of the sample by reducing the cohesiveness of muscle fiber bundles.

The result of cohesiveness being unaffected by temperature corresponds to cohesiveness results of small samples of hydrothermally treated chum salmon (Bhattacharya, 1993), but not to results from small beef samples retorted in pouches. Results from this experiment showed that cohesiveness slightly increased from 50°C to 70°C, then dropped from 70°C to 100°C. Cohesiveness is the least influenced by degree of compression over the range of 50 to 93%, as compared with all other ITPA parameters (Bourne and Comstock, 1981). From these data, the trend difference

between chum salmon, tuna, and beef is most likely not influenced by the degree of compression of the samples (75%, 70-80%, and 50% respectively). Cohesiveness could be influenced by the quality and quantity of fish versus beef collagen. Beef has more collagen, and it is more thermally stable fish collagen (Dunajski, 1979; Venugopal and Shahidi, 1996). The lower amount of Skipjack tuna collagen present was denatured and/or solubilized at the temperatures studied, and did not influence cohesiveness.

Instantaneous springiness was measured for small hydrothermal and whole steamed experiments only, as data were not recorded for small steamed samples (Figure 8). Whole steamed values were higher than small hydrothermal samples. Instantaneous springiness has been shown to relate to sample elasticity (Fiszman et al., 1998), and is also referred to as resilience (Veland and Torrissen, 1999). Higher instantaneous springiness values for whole steamed samples could indicate either higher sample elasticity or a difference in compression height, as whole steamed samples were not compressed to the degree that small hydrothermal samples were compressed. More sample compression might have made for a less resilient material which would not "push back" as much and reduce this measurement.

For the retarded springiness data, small steamed samples had higher values than small hydrothermal cooked and whole steamed samples (Figure 9). Retarded springiness was reported as a measure of the relative magnitude of the viscous component of food, which causes recovery of the sample to its initial height to be delayed (Fiszman et al., 1998). A small value for retarded springiness would indicate a sample recovered less of its original height, and would have more of a viscous component. The degree of compression was the same for small hydrothermal and small steamed samples, therefore degree of compression did not influence retarded springiness values for these treatments, and small steamed samples reacted less

viscously than small hydrothermal samples. This is likely due to more water contained in the small hydrothermal than the small steamed samples.

Retarded springiness of small hydrothermally treated chum salmon generally increased with increased temperatures over 60°C to 100°C, but not as linearly as Skipjack (Bhattacharya, 1993). Small beef samples retorted in pouches did not follow a linear increase of retarded springiness with increased temperature (Palka and Daun, 1999), For these samples, retarded springiness decreased from 50°C to 60°C, then increased and plateaued from 70°C to 80°C, then again decreased from 80°C to 100°C. This phenomenon was attributed to actin and myosin denaturation over the tested temperature range, and also with beef fiber diameter changes, as instantaneous springiness changed up and down with increased and decreased fiber diameter. A linear increase of retarded springiness for Skipjack tuna over the same temperature range indicate tuna actin and myosin are more susceptible to denaturation and agglomeration. Increased fiber diameters causing increased retarded springiness levels are not suspected, as other researchers have noted decreased fiber diameter from raw to precooked Skipjack (Lampila and Brown, 1986)

Relational equations between treatments

Slopes of linear models for small hydrothermal and small steamed sample measured variables were similar to slopes of linear models for measured variables for whole steamed fish, even though whole steamed fish had the greatest data variability. Table 5 shows the relationship equations between measured values of small steamed, small hydrothermal, and whole steamed samples. These equations can be used to convert data gathered by the listed experiment methods applied to small steamed and small hydrothermal samples to that of the meat of whole fish processed by the whole

steamed fish method. These relational equations can be used by processors to predict texture, weight, and moisture content changes of whole fish from measurements taken from small sample experiments.

Table 5 Linear prediction equations of listed dependent variables for whole fish as a function of small steamed and small hydrothermal values for Skipjack tuna samples.

Whole steamed (Predicted variable = y)	Small steamed (Measured variable = x)	Small hydrothermal (Measured variable = x)
Weight loss (%)	$y = 0.8587x + 10.1712$	$y = 7.15x - 100.090$
Moisture content (% wb)	$y = 0.1148x + 61.7042$	$y = 0.9681x + 1.1312$
H (N)	$y = 0.9677x + 102.6645$	$y = 1.1160x + 86.2758$
C (N s/N s)	$y = x - 0.1278$	$y = -1.3333x + 0.8579$
S_{inst} (s/s)	--	$y = 0.9216x + 0.0835$
S_{ret} (s/s)	$y = 0.7317x + 0.0514$	$y = 0.5455x + 0.2052$

CONCLUSIONS

For all treatments, weight loss and moisture content linearly decreased with increased temperature, and hardness, instantaneous springiness, and retarded springiness increased with linearly increased temperature. Cohesiveness did not vary with temperature. Weight loss, moisture content, and ITPA values reacted similarly, regardless of experiment method. Data variability was greatest for whole steamed fish, and is a result of fish to fish variability and the difficulty of handling whole fish for texture measurements.

Because linear models of measured variables had similar trends, ITPA, weight loss, and moisture content data from small steamed and small hydrothermal samples were related to ITPA, weight loss, and moisture content values of whole steamed fish by linear fit models. These conversion equations can be used to relate texture, weight, and moisture changes of precooked whole fish from small samples which are more easily processed.

ACKNOWLEDGMENTS

This work was supported by a grant from the StarKist Seafood Company and the USDA National Needs Fellowship program. The authors would also like to thank Tim Seaboch for his assistance in this work.

REFERENCES

AOAC, 1995. Official Methods of Analysis, 16th ed. Association of Official Analytical Chemists, 39.1. Washington, DC.

Bell, J.W., Farkas, S.A., Hale, S.A., and Lanier, T.C., 2001. Effect of thermal treatment on moisture transport during steam cooking of Skipjack tuna (Katsuwonas pelamis). Journal of Food Science, 66 (2), 307-313.

Bell, J., 1999. Unpublished data. North Carolina State University, Department of Food Science, Raleigh, North Carolina.

Bell, J., 1998. Personal communication. North Carolina State University, Dept. of Food Science, Raleigh, North Carolina.

Bertola, N.C., Bevilacqua, A.E., and Zaritzky, N.E. 1994. Heat treatment effect on texture changes and thermal denaturation of proteins in beef muscle. Journal of Food Processing and Preservation, 18, 31-46.

Bhattacharya S., Choudhury, G.S., and Studebaker, S. 1993. Hydrothermal processing of Pacific chum salmon: effects on texture and in-vitro digestibility. Journal of Food Quality, 16, 243-251.

Bourne, M.C., 1978. Texture profile analysis. Food Technology, July 62-66, 72.

Bourne, M.C. and Comstock, S.R., 1981. Effect of degree of compression on texture profile parameters. Journal of Texture Studies, 12, 201-216.

Bouton, P. E. and Harris, P. V. 1972. The effects of cooking temperature and time on some mechanical properties of meat. Journal of Food Science, 37, 140-144.

Bouton, P.E., Harris, P.V., and Shorthose, W.R. 1975. Possible relationships between shear, tensile, and adhesion properties of meat and meat structure. Journal of Texture Studies, 6 (3), 297-314.

Califano, A.N., Bertola, N.C., Bevilacqua, A.E., and Zaritzky, N.E. 1997. Effect of processing conditions on the hardness of cooked beef. Journal of Food Engineering, 34, 41-54.

Duizer, L.M., Gullett, E.A., and Findlay, C.J. 1996. The relationship between sensory time-intensity, physiological electromyography, and instrumental Texture Profile Analysis measurements of beef tenderness. Meat Science, 42, 215-224.

Fiszman, S.M., Pons, M., and Damasio, M.H. New parameters for instrumental texture profile analysis: instantaneous and retarded recoverable springiness. Journal of Texture Studies, 29, 499-508.

Hamann, D.D. and Lanier, T.C. 1986. Instrumental methods for predicting seafood sensory texture quality. Seafood Quality Determination, Proceedings of an international symposium coordinated by the University of Alaska Sea Grant College program, Anchorage, Alaska, 10-14 November 1986.

Hedrick, H.B., Aberle, E.D., Forrest, J.C., Judge, M.D., Merkel, R.A. 1989. Palatability and cookery of meat. Ch. 12 in Principles of Meat Science, 3rd ed., p. 269-287, Kendall/Hunt Publishing Co., Dubuque, Iowa.

Kanoh, S., Polo, J.M.A., Kariya, Y., Kaneko, T., Watabe, S., and Hashimoto, K. 1988. Heat-induced textural and histological changes of ordinary and dark muscles of Yellowfin tuna. Journal of Food Science, 53 (3), 673-678.

Lampila, L.E. and Brown, W.D. 1986. Changes in the microstructure of Skipjack tuna during frozen storage and heat treatment. Food Microstructure, 5, 25-31.

Lassen, S., 1965. Tuna Canning and the Preservation of the Raw Material through Brine Refrigeration. Ch. 4 in Fish as Food, v 4, part 2, G. Borgstrom (Ed.) p. 207-245, Academic Press, New York and London.

Martens, H., Stabursvik, E., and Martens, M. 1982. Texture and colour changes in meat during cooking related to thermal denaturation of muscle proteins. Journal of Texture Studies, 13, 291-309.

Mathevon, E., Mioche, L., Brown, W.E., and Culioli, J. 1995. Texture analysis of beef cooked at various temperature by mechanical measurements, sensory assessments, and electromyography. Journal of Texture Studies, 26, 175-192.

Mohsenin, N.N., 1986. Physical properties of plant and animal materials. Gordon and Breach Science Publishers, New York.

Palka, K. and Daun, H. 1999. Changes in texture, cooking losses, and myofibrillar structure of bovine *M. semitendinosus* during heating. Meat Science, 51, 237-243.

Segars, R.A. and Johnson, E.A. 1986. Instrumental measurement of the textural quality of fish flesh: effect of pH and cooking temperature. Seafood Quality Determination, Proceedings of an international symposium coordinated by the University of Alaska Sea Grant College program, Anchorage, Alaska, 10-14 November 1986.

Veland, J.O. and Torrissen, O.J., 1999. The texture of Atlantic salmon (*Salmo salar*) muscle as measured instrumentally using TPA and Warner-Brazler shear test. Journal of Science in Food and Agriculture, 79, 1737-1746.

Venugopal, V. and Shahidi, F. 1996. Structure and composition of fish muscle. Food Review International, 12 (2), 175-197.

Webb, E.L., Hale, S.A., and Farkas, B.E., 2003. Relating texture and protein changes of Skipjack tuna (*Katsuwonas pelamis*) loin meat to different time and hydrothermal treatments by ITPA and DSC analysis. Manuscript in preparation.

Wheaton, F.W. and Lawson, T.B. 1985. Processing aquatic food products., p. 158-162, John Wiley & Sons, New York.

5.0 MANUSCRIPT 3

Comparison of multiple linear regression, fuzzy logic, and neural network models for predicting Skipjack tuna (*Katsuwonus pelamis*) pre-cooking effects

ABSTRACT

Fuzzy logic, neural network, and multiple linear regression models were used to predict precook time, weight loss, friability, and edible weight using inputs of frozen weight, final backbone temperature, and storage time of 2.8 to 5.2 kg Skipjack tuna over the range of 63.7°C to 80.0°C final cook temperature. The fuzzy logic and neural network models outperformed the multiple linear regression model. Cook time and weight loss were better predicted by all models than friability and edible weight. More data is needed to quantify friability and edible weight. Frozen storage time was not needed as a model input except when predicting fish weight loss. The difference in fish weight losses due to frozen storage time is most probably the result of the different water contents of the fish after freezing but before cooking.

Key Words – Tuna, weight, time, edible, friability, fuzzy logic, neural network, multiple linear regression

INTRODUCTION

Thermal processing of food is a study in optimization. Processor's goals are to heat their product enough to obtain the desired texture, microbial, and/or enzymatic parameters without over treating the product and diminishing yield and quality. Accurate models of the outcomes of thermal processes are necessary to understand the effect of different process variables on quality and yield. Processors use mathematical models to predict the impact of thermal processing, for instance predicting the change in vitamin content of a food as a function of time with a first order model (Taoukis and Labuza, 1996). Other effects of thermal processing on food, such as texture and weight changes, are not as easily quantified by mathematical models due to the heterogeneous nature of most food systems and our incomplete knowledge of the effect of heat on the system's components.

One strategy for modeling food processes is to modify the knowledge gained from the system as little as possible. In this approach, the underlying physical phenomena are represented by a shallow knowledge base, and the sum of the knowledge is represented by quantitative data as equations, measurements, and conditional statements (Dohnal et. al. 1993). Multiple linear regression, fuzzy logic, and neural network models are all variations of this technique in that they model available data without applying any fundamental rules of system behavior.

Multiple linear regression (MLR) is a modeling technique where measured variables are modeled as linearly dependent on system inputs. This technique can predict linear changes in multiple independent variables as a result of dependent variable manipulation. The advantage of using MLR is that it is a simple statistical model that assumes no underlying physical phenomena. Studies have found MLR correlated soak time and soak temperature with drain weight and texture of cowpeas (Taiwo et. al.

1998). Other studies noted that MLR outperformed neural networks when modeling sensory color quality of tomatoes and peaches, although the neural network models were less complex (Thai and Shewfelt, 1991). The disadvantage of MLR is that it fails to predict nonlinear behavior. Researchers proved that surimi quality was a nonlinear function of harvesting/processing input combinations and product quality attributes, and MLR was inadequate to describe quality behavior. Neural networks were a better choice to model surimi quality (Peters et. al. 1996).

Fuzzy logic is a modeling technique that makes decisions much like a human operator would – by logical decisions based on imprecise linguistic descriptions of variables and processes. Fuzzy logic can give accurate models where variables are measurable, repeatable, yet vaguely described and the underlying mathematical relationships are not known. This modeling technique is advantageous because it can deal with human interpretations of processes which are complex and non linear. Fuzzy logic is a good choice to model food systems behaviors, and has been used to determine the degree of doneness of beef steaks (Unklesbay et. al. 1988). Meat chilling and brewing malt modification have each been successfully modeled using fuzzy logic (Donhal et. al 1993). Other examples include fuzzy logic controllers for both continuous and batch fermentation processes and sunflower oil extraction (Zhang et. al. 1993). Several studies were successful in using fuzzy logic to control grain drying (Zhang and Litchfield, 1993) and to model cooked pea texture (Xie et al., 1998).

An artificial neural network is a modeling method that mimics biological neural processes by assigning connection strength between inputs and outputs. These models adapt, or learn, by trial and error. Paired input/output responses are presented, model responses are compared to correct responses, and model parameters are adjusted according to those responses. Neural networks model non linear behavior well, and do

not require *a priori* knowledge of the relationships between variables. A neural network outperformed principal component analysis for prediction of milk shelf life (Vallejo-Cordoba et. al. 1995). Wheat loaf volume was also better predicted by neural networks than by principle component analysis (Horimoto et. al. 1995). Other studies have shown that this modeling technique can be used to predict the temperature, moisture content, and fat in both slab shaped foods and meatballs during deep fat frying (Mittal and Zhang, 2000; Mittal and Zhang 2001). These researchers also predicted temperature and moisture content of frankfurters during thermal processing (Mittal and Zhang, 2000). Studies have shown a neural network can model generated data describing bioprocessing variable estimations and corresponding state predictions (Linko and Zhu, 1991).

The goal of this study was to develop and compare multiple linear regression, fuzzy logic, and neural network models to predict the cook time, friability, edible weight, and yield loss of Skipjack tuna during precooking.

MATERIALS AND METHODS

Precook treatment

Thirty-five fish from five different lots of Skipjack tuna shipped from Mayguez, Puerto Rico were used in this study. Fish weights ranged from 2.8 kg to 5.2 kg. Fish were almost equally split into two storage time categories, “new” fish that were stored in the –40°C freezer approximately one month prior to cooking, and “old” fish stored approximately six months prior to cooking.

Fish were tempered in 22°C water to -2.2°C center (backbone) temperature prior to cooking, as monitored by a standard meat thermometer. After thawing, a 28 ga. type

T thermocouple wire coated with Teflon heat shielding (Omega Engineering Inc., Stamford, CT) was inserted into one of the upper loins, and placed to measure "backbone" temperature, next to the backbone at the thickest part of the fish. Thermocouple location was approximately 2.54 cm back from the start of the dorsal fin, and 15° to 20° angle from vertical, towards one of the two pectoral fins.

For each experiment, one to three fish were cooked with 100°C – 104°C steam in a pilot plant retort. Fish were suspended in the retort in wire baskets and were not allowed to touch. "Pull" temperatures, temperatures at which the fish were removed from the retort, ranged from 57.2°C to 73.9°C backbone temperature. Final temperatures, maximum temperature that fish reached after they were removed from the retort, ranged from 63.7°C to 80.0°C backbone temperature. Fish weight, final temperatures, and storage time were selected to give models a broad range of training examples.

Fish were moved from steam to ambient conditions at the predetermined "pull" temperature and allowed to cool in ambient air by free convection. At ca. 35°C backbone temperature, fish were transferred to a 4°C cooler and chilled to ca. 25°C backbone temperature prior to cleaning. Fish, steam and ambient temperatures were recorded at 1 minute intervals throughout the experiment with ADAM 4018M data acquisition modules, an ADAM 4520 RS232 to RS422/RS485 converter module, and GENIE v. 2.12 data acquisition and control software (American Advantech Co., Sunnyvale, CA).

Weight loss, edible weight, and friability

After chilling to 25°C fish were taken from the cooler, weighed and cleaned. Skin was scraped off the fish with a small blunt knife, and the head and fins were removed. The meat surrounding the visceral cavity was recovered. The fish were then split in half

along the upper dorsal line and pulled apart. The spine was removed in one piece, and small bones that protect the gut cavity were removed from the lower loins. The upper and lower loins from each half were then separated, and red meat was cleaned from the loins. Constituents of each fish were then weighed. The edible portion of the fish was comprised the upper and lower loins and belly meat.

For friability measurements, one upper and one lower loin were selected from each fish, and checked to assure ambient temperature. Loins were chopped lengthwise at a ¾" center to center diagonal cut. Each loin was then placed on a stack of 1 ½", 1", ½" Tyler sieves. The sieves were shaken side to side by hand five times, and then each sieve was weighed. Friability for each fish was calculated using the friability equation listed in ASTM method D 441 – 86 (ASTM, 1994).

Model development

Model inputs were fish frozen weight, final backbone temperature, and frozen storage time as independent variables. The original data set containing 35 data points was randomly divided into a training/testing set of 28 data points and a validation set of seven data points. The training/testing set was used to find optimum parameters for all models, and the validation set was used to validate all models after the final test/train procedure.

The MLR model coefficients and fuzzy logic model input/output membership functions and rules were determined by the complete training/testing data set of 28 data points. The training data set was further partitioned for the neural network model into four data sets of seven data points each for model training using different training/testing set combinations.

A multiple linear regression (MLR) model was written in SAS 8.01 statistical analysis software (SAS, Cary NC) to obtain coefficients for the following equation:

$$Y = b_0 + b_1X_1 + b_2X_2 + b_3X_3 + b_4X_1X_2 + b_5X_1X_3 + b_6X_2X_3 + b_7X_1X_2X_3 + e$$

where *ß$_n$ are model coefficients, X_1*, *X_2*, and *X_3* are the independent variables frozen weight, final temperature, and frozen storage time, respectively, and *e* is the standard error. Dependent variables were each modeled separately and combined to calculate the root mean square error (RMSE) of the entire model. For the MLR model, a full model using all combinations of independent variables was tried first, and model terms were dropped in order to maximize the adjusted R^2, F value, and minimize the probability of a Type I error. Final MLR model structure was –

$$\begin{bmatrix} y_1 \\ y_2 \\ y_3 \\ y_4 \end{bmatrix} = \begin{bmatrix} b_{1,0} & b_{1,1}x_1 & 0 & b_{1,3}x_3 & 0 & b_{1,5}x_1x_3 & 0 & b_{1,7}x_1x_2x_3 \\ b_{2,0} & b_{2,1}x_1 & b_{2,2}x_2 & 0 & 0 & 0 & 0 & 0 \\ b_{3,0} & b_{3,1}x_1 & 0 & 0 & b_{3,4}x_1x_2 & 0 & 0 & b_{3,7}x_1x_2x_3 \\ b_{4,0} & 0 & 0 & 0 & b_{4,4}x_1x_2 & 0 & 0 & 0 \end{bmatrix}$$

where dependent model terms were percent edible weight (y_1), cook time (y_2), percent weight loss (y_3), and percent friability (y_4).

A fuzzy logic model was developed using MatLab Neural Net Toolbox (The Math Works, Natick, MA). For this model three input variables of weight, temperature, and frozen storage time and four output variables of friability, weight loss, weight edible, and cook time were used. Six fuzzy sets were used for weight, six fuzzy sets were used for temperature, and two fuzzy sets were used for frozen storage time. Sigmoidal input membership functions and trapezoidal output membership functions were used in the model to simplify computations (Figure 1). Range of crisp values for all variables were as follows: weight, 2.8 – 5.2 kg; temperature, 63.7 – 80.0°C; storage time, 0 (new fish) or 1 (old fish); cook time, 1.08 – 2.5 hours; weight loss, 16.1 – 25.1%; weight edible,

47.9 – 54.6%; and friability, 9.2 – 31.3%. Using IF THEN logic, 72 fuzzy rules were written, and membership functions were modified to minimize the RMSE of the test set. Mamdani implication and centroid defuzzification were used to map input to output variables.

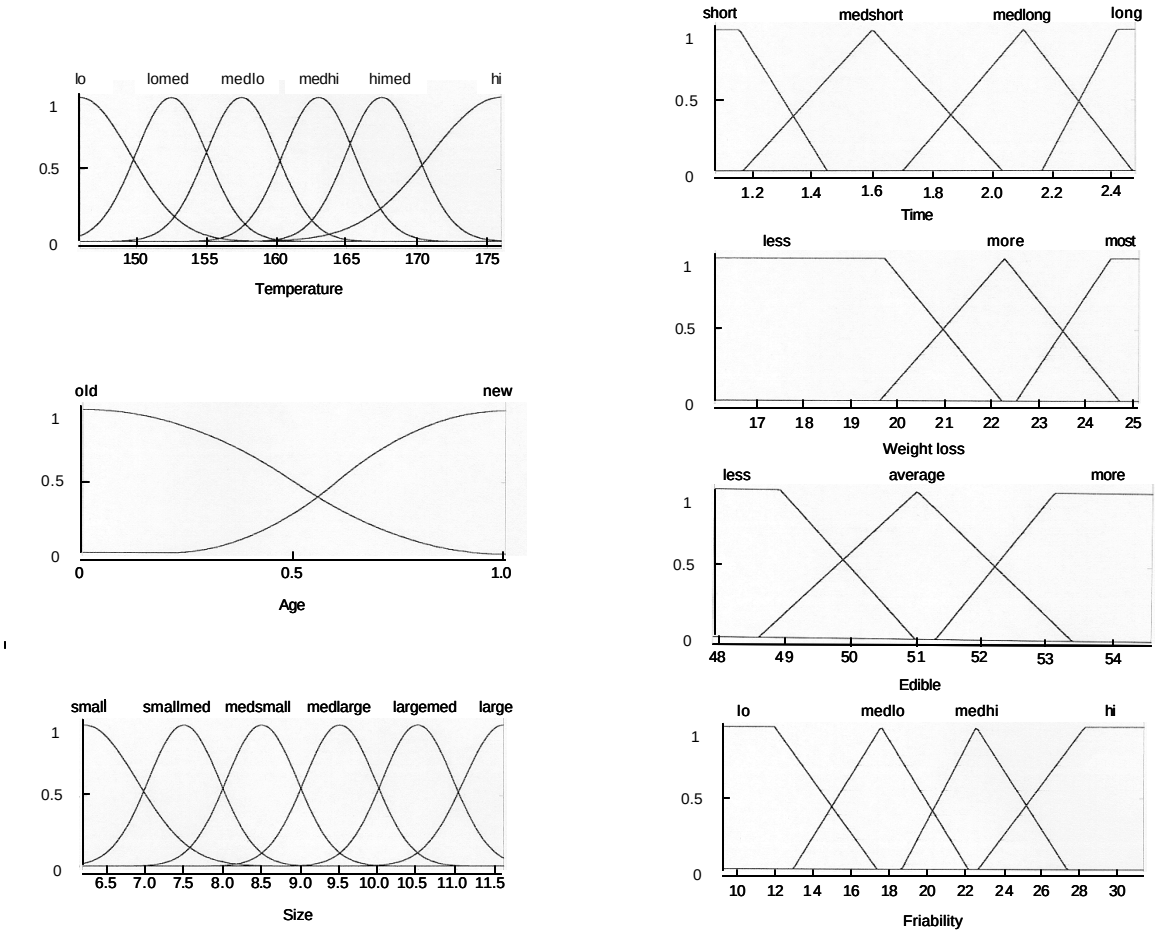

Figure 1 Fuzzy logic model input (left) and output (right) membership functions.

A neural network model with three inputs of weight, final temperature, and frozen storage time, four outputs of friability, weight loss, weight edible, and cook time, and one hidden layer was designed using MatLab Neural Network Toolbox (Demuth and Beale, 2002). Input and output data were scaled using max/min normalization to eliminate the

effect of one variable overshadowing others during modeling (Kennedy et al., 1995). A back propagation algorithm using gradient descent, fixed momentum, and adaptive learning rate was used. The network hidden layer contained log sigmoid neurons, and the output layer used linear neurons. The number of hidden neurons needed for the problem was calculated from four to nine by four different methods –

$\frac{(inputs + outputs)}{2} = \frac{(3+4)}{2} = 3.5 \approx 4$ Lawrence, 1994.

$(training\ \ patterns)^{0.5} = (28)^{0.5} = 5.3 \approx 5$ Kennedy et al., 1995.

$2(inputs + outputs)^{0.5} = 2(3+4)^{0.5} = 5.3 \approx 5$ Ward Systems Group, 1989.

$\frac{(inputs + outputs)}{2} + (training\ \ patterns)^{0.5} = 8.8 \approx 9$ Ward Systems Group, 1993.

Because of the estimated nature of assigning neuron number to a hidden layer, two to ten neurons were initially used. Momentum terms over the range of 0.0 to 1.0 (Kennedy et al., 1995) were combined with different numbers of neuron in the hidden layer. RMSE average and standard deviation for each testing/training set combination was compared over the range of momentum and hidden neuron values to optimize hidden neuron number and momentum term value. The top 5 hidden neuron/momentum combinations, as judged by the lowest average RMSE and tightest RMSE standard deviation were then tested five times over the same testing/training data set combinations to minimize the effect of random initialization weights for the network. The combination of momentum and number of neurons that gave the lowest average RMSE and tightest RMSE standard deviation was selected to train the model. Optimum

number of hidden neurons for this problem was six and optimum momentum was 0.3 using this technique (Figure 2).

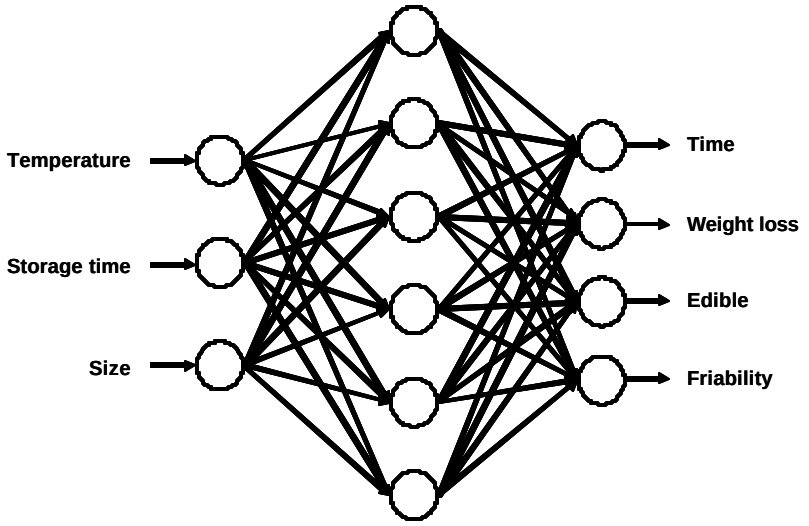

Figure 2 Three input, six hidden neuron, four output neural network model.

RESULTS AND DISCUSSION

Model best fit, as denoted by the highest R^2, was generally produced by the fuzzy logic and neural network models (Table 1). Fitness as designated by RMSE, usually followed R^2. Fuzzy logic and neural network models fit the data better due to the non-linearity of the data and the ability of these models to predict nonlinear behavior. The performance of the MLR model was less effective for both training and validation data sets for all dependent variables, with the exception of edible weight.

MLR model training set R^2 and RMSE were best for edible weight, but MLR validation set R^2 and RMSE for this variable were worse. All models had low fitness for this dependent variable, with R^2 ranging from 0.27 to 0.31 for training data and 0.03 to 0.55 for validation data. Likewise, friability had low fitness, with R^2 ranging from 0.26 to 0.35 for training data and 0.14 to 0.31 for validation data. These two variables were

hard to measure, and more training examples are needed to better quantify their behavior.

Table 1 MLR, neural network, and fuzzy logic R^2 and RMSE for time, edible weight, weight loss, and friability of Skipjack tuna.

	time		edible weight		weight loss		friability	
training	R^2	RMSE	R^2	RMSE	R^2	RMSE	R^2	RMSE
mlr	0.82	0.14	0.32	1.51	0.74	1.37	0.26	4.23
nnet	0.85	0.13	0.26	1.59	0.77	1.30	0.35	3.96
fuzzy	0.87	0.13	0.27	1.58	0.72	1.44	0.32	4.40
validation	R^2	RMSE	R^2	RMSE	R^2	RMSE	R^2	RMSE
mlr	0.77	0.17	0.03	1.54	0.80	1.26	0.30	3.70
nnet	0.81	0.20	0.29	1.29	0.80	1.25	0.31	4.11
fuzzy	0.80	0.20	0.55	1.09	0.84	1.28	0.14	5.02

Correlations of experimental values and predicted values for the entire data set of dependent variables confirm that the neural network and fuzzy logic models performed better than the MLR models (Figures 3-6). The dependent variable time had the best correlation between predicted and actual variables (Figure 3). The relationship between precook backbone "pull" temperature and time spent in the precooker for Skipjack tuna has been modeled by researchers using finite element analysis (Zhang et al., 2002). These researchers predicted time in the precooker for a backbone "pull" temperature given specific fish weights, ambient temperatures, and other thermal properties. The multiple linear regression, fuzzy logic, and neural network models presented in this research predict precook time, or "pull time" for a desired final backbone temperature, frozen fish mass, and storage time of the fish.

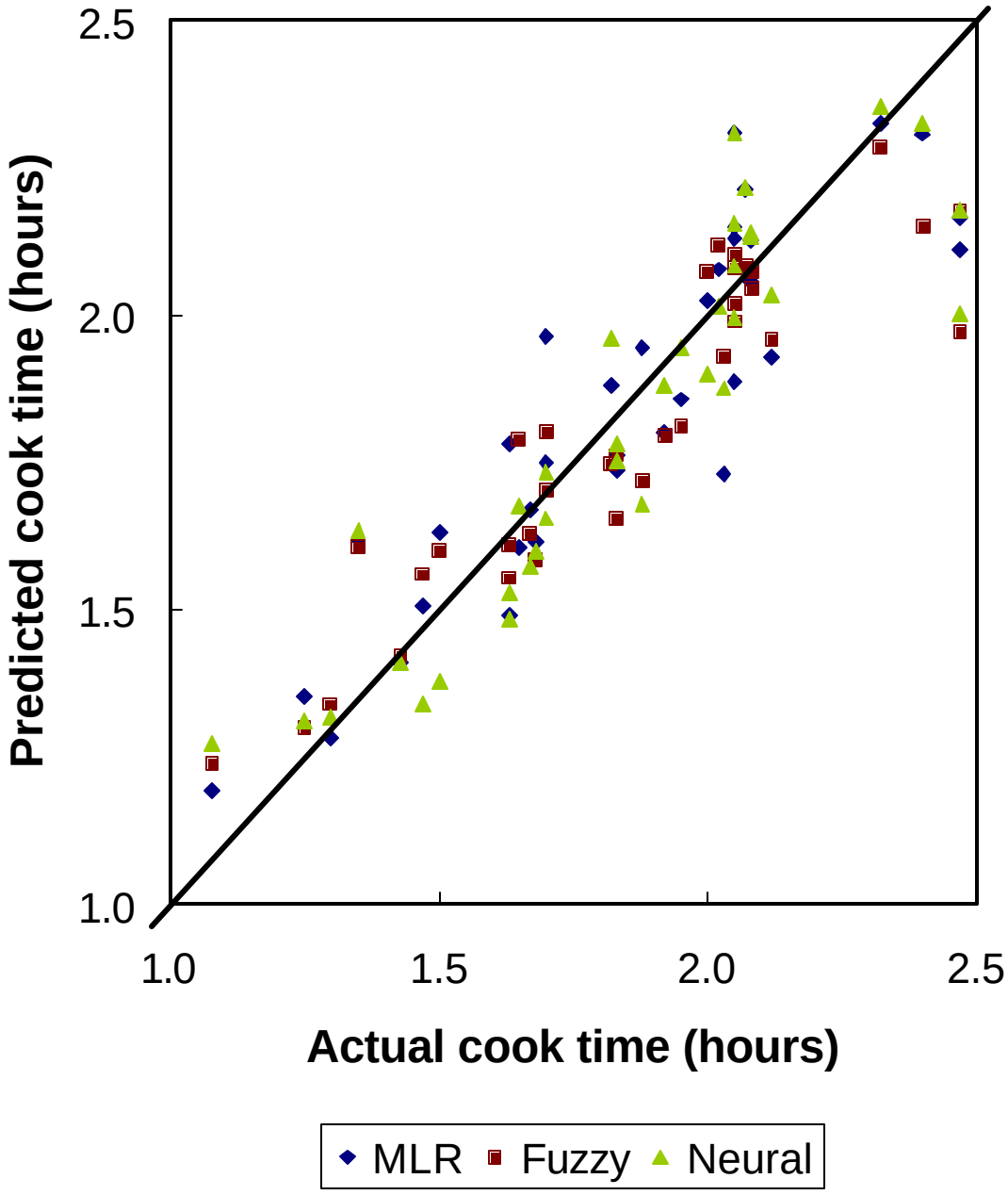

Figure 3 **Predicted versus actual cook time for multiple linear regression, fuzzy logic, and neural network models.**

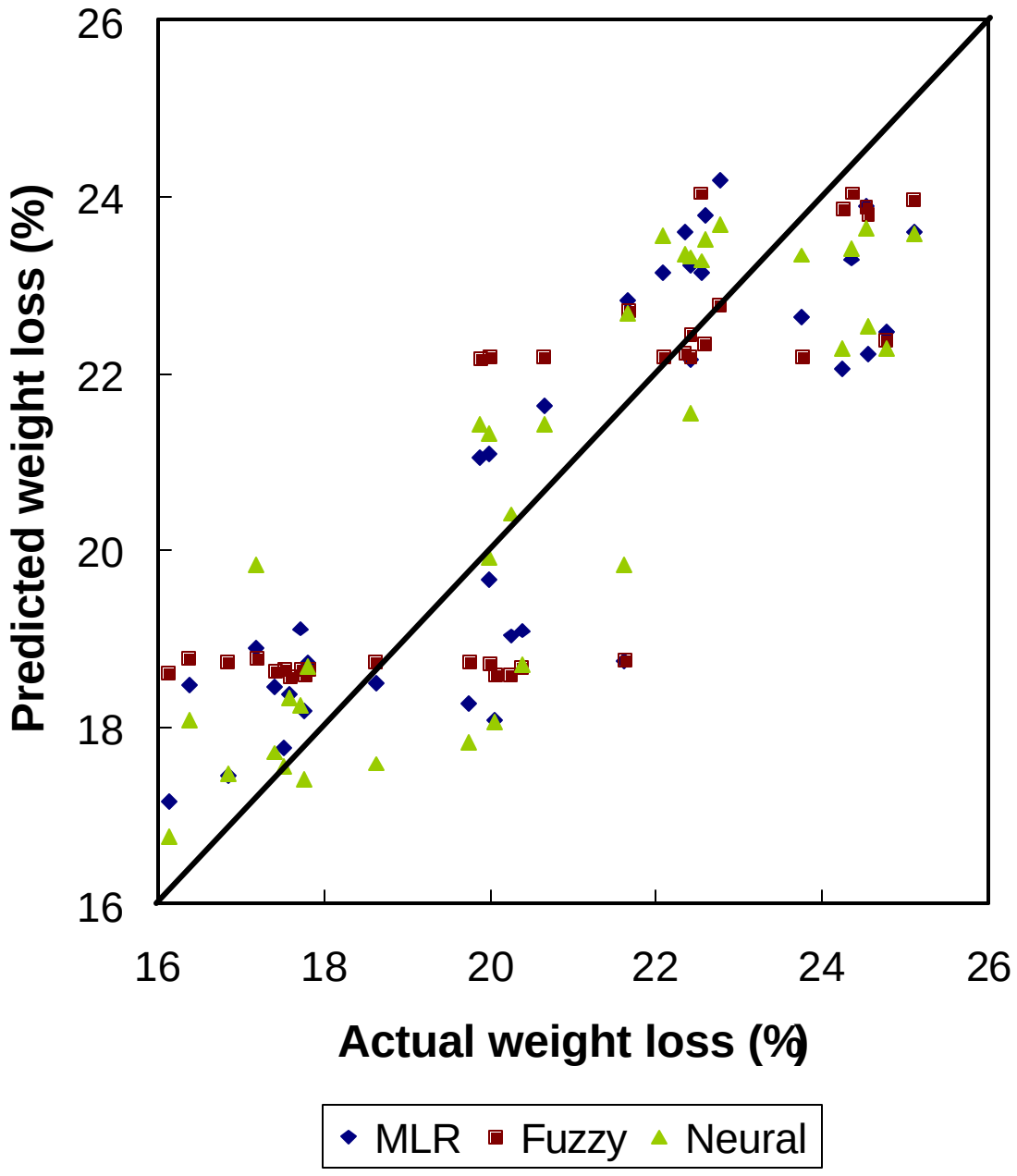

Figure 4 **Predicted versus actual weight loss for multiple linear regression, fuzzy logic, and neural network models.**

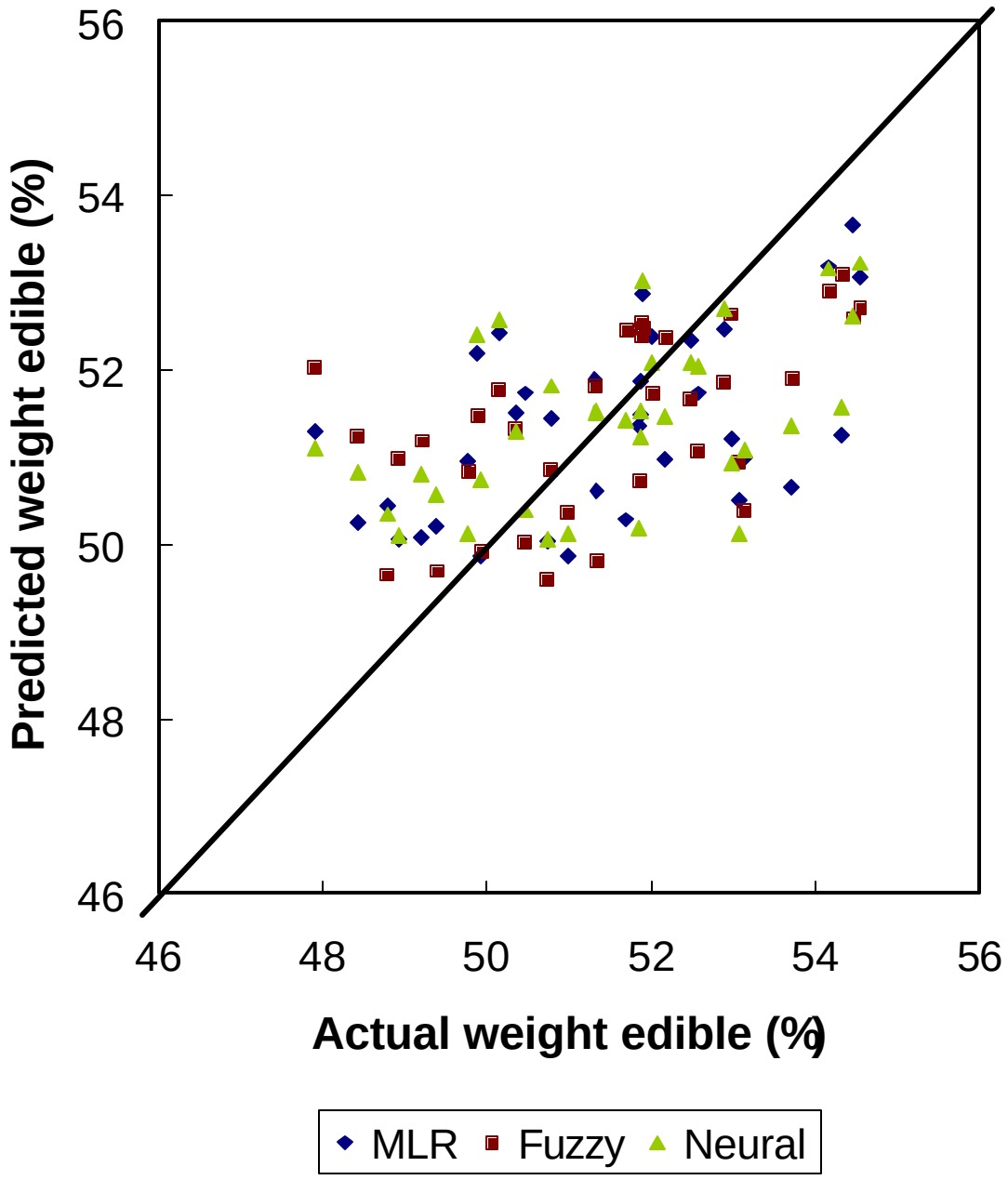

Figure 5 **Predicted versus actual weight edible for multiple linear regression, fuzzy logic, and neural network models.**

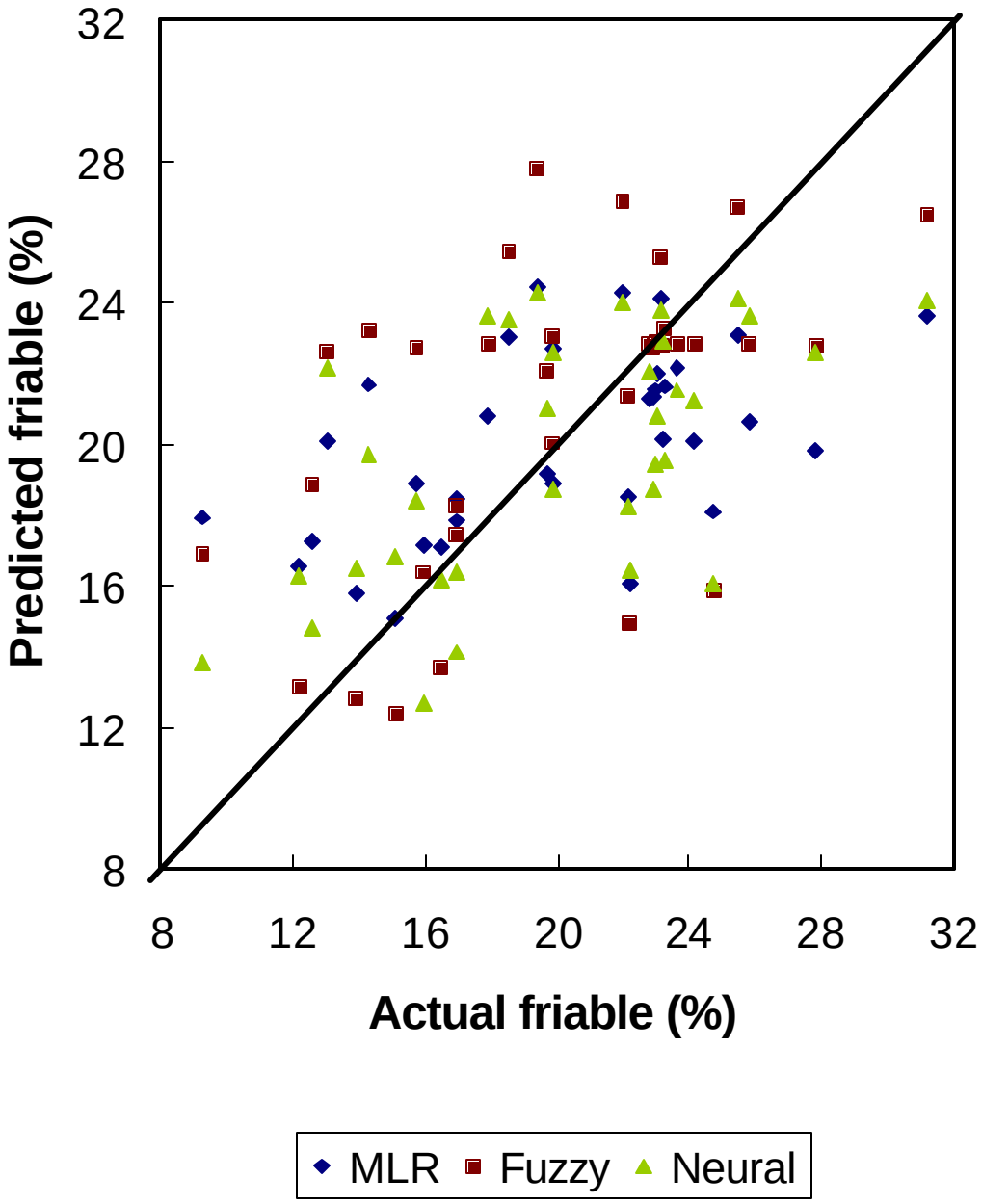

Figure 6 **Predicted versus actual friability for multiple linear regression, fuzzy logic, and neural network models.**

Predicted and actual weight loss also correlated well (Figure 4). Again, the neural net and fuzzy logic models performed better than the MLR model. Both R^2 and RMSE increased for the validation set, and indicate how a small data set, even with resampling, can influence these statistics.

All models performed poorly on the variables weight edible and friability (Figure 5 and Figure 6). These variables were difficult to quantify, and R^2 and RMSE values were not consistent with these variables. The lack of fit is also shown by the data scatter, and all signify that more data is needed to quantify any relationship between independent and these dependent variables. Measurement variability of edible weight can be attributed to the small sample size and the method of hand cleaning prior to weighing, as depth of cleaning varied from fish to fish. Thirty-five fish is not a sufficient sample size for this measurement. Greater sample size, perhaps in a production environment, would improve this measurement. Raw data range for this variable was from 47.9% to 54.5%, a 12.1% range over the variables. More measurements are needed because of the variability of the measurement and the lack of data range. For comparison, data ranges for cook time was from 1.1 hour to 2.5 hours, or a 56% range and data ranged for weight loss from 16.1% to 25.1%, or 35.9%. Measurement variability of friability also suffers from insufficient data. Again, a sample of 35 fish is insufficient to quantify this variable. More data would help to smooth out fish to fish variability, although data range was adequate at 70.2%, measured from 9.3% to 31.2%.

Frozen weight and final temperature were more relevant to the models than storage time, with the exception of percent weight loss. The influence of fish storage time on percent weight loss could be attributed to sublimation of samples when stored in the freezer. Fish stored for a longer period of time had more time for mass transfer by

subliming water, and it is theorized that these fish had less weight loss when cooking due to less water at the beginning of cooking.

CONCLUSIONS

Fuzzy logic and neural net models perform better than traditional multiple linear regression models in predicting precook time and weight loss of Skipjack tuna given final desired backbone temperature, frozen fish mass, and fish storage time in the freezer. Friabililty and edible weight were difficult to quantify with all models, and more data is needed to better quantify these variables. Fish storage time was not needed as a model input except when predicting weight loss, and could be caused by lower water content of frozen fish stored for a longer period of time before cooking.

ACKNOWLEDGMENTS

This work was supported by a grant from the StarKist Seafood Company and the USDA National Needs Fellowship program.

REFERENCES

ASTM, 1994. Standard test method for tumbler test for coal. American Society for Testing and Materials, D 441 – 86.

Demuth, H. and Beale, M., 2002. Neural Network Toolbox for use with MatLab, Users guide, version 4, release 13. The MathWorks, Natick, MA.

Donhal M, Vystrcil J, Dohnalova J, Marecek K, Kvapilik M, and Bures P. 1993. Fuzzy food engineering. Journal of Food Engineering 19, 171-201.

Horimoto Y, Durance T, Nakai S, and Lukow OM. 1995. Neural networks vs principal component regression for prediction of wheat flour loaf volume in baking tests. Journal of Food Science, 60 (3) 429-433.

Kennedy, R., Lee, Y., Reed, C., and Van Roy, B. 1995. Solving Pattern Recognition Problems. Unica Technologies Inc., Brighton, MA.

Lawrence, J., 1994. Introduction to Neural Networks – Design, Theory, and Applications. California Scientific Software, Nevada City, CA.

Linko P and Zhu Y. 1991. Neural network programming in bioprocess variable estimation and state prediction. Journal of Biotechnology 21, 253-270.

Mittal GS and Zhang J. 2000. Prediction of temperature and moisture content of frankfurters during thermal processing using neural network. Meat Science 55, 13-24.

Mittal GS and Zhang J. 2000. Use of artificial neural network to predict temperature, moisture, and fat in slab-shaped foods with edible coatings during deep-fat frying. Journal of Food Science, 65 (6) 978-983.

Mittal GS and Zhang J. 2001. Artificial neural network for the prediction of temperature moisture and fat contents in meatballs during deep-fat frying. International Journal of Food Science and Technology 36, 489-497.

Peters G, Morrissey MT, Sylvia G, and Bolte J. 1996. Linear regression, neural network, and induction analysis to determine harvesting and processing effects on surimi quality. Journal of Food Science 61 (5) 876-880.

Taiwo KA, Akanbi CT, and Ajibola OO. 1998. Regression relationships for the soaking and cooking properties of two cowpea varieties.

Taoukis, P. and Labuza, T.P., 1996. Summary: Integrative concepts. In Food Chemistry, Fennema, O. (ed). Marcel Dekker, New York, NY.

Thai CN and Shewfelt RL. 1991. Modeling sensory color quality of tomato and peach: neural neworks and statistical regression. Transactions of the ASAE, 950-955.

Unklesbay K, Keller J, Unklesbay N, and Subhangkasen D. 1988. Determination of doneness of beef steaks using fuzzy pattern recognition. Journal of Food Engineering 8, 79-90.

Vallejo-Cordoba B, Arteaga GE, and Nakai S. 1995. Predicting milk shelf-life based on artificial neural networks and headspace gas chromatographic data. Journal of Food Science, 60 (5) 885-888.

Ward Systems Group, 1989. NeuroShell: Neural Network Shell Program. Ward Systems Group, Inc., Frederick, MD.

Ward Systems Group, 1993. NeuroShell, version 4, online documentation. Network architecture – backpropagation, number of hidden neurons. Ward Systems Group, Inc., Frederick, MD.

Xie G, Xiong R, and Church I., 1998. Comparison of kinetics, neural network and fuzzy logic in modeling texture changes of dry peas in long time cooking. Lebensm.-Wiss. u.- Technol. 31, 639-647.

Zhang, J, Farkas, B.E., and Hale, S.A., 2002. Precooking and cooling of Skipjack tuna (*Katsuwonas pelamis*): a numerical simulation. Lebensm. Wiss. u Technol., 35, 607 – 616.

Zhang, J., 2002. Numerical simulation of the commercial tuna thawing, precooking, and cooling process. Ph. D. dissertation, North Carolina State University, Raleigh, North Carolina.

Zhang Q and Litchfield JB. 1993 Fuzzy logic control for a continuous crossflow grain dryer. Journal of Food Process Engineering 16, 59-77.

Zhang Q, Litchfield JB, Bentsman J. 1993. Fuzzy logic control for food processes. Food dehydration, AIChE symposium series, 89, 90-97.

6.0 SUMMARY AND CONCLUSIONS

6.1 Project summary

The impact of precook temperature and time combinations on the Instrumental Texture Profile Analysis (ITPA) texture parameters, protein state, weight loss, and moisture content of hydrothermally treated tuna loin meat was investigated. It was found that temperature was the primary influence for all ITPA parameters, however time influences texture when samples are held at 55°C. Auto proteolysis was suspected at this temperature, as some ITPA parameters declined with increased time.

Data from small steamed and small hydrothermally treated samples was compared with data from whole steamed fish to ascertain whether small sample results could be extrapolated to data from whole precooked fish. Weight loss, moisture content, and ITPA values reacted similarly, regardless of experiment method. For all treatments, weight loss and moisture content decreased with increased temperature, and hardness, instantaneous springiness, and retarded springiness increased with increased temperature. Cohesiveness did not vary with temperature. Linear conversion equations were written to predict texture, weight loss, and moisture content results of whole precooked fish from small steamed and small hydrothermal samples.

Process inputs which are available from a commercial precooking unit operation were used to model effects of precooking Skipjack tuna. Fuzzy logic, neural network, and multiple linear regression models were written to predict precook time, weight loss, friability, and edible weight of precooked fish from final backbone temperature, frozen weight, and storage time inputs. Both fuzzy logic and neural net models perform better than traditional multiple linear regression models in predicting cook time and weight loss.

Friability and edible weight were difficult to quantify with all models, and more data was needed to better quantify these variables.

In summary, Skipjack tuna texture, protein, moisture content, and weight changes during hydrothermal cooking were quantified over the range of precook times and temperatures found in a commercial cannery. Hydrothermal data was compared to data from whole steamed fish and small steamed samples. Cooking method differences were found, although general trends between cooking methods were the same. Linear relationships were defined to translate between cooking methods. Final backbone temperature, frozen weight, and storage time of whole fish were used to predict precook time, weight loss, friability, and edible weight with fuzzy logic, neural network, and multiple linear regression models. Although more research is required to fully control the precook unit operation to maximize plant yield, the results presented here are an important first step in achieving this goal. Therefore the ultimate purpose of this research for defining the texture and mass changes associated with precooking Skipjack tuna have been met.

6.2 Recommendations for the tuna canning industry

The overall findings of this research, the texture and mass loss dynamics during precooking Skipjack tuna as related to temperature and time, gives a starting point for better control of the precook unit operation. The following recommendations are made to the tuna canning industry –

1) Limit the amount of time Skipjack experience 55°C. 55°C has been shown to degrade meat texture parameters.

2) Cook fish in such a way to reduce the amount of time needed to raise a fish to the desired precook temperature. This will limit the amount of time at 55°C. One way would be to cook fillets instead of whole fish. Smaller portions of fish also exhibit greater compressive strength than whole steamed fish, which could indicate smaller portions are stronger and less friable than larger, whole fish.

3) Try to target a 60 - 65°C final backbone temperature. Higher final backbone temperatures appear to cause increased friability, as seen in larger error bars from texture measurements of fish treated at higher temperatures, and from data included in the Appendix, which shows higher sample friability at a higher process temperature. Less friable fish at cleaning will increase plant yield by decreasing the amount of edible meat lost to dark meat and fish meal. Lower final backbone temperatures can result in undesirable texture changes, decreased carcass yields due to reduced "cleanability" of the carcass, and unacceptable canned product quality.

4) Use a model that accurately predicts precooking time given frozen fish mass and desired final backbone temperature. Checking backbone temperature right out of the precooker does not give the final temperature, or temperature profile, that the fish experienced. In addition, final temperature, not precook time, for most treatment regimes was the only variable which affected tuna texture. An accurate model which can translate final fish temperature, a difficult variable to measure, to precook time, a simple measurement, would help canneries control final fish temperature and process fish more consistently.

6.3 Future work

Proposed future research includes the following –

- Make a texture model given a final backbone temperature for a Skipjack tuna. Researchers have proposed such a model for cooked beef –

Califano, A.N., Bertola, N.C., Bevilacqua, A.E., and Zaritzky, N.E., 1997. Effect of processing conditions on the hardness of cooked beef. Journal of Food Engineering, 34, 41-54.

- Further investigate the influence of frozen fish mass and final backbone temperature on the friability and edible weight of precooked Skipjack. More data points are needed to refine the model fits of paper three, and it is recommended these data are gathered in a production environment.

- Write multiple linear regression, fuzzy logic, and neural network models using inputs of final temperature and frozen fish weight to predict cook time, weight loss, edible weight, and friability for a simulated precooking unit operation of one fish. Compare and contrast the model results.

- If one model shows promise, adapt it to control a pilot plant precooker, and quantify results.

- If the pilot plant experiment goes well, scale up the control scheme to a production precooker and quantify results.

APPENDIX

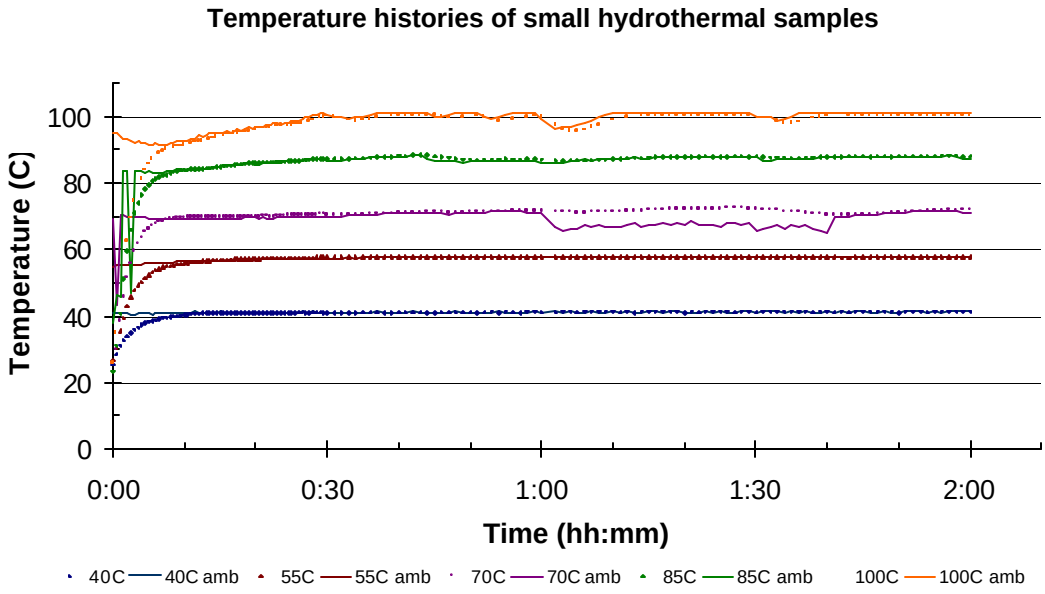
Temperature histories of small hydrothermal samples
Temperature (C)
100
80
60
40
20
0
0:00
0:30
1:00
1:30
2:00
Time (hh:mm)
40C
40C amb
55C
55C amb
70C
70C amb
85C
85C amb
100C
100C amb

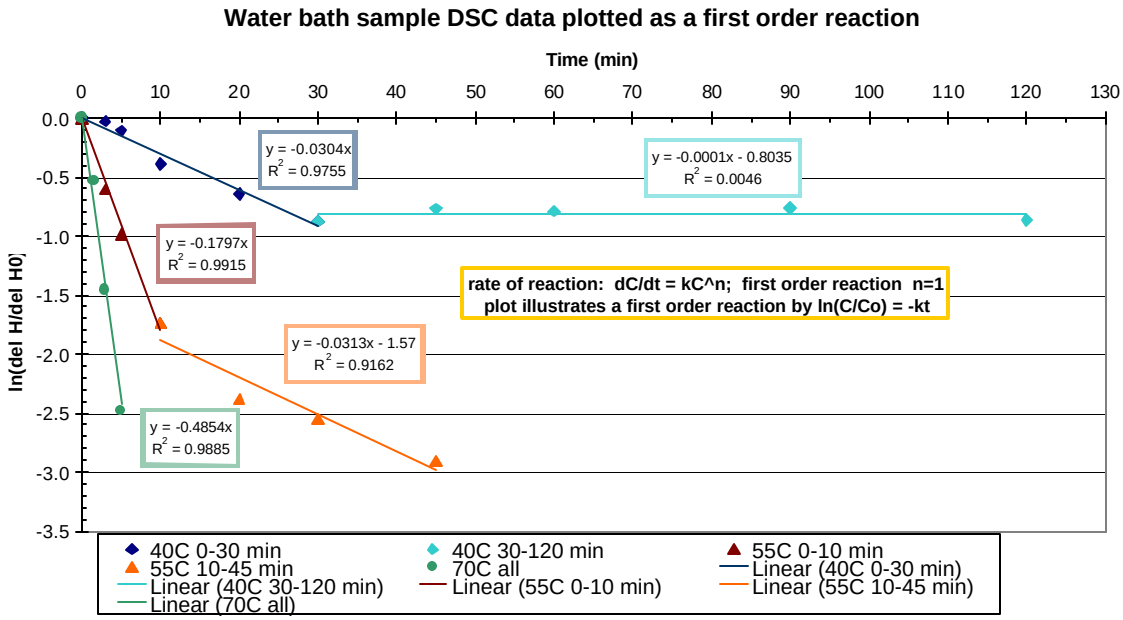
Water bath sample DSC data plotted as a first order reaction
Time (min)
0
10
20
30
40
50
60
70
80
90
100
110
120
130
0.0
-0.5
-1.0
-1.5
-2.0
-2.5
-3.0
-3.5
ln(del H/del H0)
y = -0.0304x
R2 = 0.9755
y = -0.0001x - 0.8035
R2 = 0.0046
y = -0.1797x
R2 = 0.9915
rate of reaction: dC/dt = kC^n; first order reaction n=1
plot illustrates a first order reaction by ln(C/Co) = -kt
y = -0.0313x - 1.57
R2 = 0.9162
y = -0.4854x
R2 = 0.9885
40C 0-30 min
40C 30-120 min
55C 0-10 min
55C 10-45 min
70C all
Linear (40C 0-30 min)
Linear (40C 30-120 min)
Linear (55C 0-10 min)
Linear (55C 10-45 min)
Linear (70C all)

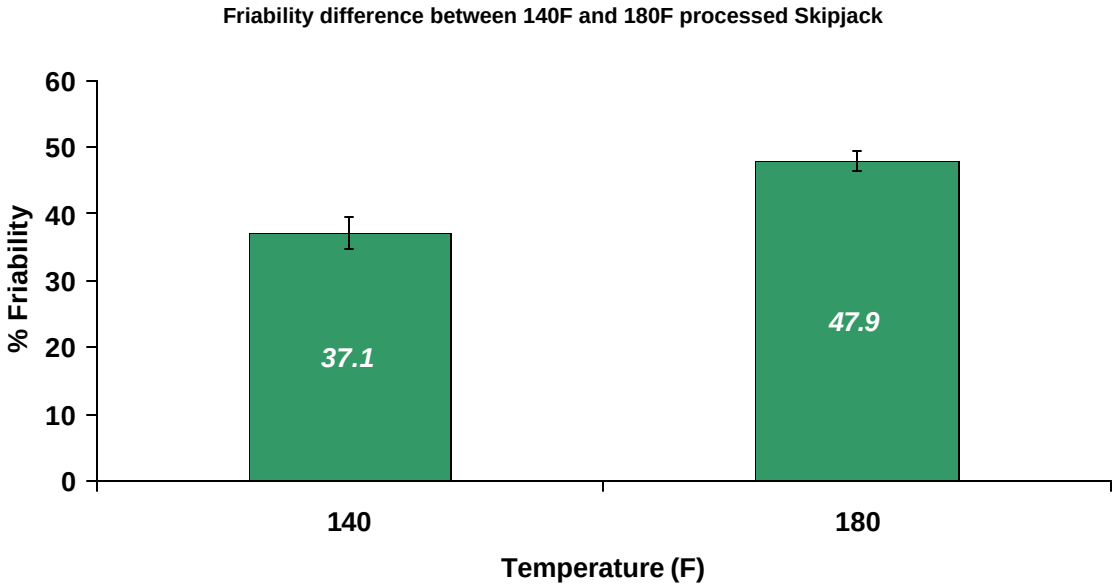
Friability difference between 140F and 180F processed Skipjack
% Friability
60
50
40
30
20
10
0
37.1
47.9
140
180
Temperature (F)

SENSITIVITY CALCULATION FOR NEURAL NETWORK BACKPROPAGATION ALGORITHM

Mathematics behind the backpropagation algorithm for multilayer, nonlinear networks

Backpropagation is an approximate steepest descent algorithm which uses mean square error (MSE) as a performance index. Backpropagation is descendent of the least mean square (LMS) algorithm, which uses the same concept of approximate steepest descent, except is only valid for a single layer network with linear transfer functions. LMS is limited to single layer, linear transfer function networks because the error of these networks is an explicit linear function and derivatives with respect to the weights can be easily calculated. Backpropagation is used in multilayer networks with nonlinear transfer functions, and the relationship between network weights and error is more complex. The chain rule of calculus is needed in order to calculate the derivatives for error backpropagation. In fact, the backpropagation error through a multilayer neural network with nonlinear transfer functions is primarily an exercise in using the chain rule of calculus.

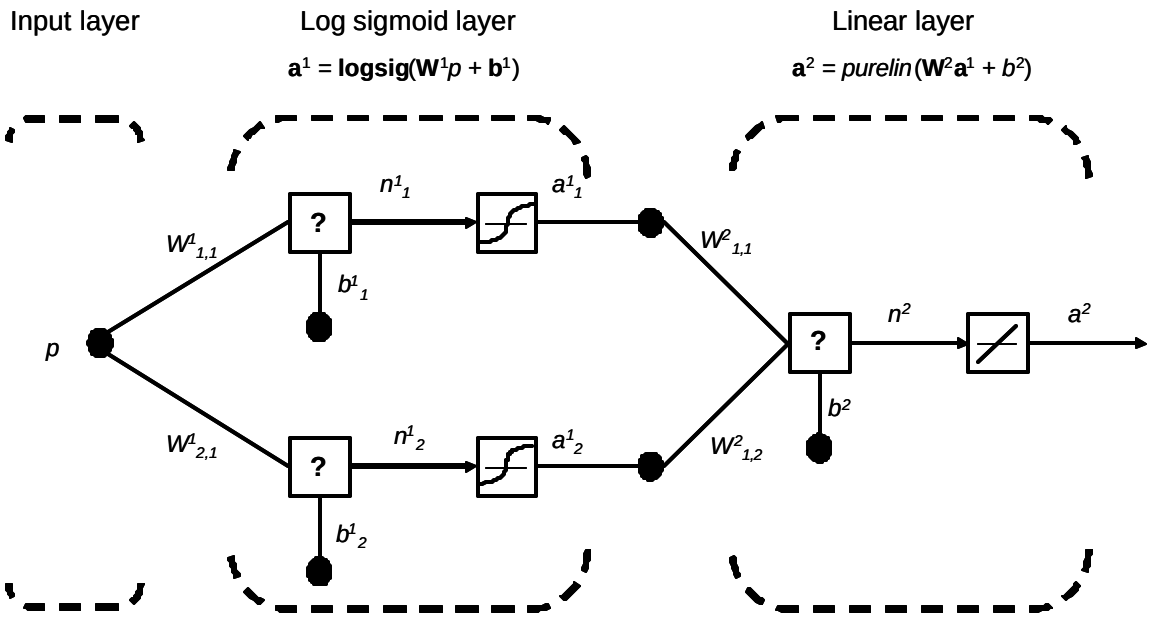

Figure A1 **Neural network example with one input, two log sigmoid neurons in one hidden layer, and one linear neuron in the output layer.**

Figure A1 shows a one input, two log sigmoid hidden layer, one linear output neural network. The hidden layer transfer function f^1 is log sigmoid and the output layer transfer function f^2 is linear. These transfer functions can be represented by

$$f^1(n) = \frac{1}{1+e^{-n}}, \quad f^2(n) = n \quad \text{..... (1)}$$

For multilayer networks, Figure A1 as an example, the output of one layer is the input to the next layer. For a network of M layers with a preceding layer output of a^m, the output a^{m+1} can be represented by

$$\mathbf{a}^{m+1} = \mathbf{f}^{m+1}(\mathbf{W}^{m+1}\mathbf{a}^m + \mathbf{b}^{m+1}), \quad for\ m = 0, 1, \ldots, M-1 \quad \text{..... (2)}$$

Neurons in the first layer receive external inputs p, which is a starting point for the above equation, and is represented by

$$\mathbf{a}^0 = \mathbf{p} \quad \text{..... (3)}$$

Neuron outputs in the last layer, or the network outputs, are represented by

$$\mathbf{a} = \mathbf{a}^M \quad \text{..... (4)}$$

The backpropagation algorithm for multilayer networks is a generalization of the least mean square (LMS) algorithm for single layer networks. Both algorithms use the same error metric, or performance index: mean square error (MSE). To train a neural network, examples of proper network behavior are presented in input $\boldsymbol{p}_q$ and output $\boldsymbol{t}_q$ examples, where $\boldsymbol{p}_q$ is the network input and $\boldsymbol{t}_q$ is the target network output. These inputs and targets can be represented by

$$\{\mathbf{p}_1, \mathbf{t}_1\}, \{\mathbf{p}_2, \mathbf{t}_2\}, \ldots, \{\mathbf{p}_Q, \mathbf{t}_Q\} \quad \text{..... (5)}$$

Each input $\boldsymbol{p}_q$ to the network will return an output $\boldsymbol{a}_q$, which is compared to the corresponding target $\boldsymbol{t}_q$. The backprop algorithm should adjust the network parameters, in other words the weights and biases, in order to minimize the MSE –

$$F(\mathbf{x}) = E\left[e^2\right] = E\left(t - a\right)^2 \quad \text{..... (6)}$$

where $\boldsymbol{x}$ is a vector containing network weights and biases. If the network has multiple outputs, the above MSE equation generalizes to

$$F(\mathbf{x}) = E\left[\mathbf{e}^T \mathbf{e}\right] = E\left[(\mathbf{t} - \mathbf{a})^T (\mathbf{t} - \mathbf{a})\right] \quad \text{..... (7)}$$

In backpropagation, as in the LMS algorithm, the MSE is approximated by

$$\hat{F}(\mathbf{x}) = (\mathbf{t}(k) - \mathbf{a}(k))^T (\mathbf{t}(k) - \mathbf{a}(k)) = \mathbf{e}^T(k)\mathbf{e}(k) \quad \text{..... (8)}$$

where the squared error at *k* iteration has been substituted for the expectation of squared error.

The steepest descent algorithm to update the weights and biases using the approximate MSE is

$$w_{i,j}^{m}(k+1) = w_{i,j}^{m}(k) - a\,\frac{\partial \hat{F}}{\partial w_{i,j}^{m}}\,,$$
$$b_{i}^{m}(k+1) = b_{i}^{m}(k) - \frac{\partial \hat{F}}{\partial b_{i}^{m}} \quad \text{..... (9)}$$

where *a* is the learning rate.

The error in a multilayer network is not an explicit function of the weights in the hidden layers, therefore the error derivatives must be calculated using the chain rule. To review the chain rule, suppose a function *f* which is an explicit function only of variable *n*. For the derivative of *f* with respect to a third variable *w*, the chain rule is then

$$\frac{df(n(w))}{dw} = \frac{df(n)}{dn} \times \frac{dn(w)}{dw} \quad \text{..... (10)}$$

Using the chain rule, the derivatives to calculate the weight and bias modifications would be

$$\frac{\partial \hat{F}}{\partial w_{i,j}^{m}} = \frac{\partial \hat{F}}{\partial n_{i}^{m}} \times \frac{\partial n_{i}^{m}}{\partial w_{i,j}^{m}}\,,$$
$$\frac{\partial \hat{F}}{\partial b_{i}^{m}} = \frac{\partial \hat{F}}{\partial n_{i}^{m}} \times \frac{\partial n_{i}^{m}}{\partial b_{i}^{m}} \quad \text{..... (11)}$$

The second term of each of these equations can be calculated because the net input to layer *m* is an explicit function of the weights and biases in that layer –

$$n_{i}^{m} = \sum_{j=1}^{S^{m-1}} w_{i,j}^{m} a_{j}^{m-1} + b_{i}^{m} \quad \text{..... (12)}$$

so

$$\frac{\partial n_{i}^{m}}{\partial w_{i,j}^{m}} = a_{j}^{m-1},\ \frac{\partial n_{i}^{m}}{\partial b_{i}^{m}} = 1 \quad \text{..... (13)}$$

If we define s_i^m as the sensitivity of F to changes in the *ith* element of the net input at layer *m,* defined as

$$s_i^m \equiv \frac{\partial \hat{F}}{\partial n_i^m} \quad \text{..... (14)}$$

then the chain rules for calculating the MSE for weights and biases for layer *i* become

$$\frac{\partial \hat{F}}{\partial w_{i,j}^m} = s_i^m a_j^{m-1} \text{ ,}$$
$$\frac{\partial \hat{F}}{\partial b_i^m} = s_i^m \quad \text{..... (15)}$$

The approximate steepest descent algorithm can now be written as

$$w_{i,j}^m(k+1) = w_{i,j}^m(k) - a s_i^m a_j^{m-1} \text{ ,}$$
$$b_i^m(k+1) = b_i^m(k) - a s_i^m \quad \text{..... (16)}$$

or, in matrix form

$$\mathbf{W}^m(k+1) = \mathbf{W}^m(k) - a\mathbf{s}^m(\mathbf{a}^{m-1})^T \text{ ,}$$
$$\mathbf{b}^m(k+1) = \mathbf{b}^m(k) - a\mathbf{s}^m \quad \text{..... (17)}$$

where the sensitivities can be expressed as

$$\mathbf{s}^m \equiv \frac{\partial \hat{F}}{\partial \mathbf{n}^m} = \begin{bmatrix} \frac{\partial \hat{F}}{\partial n_1^m} \\ \frac{\partial \hat{F}}{\partial n_2^m} \\ \vdots \\ \frac{\partial \hat{F}}{\partial n_{s^m}^m} \end{bmatrix} \quad \text{..... (18)}$$

To calculate the sensitivities s^m, the chain rule is applied again. To calculate the sensitivies, the error must be backpropagated through the network – a recurrence relationship exists between layers, as the sensitivity at layer m is calculated from the

sensitivity at layer m + 1. The recurrence relationship for the sensitivities is derived by using a Jacobian matrix

$$\frac{\partial \mathbf{n}^{m+1}}{\partial \mathbf{n}^{m}} \equiv \begin{bmatrix} \frac{\partial n_1^{m+1}}{\partial n_1^m} & \frac{\partial n_1^{m+1}}{\partial n_2^m} & \cdots & \frac{\partial n_1^{m+1}}{\partial n_{s^n}^m} \\ \frac{\partial n_2^{m+1}}{\partial n_1^m} & \frac{\partial n_2^{m+1}}{\partial n_2^m} & \cdots & \frac{\partial n_2^{m+1}}{\partial n_{s^n}^m} \\ \vdots & \vdots & & \vdots \\ \frac{\partial n_{s^{m+1}}^{m+1}}{\partial n_1^m} & \frac{\partial n_{s^{m+1}}^{m+1}}{\partial n_2^m} & \cdots & \frac{\partial n_{s^{m+1}}^{m+1}}{\partial n_{s^m}^m} \end{bmatrix} \quad \text{..... (19)}$$

For the *i,j* element of this matrix

$$\frac{\partial n_i^{m+1}}{\partial n_j^m} = \frac{\partial \left(\sum_{l=1}^{s^m} w_{i,l}^{m+1} a_l^m + b_i^{m+1} \right)}{\partial n_j^m} = w_{i,j}^{m+1} \frac{\partial a_j^m}{\partial n_j^m} = w_{i,j}^{m+1} \frac{\partial f^m(n_j^m)}{\partial n_j^m} = w_{i,j}^{m+1} \dot{f}^m(n_j^m) \quad \text{..... (20)}$$

where

$$\dot{f}^m(n_j^m) = \frac{\partial f^m(n_j^m)}{\partial n_j^m} \quad \text{..... (21)}$$

The Jacobian matrix can then be written as

$$\frac{\partial \mathbf{n}^{m+1}}{\partial \mathbf{n}^{m}} = \mathbf{W}^{m+1} \dot{\mathbf{F}}^m(\mathbf{n}^m) \quad \text{..... (22)}$$

where

$$\dot{\mathbf{F}}^m(\mathbf{n}^m) = \begin{bmatrix} \dot{f}^m(n_1^m) & 0 & \cdots & 0 \\ 0 & \dot{f}^m(n_2^m) & \cdots & 0 \\ \vdots & \vdots & & \vdots \\ 0 & 0 & & \dot{f}^m(n_{s^m}^m) \end{bmatrix} \quad \text{..... (23)}$$

The recurrence relationship for the sensitivity can then be expressed using the chain rule in matrix notation

$$\mathbf{s}^m = \frac{\partial \hat{F}}{\partial \mathbf{n}^m} = \left(\frac{\partial \mathbf{n}^{m+1}}{\partial \mathbf{n}^m} \right)^T \frac{\partial \hat{F}}{\partial \mathbf{n}^{m+1}} = \dot{\mathbf{F}}^m(\mathbf{n}^m)(\mathbf{W}^{m+1})^T \frac{\partial \hat{F}}{\partial \mathbf{n}^{m+1}} = \dot{\mathbf{F}}^m(\mathbf{n}^m)(\mathbf{W}^{m+1})^T \mathbf{s}^{m+1} \quad \text{..... (24)}$$

The above equation illustrates where the backpropagation algorithm derives its name – the sensitivities are propagated backward through the network from the last to first layers

$$\mathbf{s}^M \rightarrow \mathbf{s}^{M-1} \rightarrow \ldots \rightarrow \mathbf{s}^2 \rightarrow \mathbf{s}^1 \quad \text{..... (25)}$$

The starting point s^M for the network can now be computed

$$s_i^M = \frac{\partial \hat{F}}{\partial n_i^M} = \frac{\partial (\mathbf{t}-\mathbf{a})^T(\mathbf{t}-\mathbf{a})}{\partial n_i^M} = \frac{\partial \sum_{j=1}^{s^M} (t_j - a_j)^2}{\partial n_i^M} = -2(t_i - a_i)\frac{\partial a_i}{\partial n_i^M} \quad \text{..... (26)}$$

Since

$$\frac{\partial a_i}{\partial n_i^M} = \frac{\partial a_i^M}{\partial n_i^M} = \frac{\partial f^M(n_j^M)}{\partial n_i^M} = \dot{f}^M(n_j^M) \quad \text{..... (27)}$$

then

$$s_i^M = -2(t_i - a_i)\dot{f}^M(n_j^M) \quad \text{..... (28)}$$

The above equation can be expressed in matrix form

$$\mathbf{s}^M = -2\dot{\mathbf{F}}^M(\mathbf{n}^M)(\mathbf{t}-\mathbf{a}) \quad \text{..... (29)}$$

SUMMARY IN MATRIX NOTATION

Propagate input forward through the network –

$$\mathbf{a}^0 = \mathbf{p}\ ,$$
$$\mathbf{a}^{m+1} = \mathbf{f}^{m+1}(\mathbf{W}^{m+1}\mathbf{a}^m + \mathbf{b}^{m+1}) \quad for\ m = 0, 2, \ldots, M-1\ , \quad \text{..... (30)}$$
$$\mathbf{a} = \mathbf{a}^M$$

Propagate sensitivities backwards through the network –

$$\mathbf{s}^{M} = 2\dot{\mathbf{F}}^{\mathrm{M}}(\mathbf{n}^{M})(\mathbf{t}-\mathbf{a}),$$
$$\mathbf{s}^{m} = \dot{\mathbf{F}}^{m}(\mathbf{n}^{m})(\mathbf{W}^{m+1})^{T}\mathbf{s}^{m+1}, \quad for\ m = M-1, \ldots, 2, 1 \qquad \text{..... (31)}$$

Update weights and biases with approximate steepest descent rule –

$$\mathbf{W}^{m}(k+1) = \mathbf{W}^{m}(k) - a\mathbf{s}^{m}(\mathbf{a}^{m-1})^{T},$$
$$\mathbf{b}^{m}(k+1) = \mathbf{b}^{m}(k) - a\mathbf{s}^{m} \qquad \text{..... (32)}$$

Adapted from –

Hagan, M.T., Demuth, H.B., and Beale, M., 1996. Backpropagation. Ch 11, 11-1 – 11-47, in Neural Network Design, PWS Publishing Company, Boston MA,